MARTIN MARIETTA ENERGY SYSTEMS LIBRARIES
3 4456 0049756 7

CENTRAL RESEARCH LIBRARY
DOCUMENT COLLECTION

ORNL-3004
UC-81 - Reactors-Power

HOMOGENEOUS REACTOR PROGRAM

QUARTERLY PROGRESS REPORT

FOR PERIOD ENDING JULY 31, 1960

CENTRAL RESEARCH LIBRARY
DOCUMENT COLLECTION
LIBRARY LOAN COPY
DO NOT TRANSFER TO ANOTHER PERSON
If you wish someone else to see this document, send in name with document and the library will arrange a loan.

OAK RIDGE NATIONAL LABORATORY
operated by
UNION CARBIDE CORPORATION
for the
U.S. ATOMIC ENERGY COMMISSION

Printed in USA. Price $2.50. Available from the

Office of Technical Services
Department of Commerce
Washington 25, D.C.

LEGAL NOTICE

This report was prepared as an account of Government sponsored work. Neither the United States, nor the Commission, nor any person acting on behalf of the Commission:

A. Makes any warranty or representation, expressed or implied, with respect to the accuracy, completeness, or usefulness of the information contained in this report, or that the use of any information, apparatus, method, or process disclosed in this report may not infringe privately owned rights; or

B. Assumes any liabilities with respect to the use of, or for damages resulting from the use of any information, apparatus, method, or process disclosed in this report.

As used in the above, "person acting on behalf of the Commission" includes any employee or contractor of the Commission, or employee of such contractor, to the extent that such employee or contractor of the Commission, or employee of such contractor prepares, disseminates, or provides access to, any information pursuant to his employment or contract with the Commission, or his employment with such contractor.

ORNL-3004
Reactors-Power
TID-4500 (15th ed.)

Contract No. W-7405-eng-26

HOMOGENEOUS REACTOR PROGRAM
QUARTERLY PROGRESS REPORT

FOR PERIOD ENDING JULY 31, 1960

Program Director - R. B. Briggs

Homogeneous Reactor Test - S. E. Beall
Reactor Analysis and Engineering Development - R. N. Lyon
Reactor Materials Research - E. G. Bohlmann
Chemical Engineering Development - D. E. Ferguson
Supporting Chemical Research - H. F. McDuffie
Analytical Chemistry - M. T. Kelley

DATE ISSUED

OCT 28 1960

OAK RIDGE NATIONAL LABORATORY
Oak Ridge, Tennessee
operated by
UNION CARBIDE CORPORATION
for the
U.S. ATOMIC ENERGY COMMISSION

MARTIN MARIETTA ENERGY SYSTEMS LIBRARIES

3 4456 0049756 7

SUMMARY

PART I. HOMOGENEOUS REACTOR TEST

1. HRT Remote Operations, Maintenance and Testing

The program of reactor maintenance and major repairs to the core tank was continued. Approximately 90% of this program has now been completed.

A sample of the core wall at the edge of the upper hole was cut and removed from the reactor for metallographic examination, and the circular opening left by the core sample was reamed to receive a conical patch. The inside surface of the core vessel was cleaned by wire-brushing to remove zirconia-urania scale. At the end of the period a patch was installed on the lower core hole.

Tools were developed and used successfully to remove cut-up screen strips from the tee-section of the core access piping. A tool was designed for manipulating an ultrasonic core-wall thickness gauge in the HRT core so that measurements of the core wall in the 30- and 90-deg cone could be made.

Maintenance on other reactor parts included the replacement of the fuel-system primary and secondary recombiners and the replacement of the fuel condensate block valves.

Instrument maintenance was also performed. Three additional block-valve systems were installed to reduce the possibility of the escape of radioactive materials from the reactor container. A new and more sensitive stack-activity monitor was installed on the stack inlet gas, and circuit revisions were made to permit reactor operation with reverse flow and a continuous transfer of condensate between the low-pressure systems.

Macro- and micro-examinations of the specimen from the core wall showed conclusively that the hole was formed by melting through the core wall with an external heat source, presumably a deposit rich in uranium. The reaction or melting of the Zircaloy-2 was not self-sustaining and quenched out after the external heat source was removed. The microstructure of the specimen indicates that the total time of the temperature excursion from 800°C to melting and back to 800°C was 2 to 5 sec.

The HRT core-vessel thickness was measured, using a remote manipulator and ultrasonic measuring equipment. A comparison of these data and measurements taken after run 20 and in the original condition indicates an over-all loss in core thickness in the upper region of 14 mils. The area between 20 deg below the equator and the region of the top screen exhibited greater loss.

2. HRT Processing Plant

The improved multiclone was fabricated and tested in preparation for installation with the reverse-flow fuel-circulating pump. Hydraulic characteristics were normal, and efficiencies measured with sized ThO_2 in room-temperature tests

were typical of other multiple parallel hydroclone units. Basic studies initiated to provide more complete performance data on these systems show that solids-removal efficiencies decrease as the underflow-to-feed ratio is decreased. Although this is believed to be a result of small differences in individual hydroclone dimensions which result in partial bypassing of some of the parallel units, further studies are required to provide a definitive answer.

A device designed to measure quantitatively the solids accumulation in the multiclone underflow pot will be tested in the next run. The difference in specific gamma activity of the bed of solids which settles from the solution above will be detected by measuring the temperature rise which results from gamma heating of a probe in the underflow pot.

Flow-pressure-drop measurements performed on the original multiclone after removal from the cell indicated several feed ports were partially plugged. A gamma survey revealed an accumulation of solids estimated at approximately 100 g in the feed chamber.

Laboratory studies of a proposed on-site fuel-cleanup procedure based on uranyl peroxide precipitation indicated that the process is feasible. Uranium recoveries are acceptable, and decontamination from nickel and other soluble constituents should exceed a factor of 10.

3. HRT Component Testing and Development

A 450-gpm canned-motor fuel-circulation pump, which will be used to reverse the direction of flow in the reactor, was pretreated and tested to obtain hydraulic performance data.

New primary and secondary recombiners of improved design were tested and found to have satisfactory recombination efficiencies.

Replacement feed-pump assemblies were tested prior to installation in the HRT. A fuel solution was pumped at a constant flow rate for more than 2000 hr at a discharge pressure of 1500 psi without adjustment of the pump.

A new experimental technique was developed for measuring the local age of fluid within a core model, and fluid-age distribution data were measured in the HRT reversed-flow core model. These data were used to infer that the HRT in reverse flow with 250°C inlet will operate at 5 Mw with a maximum wall temperature of 301°C, if no uranium-bearing scale is deposited. The maximum interior fluid temperature is estimated to be 310°C.

4. HRT Reactor Analysis

The maximum pressure rise in the HRT following a cold-water accident was calculated for upward core-fluid flow and for reversed flow. With the reactor initially critical at 260°C and a power level of 0.04 w, fuel solution at 100°C was considered to enter the core at a flow rate of 150 gpm. With reversed flow, reactivity was added at an average rate of 1.7% Δk_e/sec, while with upward flow the rate was 0.67% Δk_e/sec. The core pressure increased rapidly to a maximum of 550 psi above normal pressure with reversed flow and 400 psi with upward flow when only the core pressurizer was available for fluid expansion. With the core and blanket pressurizers connected, the pressure increases were 380 and 210 psi, respectively.

The possibility of a criticality accident in transferring irradiated fuel solution from the HRT was investigated. The transfer vessel is cylindrical, with a diameter of 19-1/4 in. and a height of 30-1/2 in. and is shielded with 9 in. of lead. It will be loaded with 100 liters of fluid containing 8 kg of enriched uranium in an aqueous solution (25% D_2O - 75% H_2O); 250 g of gadolinium will be present for neutron poisoning. The infinite multiplication constant is 0.59 when the fuel is uniformly dispersed. Settling of the uranium would increase reactivity, but would not cause the effective multiplication constant to exceed 0.86.

PART II. ENGINEERING DEVELOPMENT

5. Development of Reactor Components and Systems

The cylindrical re-entrant core model, 2 ft in diameter and 6 ft long, was tested further. Modified inlet vanes, increased inlet velocities, and outlet pipe baffles did not prevent the by-passing of about half the fluid directly from inlet to outlet. Re-entrant cylindrical core models with new inlet-nozzle designs and straight-through cylindrical core models were designed and fabricated for test.

A general arrangement layout of a 400-MwT reactor vessel with a thoria pellet blanket was completed to define the mechanical details of this type of reactor vessel. A pellet-blanket test model was designed to be used for developing pellet-transport techniques and means for cooling stationary pellet beds.

A 200Z pump fitted with alumina bearings continued to operate satisfactorily for 4200 hr. Increased-capacity solution feed pumps were endurance-tested to more than 10,000 hr, and the test was terminated. Pumps of this type can be expected to give reliable performance in future fluid-fuel reactors.

The 300-SM slurry system was tested successfully for almost 2000 hr. A shell-and-tube slurry heat exchanger performed well; aluminum-oxide-trimmed ball valves were used to shut off flowing slurry with little damage to the valve trim; and the slurry feed pumps and letdown equipment were used to regulate the slurry concentration in the high-pressure loop over the range of concentrations of essentially water to 1000 g of Th per liter.

A slurry of 1600°C-fired thoria circulated in 200B loop for 3200 hr showed no deposition of thoria on a heat transfer test surface. There was negligible degradation of the 1.8-μ-dia slurry particles.

6. Instrument and Valve Development

Four sets each of Kennametal grade KH (tungsten carbide) and Kentanium 162B (titanium carbide) valve trim were received and will be tested in slurry service. One set of grade KH has performed satisfactorily in the 300-SM slurry loop.

After approximately 4-1/2 months in the 300-SM loop, two Annin valves incorporating aluminum oxide ball-plugs and seats were found to have almost identical leak rates of 20 cc of water per minute with 2000 psi differential pressure across the valve seat.

Life tests were made on five Fulton Sylphon bellows test assemblies with 1000 psig applied externally at 225°C. Four units, which were stroked 1/8 in., had an average life of 3950 strokes. The fifth assembly, which was tested in a similar manner but with a stroke of 1/16 in., exhibited a life of 55,160 strokes.

PART III. SOLUTION FUELS

7. Reactions in Aqueous Solutions

Measurements were made of the relative dissolution rates of various solids at 250°C in oxygenated, well-stirred, synthetic HRT fuel solution. The solids tested were UO_2, U_3O_8, UO_3, $CuO \cdot 3UO_3$, and reactor-fuel solids prepared by evaporating fuel solution to dryness and calcining at 500°C. The solids, representing those which could conceivably have existed in the HRT under conditions of off-design operation, dissolved rapidly, with half lives of from less than 0.5 min to 2.5 min. These results indicate that such solids, if formed, should redissolve promptly under the conditions of good agitation and removal from regions of neutron flux which are being provided by the present modifications in the reactor flow pattern.

8. Heterogeneous Equilibria in Aqueous Solutions

Liquid-liquid equilibria and critical temperatures were determined in the system UO_3-SO_3-D_2O for solutions from 0.05 to 1.0 *m* in SO_3 and for mole ratios, UO_3/SO_3, from 0 to 1.0. These investigations covered temperatures from 275 to 405°C. At mole ratios between 0.3 and 1.0 for all SO_3 concentrations studied, a second liquid phase appeared as the temperature was raised. Below this ratio, critical phenomena occurred; i.e., the liquid-phase composition became equivalent to the vapor phase.

The system NiO-SO_3-H_2O was investigated at temperatures above 300°C in an attempt to find liquid-liquid immiscibility and to define this subsystem of the multicomponent system UO_3-CuO-NiO-SO_3-H_2O. Apparently, liquid-liquid immiscibility does not exist in this system at saturation vapor pressure. The solubility of NiO above 400°C in the supercritical fluid may exceed 0.6 *M* in 6 *M* H_2SO_4. Solid-liquid equilibria as well as critical temperatures were determined for this system.

Previous studies of thorium nitrate solutions were extended by an investigation of the solution-solid equilibrium boundaries of the system ThO_2-HNO_3-H_2O at 200 and 300°C. Saturation mole ratios, Th^{+4}/NO_3^-, in solutions containing 9.0 *M* nitrate were 0.20 and 0.18 at 200 and 300°C, respectively; in 2.0 *M* total nitrate the ratios were 0.18 and 0.03, illustrating the pronounced tendency toward hydrolysis of thorium at higher temperatures. The rapid rates at which solubility equilibria were established at these temperatures, in marked contrast to the very slow dissolution of refractory thoria at temperatures below 100°C, suggest applications to the chemical processing of solid fuel elements incorporating refractory oxides.

The compilation of solubility information for the system UO_3-HNO_3-H_2O was revised to incorporate the results of additional studies at temperatures of 325 and 350°C.

A program was initiated to study the electrical conductivity of aqueous systems at elevated temperatures and pressures. Apparatus has been assembled for initial measurements on sulfuric acid solutions.

A 200-fold dilution of a simulated fuel solution (0.04 *m* UO_2SO_4, 0.025 *m* $CuSO_4$, 0.035 *m* H_2SO_4) was not completely stable when circulated in a stainless steel loop at temperatures of 200 to 325°C. At 200°C about 3% of the uranium was lost from solution, and at 325°C, 45% was lost. A 50-fold dilution of the solution lost 40% of its uranium content when circulated at 300°C, but a 10-fold dilution appeared to be completely stable at 325°C.

9. Solution Corrosion

The corrosion of types 347 and cast CD4MCu stainless steel was investigated in a simulated fuel solution containing 0.04 *m* UO_2SO_4, 0.025 *m* $CuSO_4$, and 0.05 *m* H_2SO_4 at 250 and 300°C. At 250°C, critical velocities were about 10 fps for type 347 and less than 10 fps for cast CD4MCu; at 300°C, respective critical velocities were 45 to 50 fps and about 30 fps.

Pretreatment of the type 347 stainless steel specimens in water at 280°C for two days before exposure to the 250°C solution resulted in a critical velocity of 15 to 20 fps. When the specimens were pretreated in water at 280°C and then exposed to the fuel solution at 300°C for about 300 hr, a relatively thick, adherent oxide film developed on the specimens at velocities up to about 50 fps. Subsequent exposure of these specimens to the fuel solution for 560 hr at 250°C did not cause disintegration of the oxide film, and essentially no corrosion occurred over the entire velocity range. No pretreatments were attempted with the CD4MCu specimens.

Corrosion tests with Coors aluminum oxide in water at 100 and 300°C and in a simulated fuel solution at 100°C showed the material to have good corrosion resistance in water at both temperatures and poor resistance to the fuel solution at 100°C. Rates between 20 and 30 mpy were observed in the fuel solution.

Specimens in which aluminum oxide was brazed to titanium with zirconium-base braze alloys showed reasonably good corrosion resistance to a simulated fuel solution at 100°C and to oxygenated water at 300°C during 1500-hr tests. Neither corrosion nor thermal cycling resulted in the aluminum oxide being detached from the titanium.

10. Radiation Corrosion

Corrosion specimens from the first ORR in-pile solution loop experiment, 0-1-25, were examined for weight loss, induced activity, and composition of materials retained on surfaces. Some chemical, metallurgical, and visual examinations of the experiment are still in progress, and the experiment will be reported in detail when all data have been received.

Total circulation time for the experiment was 2741 hr. The ORR energy during this time was 36,895 Mwhr, about 90% of which was liberated at the 16- and 20-Mw levels. The loop, exposed in beam hole HN-1, was operated for several periods in the fully or partially retracted positions, and, as a result, was exposed to a calculated amount of radiation equivalent to that prevailing during 30,598 Mwhr of reactor energy with the loop in the fully inserted position.

The solution for this experiment was 0.04 *m* UO_2SO_4, 0.016-0.036 *m* H_2SO_4, and 0.006 *m* $CuSO_4$ in D_2O, and the main-stream temperature was 280°C. The loop was constructed of type 347 stainless steel, and corrosion of this material, during some portions of the exposure, was greater than that encountered in prior LITR loops which employed similar solutions in H_2O.

Specimens of Zircaloy-2 contained in the loop were taken from stock fabricated according to specifications of the HRT Metallurgy Section, and the Zircaloy-2, as well as other zirconium-alloy specimens contained in the loop, were chemically polished.

The induced-activity results show that at the reactor power of 16 Mw the neutron fluxes on specimens ranged from 2×10^{13} to 10^{12} neutrons/$cm^2 \cdot sec$ and the calculated solution power density ranged from 6.6 to 0.3 w/ml. The maximum fluxes are greater than those experienced in the LITR HB-2 facility by a factor of about 1.5.

The relation between corrosion rate and power density for the chemically polished Zircaloy-2 specimens in this experiment was probably the same as for Zircaloy-2 in previous loop and autoclave experiments which, in general, employed H_2O solutions, Zircaloy-2 specimens with machined surfaces, and specimen material from stock fabricated to give preferred grain orientations. Both types of material indicate a maximum corrosion rate of 40 mpy at infinite power density.

Substantially greater corrosion rates were observed on covered portions of Zircaloy-2 coupons than on exposed portions of the same coupons. Values for α, a factor by which the effective power density at a corroding surface is greater than that in solution due to uranium sorption on the surface, may have been as high as 15.0 for the covered portions. For the exposed portions, which were exposed to higher solution velocities, the values were as low as 1.5 to 2.0. The value of α for the covered surfaces was probably greater, by almost a factor of 2, than values indicated by results from previous experiments which employed H_2O solutions of UO_2SO_4.

Under a given set of conditions in this experiment, surfaces which were chemically polished, overground, or sandblasted followed by chemical polishing corroded to about equal extents. Sandblasting alone had a deleterious effect on the corrosion of Zircaloy-2 at some power-density levels. Specimens of Zircaloy-2 weld material and Zircaloy-2 air-contaminated weld material corroded at about the same rates as the Zircaloy-2 coupons.

Corrosion rates for the two chemically polished crystal-bar zirconium core annulus coupons were observed to be greater than for similarly located chemically polished Zircaloy-2 coupons. However, extrapolation of the crystal-bar zirconium data indicates a maximum corrosion rate of only 20 mpy at infinite power density.

Three chemically polished Zr-1Cr core channel coupons corroded at about the same rates as Zircaloy-2.

Specimens of Zr-15Nb, Zr-15Nb-2Mo, and Zr-15Nb-1Cu in the beta-quenched condition showed better corrosion resistance than Zircaloy-2. However, specimens of these materials which had been heat-treated at 400 to 500°C for one to two weeks showed poorer corrosion resistance than Zircaloy-2.

The apparatus for the electrochemical measurement of corrosion rates was modified to permit measurements to be made above 250°C. The rate-time results obtained gave further support to the logarithmic oxidation kinetics for Zircaloy-2. The potential-time and current-potential behaviors are similar to previous observations on the Firth-Sterling Zircaloy-2 at 208°C.

PART IV. SLURRY FUELS

11. Engineering and Physical Properties

The effect of pH level on the laminar-flow properties of flocculated ThO_2 suspensions was determined over a pH range of 1.6 to 12 with 1.35-micron (mean particle diameter) thorium oxide. Between the limits of pH = 4 and 10, there seems to be little effect on the coefficient of rigidity. In contrast, the yield stress shows a variation of ±20% about the mean; this may explain in part the data scatter observed in previous correlations in which the pH parameter was neglected.

12. Thorium Oxide Irradiations

Sedimentation particle-size analyses of two sets of thoria powders fired at 650, 800, 900, 1100, and 1500°C and irradiated to nvt's of 7 and 6 x 10^{20} (about 0.1% of the initial thoria atoms fissioned) showed decreases in the average particle sizes of the oxides and substantial production of fines less than 0.6 μ in size. The production of fines less than 0.6 μ in the irradiated material was less for the 1500°C-fired material than for the lower fired materials. Specific surface areas of all powders fired at less than or equal to 1100°C were reduced to 0.6 m^2/g or less by the 22 months of irradiation, while the specific surface area of the 1500°C-fired powder was essentially unchanged.

A heavy-water slurry of Houdry spheres, 18 μ average size, containing 0.12% of adsorbed natural uranium and irradiated to an nvt of 8 x 10^{19} (0.0004% of total atoms fissioned) at 180 to 280°C in the LITR in a settled condition, showed a substantial increase in the particle-size fraction between 1 and 9.6 μ. A similar sphere preparation of 11 μ average size showed essentially no degradation upon being pumped as a slurry for 550 hr at 175°C in a 100A loop.

13. Development of Gas-Recombination Catalyst

Gas recombination studies with aqueous thorium-uranium oxide slurries containing a palladium catalyst indicated that recombination was influenced by the past history of the slurry-catalyst system. In some cases recombination was only partial, the reaction terminating in an apparent equilibrium or very slow recombination-rate condition in which both hydrogen and oxygen were present in the gas phase. The calculated H_2/O_2 ratio in the residual gas increased with successive experiments in a given slurry-catalyst system to as high as 2.5. An explanation for the apparent deactivation or poisoning of the catalyst has not yet been obtained. Reaction rates obtained at a constant hydrogen and varying oxygen partial pressure indicate that the recombination mechanism involved a strong adsorption of oxygen on the catalyst.

14. Slurry Corrosion and Blanket Materials Tests

A group of thoria pellets consisting of 24 different preparations which had been fabricated using the same 800°C-calcined ThO_2 powder was tested to determine the effects of ThO_2 prefabrication firing temperature (800, 1200, and 1425°C), pellet shape, 0.5 wt % CaO additive, and the effect of wet-tumbling after calcination on pellet integrity. All finished compacts were calcined at 1650°C.

Portions of each preparation were subjected, at room temperature, to two 1-hr exposures in a spouted-bed test (10 pellets, 0.2 to 0.3 fps superficial velocity), ball milling for two 1-hr periods, and to exposure for 72-hr in static autoclaves at 260°C using distilled water and ambient atmosphere. A second exposure in the spouted-bed test was made on samples from the autoclave tests.

Attrition (weight loss) rates in the various tests, expressed as %/hr, were:

In ball-mill tests, 0.22 to 4.6
In spouted-bed tests, 0.13 to 2.8
In static autoclave tests, 3 to 600 x 10^{-5}

Attrition rates of pellets fabricated with flat ends increased in both ball-mill and spouted-bed tests as ThO_2 precalcination temperature was increased from 800 to 1425°C; conversely, rates of cylinders fabricated with rounded ends decreased as the ThO_2 precalcination temperature was increased.

Prior to autoclaving, pellets containing CaO additive and all pellets which were wet-tumbled after final calcination displayed lowest weight loss rates. However, after autoclaving they exhibited the highest rates. Some calcium was leached from all pellets containing CaO during the 72-hr exposure in autoclaves.

Hydriding of zirconium-base alloys was studied in toroid tests which were conducted to evaluate the effects of slurry flow velocity and of operating temperature. Specimens of Zircaloy-2 picked up only small amounts of hydrogen during 300 hr of exposure to hydrogenated Th-U oxide slurries at 10 fps flow velocity, whereas in previous tests with comparable test conditions but 26-fps velocity gross hydriding resulted.

Specimens of Zircaloy-2, which were exposed in toroids at 26 fps to circulating D_2O at 330°C, picked up small amounts of hydrogen during 300 hr of exposure in tests employing atmospheres of oxygen and of deuterium. Zircaloy-2 specimens exposed for 300 hr to Th-U oxide slurries at 330°C, 26 fps, in oxygen atmosphere were mildly hydrided in localized areas under defects in the oxide corrosion films; however, in deuterium atmosphere, the alloys displayed a general uptake of hydrogen.

Zircaloy-2 in-pile autoclave slurry corrosion experiment L5Z-153S, containing thoria - 13% urania (enriched) at 820 g of Th per kg of D_2O and with 0.019 *m* Pd catalyst, was irradiated under oxygen atmosphere at 280°C for six days, at an average power density of 2.6 w/ml. Maximum power density of 26 w/ml could not be maintained because of low catalyst activity (millimolal catalyst performance index 0.24 w/ml at 100 psi D_2). The experiment was terminated because a partial plug developed in the pressure-cell connecting tubing.

At the low level of fission power density in this experiment, no evidence of any radiation effect on corrosion was observed.

In-pile slurry loop L-2-27S was placed under irradiation in LITR beam hole HB-2. The loop, constructed of type 347 stainless steel, is operating satisfactorily at 280°C under excess oxygen atmosphere, circulating a thoria - 0.5% enriched-urania slurry containing 1350 g of Th per kg of D_2O (approximately 1000 g of Th per liter) and 0.023 *m* Pd. Recombination tests over a 600-hr period prior to insertion indicated adequate catalyst activity, with loss of half the activity in 400 hr.

PART V. FUEL MANUFACTURE

15. Thorium Oxide Preparation

In studies of the preparation of rounded thoria pellets from a ceramic-grade powder by pressing and sintering, the major variables affecting the attrition resistance of the pellets were found to be: "stickiness" and granule strength of the powder, which was modified by prefiring the powder to 1000°C and prepressing at 4000 psi; and final firing temperature of the pellets. The optimum final firing temperature was found to be 1750°C. Decrease of the angle of curvature of the concave-rounded punch faces reduced cracking at the junction of the hemispherical and cylindrical sections of the fired pellets for both thoria and mixed-oxide pellets.

In fabrication of 0.5% uranium - thorium oxide rounded pellets, prefiring of the powder to 1100°C, prepressing to 4000 psi, prefiring and soaking of pressed pellets at 1200°C for 20 hr, and firing at 1600 to 1750°C for 4 hr was found to be the optimum procedure.

In preparation of thoria-alumina microspheres by flame calcination of aqueous thorium nitrate solutions or thoria sols, significant increases in particle sizes from 1.2 to 2.0 μ were obtained by increasing the thorium concentration in the feed from 300 to 600 g/liter and by reducing the furnace reflector temperature from 1500 to 1000°C.

PART VI. METALLURGY

16. Metallurgy

A study conducted on the effects of beta homogeneization and quenching variables on the omega-phase formation in Zr-15Nb alloy showed that higher homogeneization temperatures, longer homogeneization times, higher quenching temperatures, faster quenching rates, and shorter aging times at room temperature decrease the incubation time for the formation of omega phase at 400°C. The data are consistent with the postulation that the increased vacancy concentration in the specimen increases the nucleation rate of omega phase, decreasing the incubation time for its formation.

Early results from a study of the beta-quench and reheat and of the true isothermal transformation behavior of Zr-1Cu, Zr-1.6Cu, Zr-4Mo, Zr-7.5Mo alloys indicate that age-hardening transformations occur at 400 and 500°C and that, if such transformations occur at 600 and 700°C, the alloys have overaged at the shortest times studied. Shorter and longer times of transformation at the same temperatures and at intermediate temperatures will be included in the study in the near future.

The study of the effects of fabrication variables on the preferred orientation and anisotropy of mechanical properties in plate Zircaloy-2 has been terminated. The data collected and the conclusions drawn are reported in two topical reports now in press. The principal conclusions reported previously are unchanged. The fabrication procedure producing the least preferred orientation is that used for fabrication of HRP material for the past several years.

CONTENTS

SUMMARY iii

PART I. HOMOGENEOUS REACTOR TEST

1. HRT REMOTE OPERATIONS, MAINTENANCE, AND TESTING 1
   1.1 Core-Vessel Repair and Cleaning 1
      1.1.1 Core-Sample Cutting and Upper-Hole Reaming 1
      1.1.2 Core-Vessel Cleaning 2
      1.1.3 Installation of Patch on Lower Core-Wall Hole 2
   1.2 Related Maintenance in Core Vessel 3
      1.2.1 Removal of Screen Strips from Piping 3
      1.2.2 Dual-Vision Omniscope Sheath 3
      1.2.3 Hydraulic Shearing Tool 3
      1.2.4 Core-Wall Thickness Measurements 5
   1.3 Maintenance and System Alterations 5
      1.3.1 Recombiner Replacements 5
      1.3.2 Valve Replacements 7
      1.3.3 Pressurizer-Heater Repair 7
      1.3.4 Radiation Containment Experience 7
   1.4 Instrument and Control-System Modifications 7
      1.4.1 Activity Containment 7
      1.4.2 Stack-Activity Monitor 8
      1.4.3 Reactor-Cell Sump Level 8
      1.4.4 Public-Address-System Emergency Power 8
      1.4.5 Control Modifications Required for Operation After Patching the Core 8
   1.5 Examination of Specimen from Core-Tank Wall 9
   1.6 Measurements of Core-Vessel Thickness 18

2. HRT PROCESSING PLANT 20
   2.1 Multiclone Tests 20
      2.1.1 Tests of Original Multiclone After Removal from Reactor 20
      2.1.2 Tests of the Replacement Multiclone and Performance of Multiple Hydroclone Systems 21
      2.1.3 Multiclone Solids Detector Probe 21
   2.2 Proposed Fuel Processing by Peroxide Precipitation 24
      2.2.1 Laboratory Studies 24
   2.3 Shield-Water Decontamination 27

3. HRT COMPONENT TESTING AND DEVELOPMENT 28
   3.1 Test of the HRT Replacement Fuel-Circulation Pump 28
   3.2 HRT Recombiner Test 28
   3.3 HRT Feed-Pump Test 28
   3.4 Temperature Distribution for Reverse Flow in the HRT 29

4. HRT REACTOR ANALYSIS 33
   4.1 Pressure Rise Following a Cold-Water Accident with Reversed Fluid Flow 33
   4.2 Criticality Conditions in the HRT Fuel-Transfer Vessel 34

PART II. ENGINEERING DEVELOPMENT

5. DEVELOPMENT OF REACTOR COMPONENTS AND SYSTEMS 37
   5.1 Development of Cylindrical Re-Entrant Core Vessel 37
   5.2 Thoria Breeder Reactors with Pellet Blankets 37
      5.2.1 Pellet-Blanket Test Model 39
   5.3 Circulation-Pump Development 39
      5.3.1 200Z Pump and Loop 39
      5.3.2 Stator Irradiation Test 39
   5.4 Feed Pumps 39
      5.4.1 Oxygen Compressor 39
      5.4.2 Increased-Capacity Solution Feed Pumps 39
   5.5 The 300-SM Slurry System 39
   5.6 Slurry Loop Experiments 42
      5.6.1 200B Loop Operation, Run 4B 42
      5.6.2 200A Loop Operation, Run 22A 42

6. INSTRUMENT AND VALVE DEVELOPMENT 43
   6.1 Valve Trim for Thorium Oxide Slurry Applications 43
      6.1.1 Valve Trim for 300-SM Loop Valves 43
   6.2 HRT Valves 43
      6.2.1 Isolation-Chamber Stem-Sealing Bellows 43

PART III. SOLUTION FUELS

7. REACTIONS IN AQUEOUS SOLUTIONS 45
   7.1 Dissolution of Inorganic Solids in HRT Fuel 45
      7.1.1 Experimental Procedure 45
      7.1.2 Results and Discussion 45
      7.1.3 Conclusions 48

8. HETEROGENEOUS EQUILIBRIA IN AQUEOUS SYSTEMS 49
   8.1 Liquid-Liquid Equilibria in the System UO_3-SO_3-D_2O 49
   8.2 Critical Curves in Solid-Liquid Equilibria in the System NiO-SO_3-H_2O Above 300°C 49
   8.3 The System ThO_2-HNO_3-H_2O at 200 and 300°C 51
   8.4 The System UO_3-HNO_3-H_2O at 25 to 350°C 54
   8.5 Conductivity of Aqueous Solutions at Elevated Temperatures 54
   8.6 Chemical Stability of Very Dilute Solutions 56

9. SOLUTION CORROSION 61
   9.1 Dynamic Tests with High-Acid UO_2SO_4 Solutions 61
   9.2 Laboratory Corrosion Studies 62
      9.2.1 Aluminum Oxide Corrosion Tests 62
      9.2.2 Brazed Aluminum Oxide - Titanium Tests 62

10. RADIATION CORROSION 65
   10.1 In-Pile Loops 65
      10.1.1 Introduction 65
      10.1.2 Experimental Methods and Procedures 67
      10.1.3 Results and Discussion 67
      10.1.4 Conclusions 75
   10.2 Supporting Research 75
      10.2.1 Electrochemical Studies of Zircaloy-2 Corrosion 75

PART IV. SLURRY FUELS

11. ENGINEERING AND PHYSICAL PROPERTIES 79
11.1 Effect of pH on the Rheological Characteristics of ThO_2 Suspensions 79

12. THORIUM OXIDE IRRADIATIONS 81
12.1 Thoria-Powder Irradiation 81
12.2 Houdry-Sphere Slurry Irradiation 83

13. DEVELOPMENT OF GAS-RECOMBINATION CATALYST 85
13.1 Slurry Sample from Out-of-Pile Test Run of In-Pile Slurry Loop 85
13.2 Slurry Sample for In-Pile Corrosion Studies 86

14. SLURRY CORROSION AND BLANKET MATERIALS TESTS 89
14.1 Thoria-Pellet Test Program 89
14.1.1 Introduction 89
14.1.2 Evaluation Tests 89
14.1.3 Test Results 91
14.2 Hydriding of Zirconium-Base Alloys: Velocity and Temperature Effects 91
14.3 In-Pile Autoclave Slurry Corrosion Studies 93
14.3.1 Introduction 93
14.3.2 Exposure of In-Pile Experiment L5Z-153S 93
14.3.3 Corrosion in Experiment L5Z-153S 94
14.4 In-Pile Slurry Loop 96
14.4.1 In-Pile Operation 96
14.4.2 Catalysis Studies 97

PART V. FUEL MANUFACTURE

15. THORIUM OXIDE PREPARATION 99
15.1 Thoria-Pellet Preparation 99
15.2 Uranium-Thorium Oxide Pellet Preparation 101
15.3 Flame-Calcination Development 101

PART VI. METALLURGY

16. METALLURGY 105
16.1 Zirconium-Alloy Development 105
16.2 Zircaloy-2 Fabrication Study 106

ORGANIZATION CHART 109

PART I. HOMOGENEOUS REACTOR TEST

1. HRT REMOTE OPERATIONS, MAINTENANCE, AND TESTING

S. E. Beall
R. L. Moore
P. N. Haubenreich
I. Spiewak
J. W. Hill, Jr.
F. N. Peebles

H. F. Bauman
R. Blumberg
N. C. Bradley
J. R. Brown
J. R. Buchanan
S. R. Buxton
J. R. Engel
D. F. Frech
R. H. Guymon
R. J. Harvey
E. C. Hise
P. P. Holz
J. E. Jones
J. O. Kolb
H. R. Payne
H. B. Piper
J. L. Redford
H. C. Roller
W. Terry
P. Vignet[1]

The program of reactor maintenance and major repairs[2] to remove the five uppermost diffuser screens, repair the core-vessel holes, reverse the direction of flow through the core, and replace several items of equipment was continued. Approximately 90% of this program has now been completed.

1.1 CORE-VESSEL REPAIR AND CLEANING

Progress on the core-vessel repair program included: cutting and removal of a sample of the core wall at the edge of the upper hole in the core vessel for metallographic examination; reaming the upper hole to provide a seating surface for a conical patch; cleaning of the inside core-vessel surface by wire-brushing; and installation and leak-testing of a patch on the lower hole in the core vessel. Following are descriptions of these repair operations and new tools developed for the work.

1.1.1 Core-Sample Cutting and Upper-Hole Reaming

A plastic impression of the upper hole in the core wall was made and replicated to provide a pilot for the core-hole sample cutter.[3] The sample cutter was then used successfully to cut a sample from the lower edge of the upper hole, after which the sample was brought out of the core vessel by means of the cutting tool and delivered to the "hot" laboratory facilities for metallographic examination. The round hole resulting from the sample cutting was then reamed with the tool described previously[4] to provide a 60-deg tapered seating surface for a conical patch. Photographs in Sec. 1.5 show the upper hole before and after removal of the core-wall sample; Fig. 1.1 shows the hole after reaming. Examination of photographs and observation of the reamed hole by means of the Omniscope confirmed that there is an uninterrupted machined surface to receive the conical patch. The irregular minor diameter of the reamed hole shown in Fig. 1.1 is due to thinning of the core wall from the blanket side.

UNCLASSIFIED
PHOTO 50735

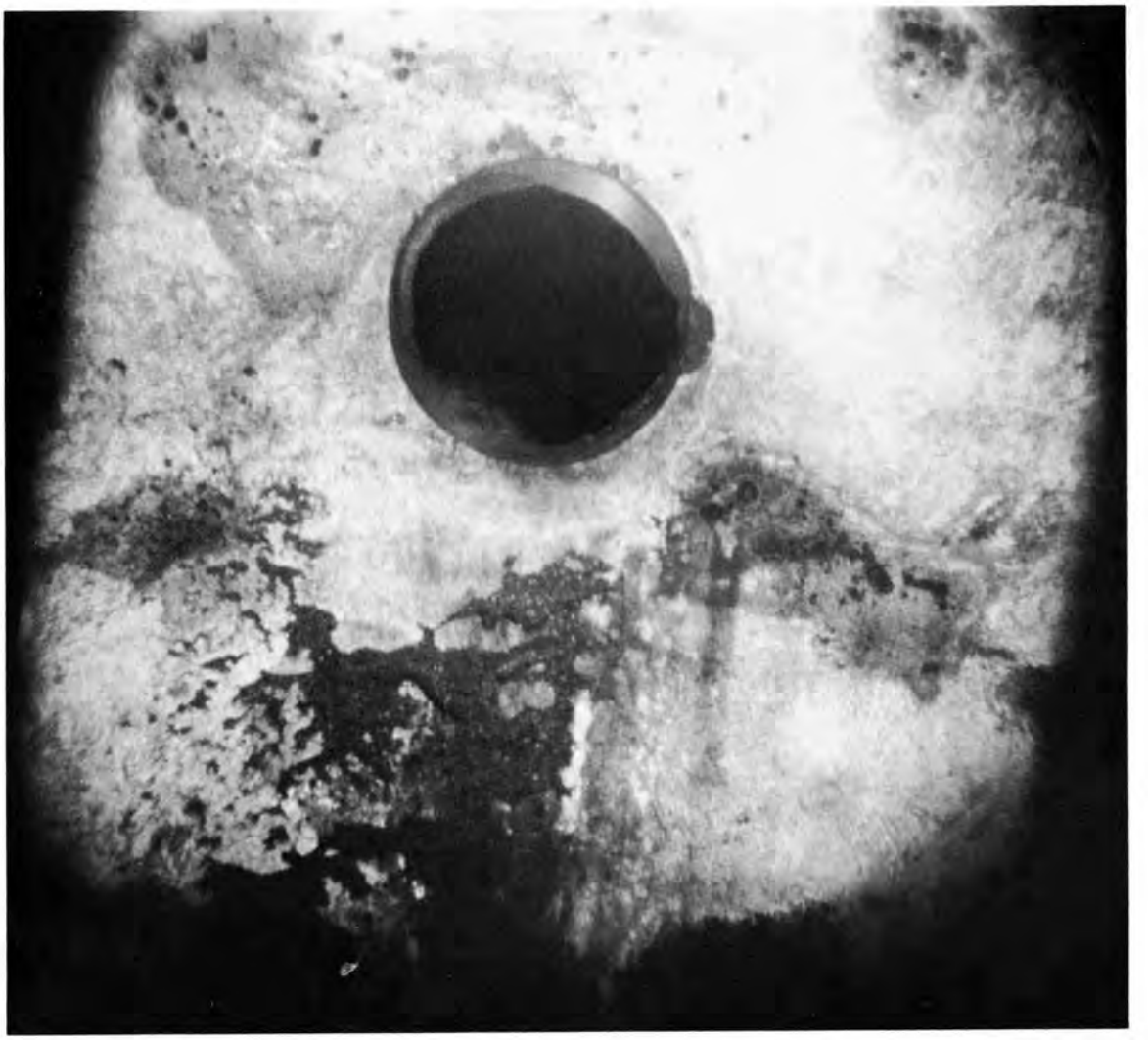

Fig. 1.1. Second Hole in HRT Core Vessel After Reaming for Conical Patch.

The core-hole sample cutting and reaming operations proceeded smoothly, partly because the Omniscope was fitted into the tool so the machining could be viewed remotely while the operation was in progress.

1.1.2 Core-Vessel Cleaning

The inside surface of the HRT core vessel was wire-brushed to remove zirconia-urania scale, by use of a tool[5] designed and constructed for this purpose. Photographic mapping of the core-vessel wall before and after the operation showed that the brushing was effective.

1.1.3 Installation of Patch on Lower Core-Wall Hole

A contour patch replicated from a plastic impression of the lower core-wall hole was installed by means of a tool designed for this operation.[6] After

installation of the patch, leakage rates were found to be undesirably large, and it was necessary to remove the patch, as planned in this eventuality. During the patch removal, the threads of the Zircaloy bolt and toggle-nut assembly galled, so that the patch insertion tool was unable to either remove or re-tighten the bolt. It was necessary to remove the patch insertion tool from the core, leaving the patch and bolt assembly hanging loosely in the hole.

The use of hooks and grapples in attempts to fold the toggle failed to remove it from the hole, and it was necessary to either shear or saw the toggle bolt. After the bolt was sawed partially with a tool having a saw blade welded to a rod, hooks were used to fracture the bolt and then remove the pieces from the core. The Omniscope and blanket viewer were used to observe these operations.

A second plastic impression of the lower hole was prepared by using a slightly modified procedure. A Dipseal plug cast in the shape of the first patch was pressed into the lower hole and heated in place by means of Teflon-insulated nichrome wire embedded in the surface of the Dipseal plug. This second plastic impression of the lower hole was replicated, and a new contour patch fabricated.

Installation of the new patch in the lower hole is in progress.

1.2 RELATED MAINTENANCE IN CORE VESSEL

1.2.1 Removal of Screen Strips from Piping

During removal of cut-up screen strips[7] from the core, four of the strips fell from the removal-hook tools and lodged in the 3-1/2-in.-ID horizontal runs of the 2-1/8-in.-ID access tee. These strips were located with special lighting and a short right-angle Omniscope sheath. Additional lights, raking tools, and a special seal for insertion into the core access line below the tee, to prevent the strips from falling back into the core, were designed and fabricated. A Greer accumulator ball, inflated with air after insertion in the tee, was used to seal the 3-1/2-in. core access line.

Figure 1.2 is a photograph, taken in a mockup of the tee section, which shows the extended rake-scribe tool, a light cage, and the support mast for the accumulator ball seal.

1.2.2 Dual-Vision Omniscope Sheath

Improvement to the Omniscope sheaths included the development of a dual-purpose sheath, containing both a right-angle and a 180-deg view window. Use of the dual-window sheath permits ready interchangeability of viewers and viewing in either plane, as well as cleaning of respective window surfaces through the slot-supported side opening. This feature permitted re-use of sheaths which were decontaminated following core applications.

The dual-vision sheath will also be used for future metallurgical examination of the core wall with a high-magnification telescope.

1.2.3 Hydraulic Shearing Tool

In attempting to install a Zircaloy patch on the first hole in the HRT core vessel, the Zircaloy bolt and toggle galled and the patch became caught in a position away from the core wall. To permit removal of the patch, a tool

Fig. 1.2. Mockup of C-100 Tee Section Showing Tool for Removal of Screen Strips.

(see Fig. 1.3) was designed to hydraulically shear the 1/4-in. Zircaloy bolt. A 1-1/4-in.-ID hydraulic cylinder is used to supply up to a 2000-lb force to a moving shear blade which is a part of the cylinder piston. The stationary shear blade or "shoe" is mounted from the cylinder wall.

The cylinder is supported from a 3/4-in. sched-160 pipe mast by means of two nonparallel arms which erect to the proper elevation with the cylinder on a 15-deg angle with the vertical (i.e., parallel with the 30-deg cone). The erecting rod is located inside the pipe mast, thus allowing room for the Omniscope, lights, and grappling hooks to be installed with the tool.

The shearing tool was fabricated and tested successfully. It was not necessary to use this device, as the toggle bolt as partially sawed and then fractured, as described in Sec. 1.1.3.

1.2.4 Core-Wall Thickness Measurements

A tool was designed for use in measuring the thickness of the 30- and 90-deg cone sections of the HRT core tank. (This device supplements the thickness gauge for the spherical portion.[8])

An ultrasonic thickness gauge (1-in. dia x 1-3/8-in. long) is mounted and supported so that it will remain near the vertical axis of the vessel. The gauge may be rotated from 10 to 50 deg of arc from the horizontal and be "aimed" normal to either the 30- or 90-deg cone (with an allowance of ±5 deg at either extreme).

A thumbscrew positioning mechanism and a position indicator are provided. The conical sections must be filled with water during the operation of this tool to provide a coupling medium between the ultrasonic gauge and the core wall.

1.3 MAINTENANCE AND SYSTEM ALTERATIONS

The normal maintenance of reactor equipment proceeded while core repair work was in progress. Approximately 80% of the scheduled maintenance is now completed. Almost half of the shield roof pans which were removed for these maintenance operations have been rewelded into position.

1.3.1 Recombiner Replacements

The fuel-system primary and secondary recombiners were replaced because they were no longer able to recombine efficiently.[9] This was the first replacement for either unit.

Causes for their decreased efficiencies are being investigated. The primary-recombiner pellet bed definitely contained void areas. Tests are being conducted to determine the characteristics of the pellets.

It was found that the secondary unit operated efficiently at bed temperatures above approximately 150°C instead of 110°C as originally designed. The new secondary recombiner has a clamp-on heater which can be operated at temperatures up to 575°C.

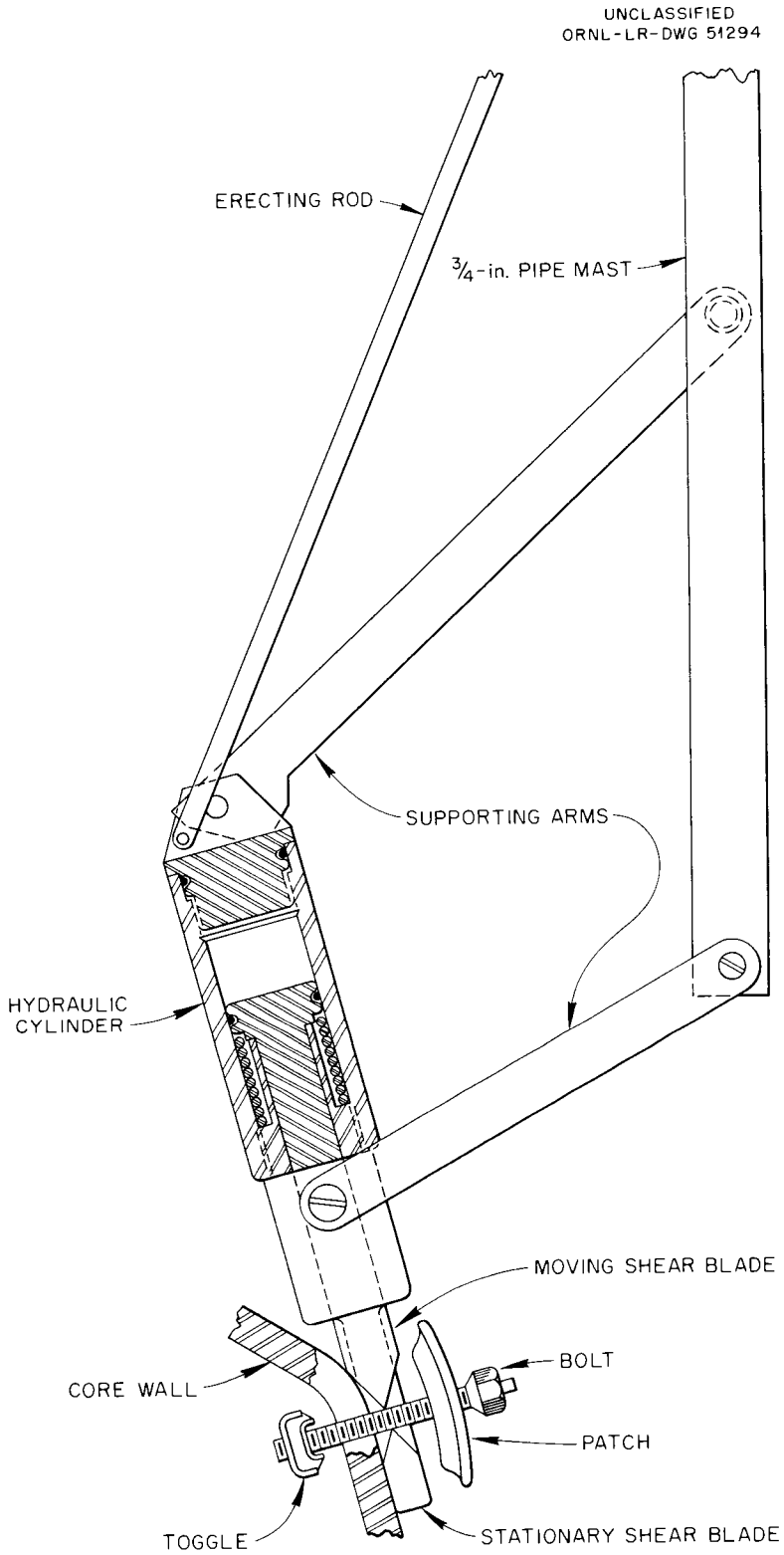

Fig. 1.3. Hydraulic Shearing Tool for Zircaloy Toggle Bolt.

1.3.2 Valve Replacements

The outlet valve (HCV-344) on the fuel-recombiner condenser was replaced because it was part of the secondary-recombiner assembly. The valve, which still operated satisfactorily, was later used to replace the fuel-condensate-tank block valve (HCV-336), which leaked excessively past the seat.

1.3.3 Pressurizer-Heater Repair

One heater unit (2-B) on the fuel pressurizer was removed long enough to replace an open thermocouple. The unit had not been operated since the thermocouple failed.

1.3.4 Radiation Containment Experience

Personnel exposures continue to be well below permissible levels in all phases of the work. During the report period the highest single exposure in a 24-hr period was approximately 200 mr. Work backgrounds have usually been less than 50 mr/hr.

The water, which has provided shielding for personnel during all the maintenance operations, has been changed only once since the current series of activities began (in February 1960). After about three months, the reactor containment tank was partially emptied to ascertain whether or not prolonged contact with water had damaged reactor components, wiring, etc. The only damage was observed at the bakelite thermocouple disconnects near the pressurizer heaters where the radiation level ($\sim 10^5$ r/hr) and temperature ($\sim 150°F$) are high. Before releasing the shield water (approximately 200,000 gal), it was treated in the waste-system pond to precipitate greater than 99% of the radioactivity, approximately 70 curies of predominantly beta activity. Maintenance activities since the shield was refilled have added only 2 curies to the water.

Leak-testing of the reactor containment-tank penetrations continued to ensure that the integrity of the secondary containment is still good. Approximately 70% of the tests have been completed.

1.4 INSTRUMENT AND CONTROL-SYSTEM MODIFICATIONS

1.4.1 Activity Containment

Three additional block-valve systems were installed to prevent possible escape of radioactive materials from the reactor containment tank through piping penetrations. Two Victoreen monitors located in the east valve pit will detect the presence of activity in the cell jet line and cause a block valve located in the jet line to close when activity in the jet line exceeds safe limits. Two similar Victoreen monitors, also located in the east valve pit, will cause a block valve located in the waste storage and sampler vent lines to close when activity in these lines exceeds safe limits. The third system is designed to prevent the escape of radioactive steam into the external steam system in the event of a failure of the heat exchanger tubing with subsequent leakage of steam through the steam safety block valves and outer steam valves. Leakage of radioactive steam through the safety block valves will be detected by the two Victoreen steam-activity monitors, located in the steam pit. If the steam activity exceeds safe limits, the steam safety block valves and the outer steam valves

will be closed and the lines connecting these valves will be vented to the reactor cell, thus reducing steam pressure in the lines and preventing leakage of radioactive steam through the outer valves into the external system. A high-shield-pressure interlock on the vent valves will prevent escape of radioactive steam through the vent lines in the event of a rupture of the system within the cell.

Dual-channel circuitry was utilized in all three systems in order to prevent inadvertent operation due to failure of a single component. Provisions were made whereby the action of the safety circuitry associated with these systems may be blocked on the jumper-board panel located in the main control room.

1.4.2 Stack-Activity Monitor

A new activity monitor was installed at the inlet to the stack. The new monitor contains a filter assembly, which will collect particulate activity in the stack gas, and a Geiger tube detector. This system is much more sensitive than the Victoreen units fastened to the outside of the stack.

1.4.3 Reactor-Cell Sump Level

A new level system was installed to provide a continuous indication and record of the reactor cell sump level and to provide a high-sump-level alarm. This system is of the dip-tube (bubbler) type and uses nitrogen as a purge gas. All associated instruments, such as recorders, differential-pressure cells, solenoids, etc., are located on a control panel adjacent to the blanket sample station in the high-bay area.

1.4.4 Public-Address-System Emergency Power

A d-c to a-c converter was installed to automatically provide emergency power for the public-address system upon loss of normal TVA power. This system obtains its power from the 48-v d-c control-system batteries. In order to conserve battery charge, provisions were made to automatically disconnect the converter from the batteries after 5 min. If additional time is required, successive 2-min periods of emergency power may be obtained by operation of a switch located in the control console.

1.4.5 Control Modifications Required for Operation After Patching the Core

Revisions were made in the control of fuel- and blanket-system pressures and levels to provide for operation with the patched core. A control system was installed to permit continuous transfer of condensate from the fuel low-pressure system to the blanket low-pressure system.

In the revised method of operation condensate will be pumped into the blanket continuously and will leak around the plugs in the core wall and into the core. There will be no letdown from the blanket high-pressure system to the blanket low-pressure system. The fuel and blanket pressurizer heaters will be controlled to maintain a constant pressure in the fuel pressurizer. Provisions are made whereby the output of the blanket pressurizer heaters can be biased below that of the fuel pressurizer heaters. This bias, which is obtained by manually setting a bias between the demand signals to the fuel and blanket D.A.T. (duration and time) heater controllers, will be adjusted to maintain a blanket-to-core differential pressure which will maintain a leakage flow through

the patches such that the flow is from blanket to core and is within the capacity of the low-pressure condensate transfer system. Fuel pressurizer level will be controlled by control of the fuel letdown as in previous operations. The rate of condensate addition to the blanket will normally be constant, but the blanket pressurizer level can be controlled, if necessary, by controlling the stroke of the blanket feed pump with a signal obtained from the blanket pressurizer level controller.

In order to maintain a constant concentration in the fuel dump tanks, and therefore a constant fuel temperature, a system was installed wherein the rate of condensate collection in the condensate tanks can be controlled from the fuel dump-tank weight. Fuel-to-blanket condensate transfer will be controlled by a cascade system to maintain a constant weight of condensate in the fuel condensate storage tanks. In this system the fuel-storage-tank condensate weight will supply a setpoint signal to a controller which positions the fuel cold-trap valves to obtain the required differential pressure between the fuel and blanket low-pressure systems. Since the condensate transfer rate will be a direct function of the differential pressure between the low-pressure systems, this differential pressure will serve as an indication of the condensate transfer rate.

These revisions required numerous changes to the control-system pneumatic piping and wiring and also required the addition of additional control devices external to the reactor cell. However, no changes have been made in instrumentation equipment within the reactor cell.

1.5 EXAMINATION OF SPECIMEN FROM CORE-TANK WALL*

The metallographic specimen cut from the Zircaloy-2 core tank (see Sec. 1.1.1) was cleaned and macro-photographs were made by the Post-Irradiation Evaluation Group of the Metallurgy Division. The metallographic preparation and the photomicrographs were made by the Remote Metallography Group of the Solid State Division. The macro- and micro-examinations of the specimen have shown conclusively, it is believed, that the hole in the core tank was formed by melting through the core wall with an external heat source, presumably a deposit rich in uranium. The reaction or melting of the Zircaloy-2 quenched out very soon after the removal of the external heat source, since the microstructural features of the specimen indicate that the total time of the temperature excursion from approximately 800°C to melting to 800°C was 2 to 5 sec.

Photographs of the site of the specimen location, Figs. 1.4 and 1.5, show the shape of the hole after removal of brittle outer scales, and after the hole sawing operation. (A photograph showing the hole as-formed was included in the last quarterly progress report, ORNL-2947, p 4.) Figures 1.4 and 1.5 also show the location, approximate orientation, and size of the metallographic specimen. Photomacrographs of the specimen, Fig. 1.6, show both ends of the specimen, the plane of cut and polishing for the metallographic specimen, and the surface of cut made by the hole saw. The burr left on the specimen at the saw kerf was caused by flexing of the specimen to fracture during the last portion of the cutting operation, due to fouling of the hole saw in the cut. It does not indicate brittle fracture of the specimen. The scratches produced on the cut surface, the lack of pitting on the cut surface, and the bending of the burr indicate that the cut was made in ductile material, quite similar to that found in and produced by an uncontaminated deposited weld.

*Contribution by F. W. Cooke and M. L. Picklesimer, Metallurgy Division.

Fig. 1.4. Upper Hole in the HRT Core Tank After Removal of Scale. ~1X. Reduced 8%.

The metallographic cross section of the specimen examined is shown in the composite photomicrograph in Fig. 1.7. The molten tip at the top of the figure was the edge of the hole, the nub at the bottom is the burr from the hole-saw cut, the core side of the specimen is on the right-hand side, the blanket side on the left, and the hole-sawed surface at the bottom. The width of the specimen, from left to right in the figure, is ~1/4-in., the cross section of the core-tank wall. The gradient of structures is representative of a temperature gradient from greater than about 1800°C (oxygen-stabilized alpha zirconium plus oxygen-rich melt) at the molten tip to approximately 950 to 1000°C just inside the core-side surface at the saw kerf. The maximum temperature in the burr, on the blanket side, is estimated to have been about 1300 to 1400°C. The region of temperatures from reactor temperature to about 950°C was removed by the cutting operation.

Fig. 1.5. Upper Hole in the HRT Core Tank After Removal of Specimen. ~1X.

The region of the molten edge and surface of the specimen is shown at higher magnification in Figs. 1.8 and 1.9. Shown are the molten zone, the oxygen-stabilized alpha rim, and depth of oxygen contamination. The temperatures experienced ranged from greater than 1800°C in the molten zone to near 1500°C in the center of the field shown in Fig. 1.8. The acicular structure produced by the transformation through quenching the high-temperature beta phase is duplex

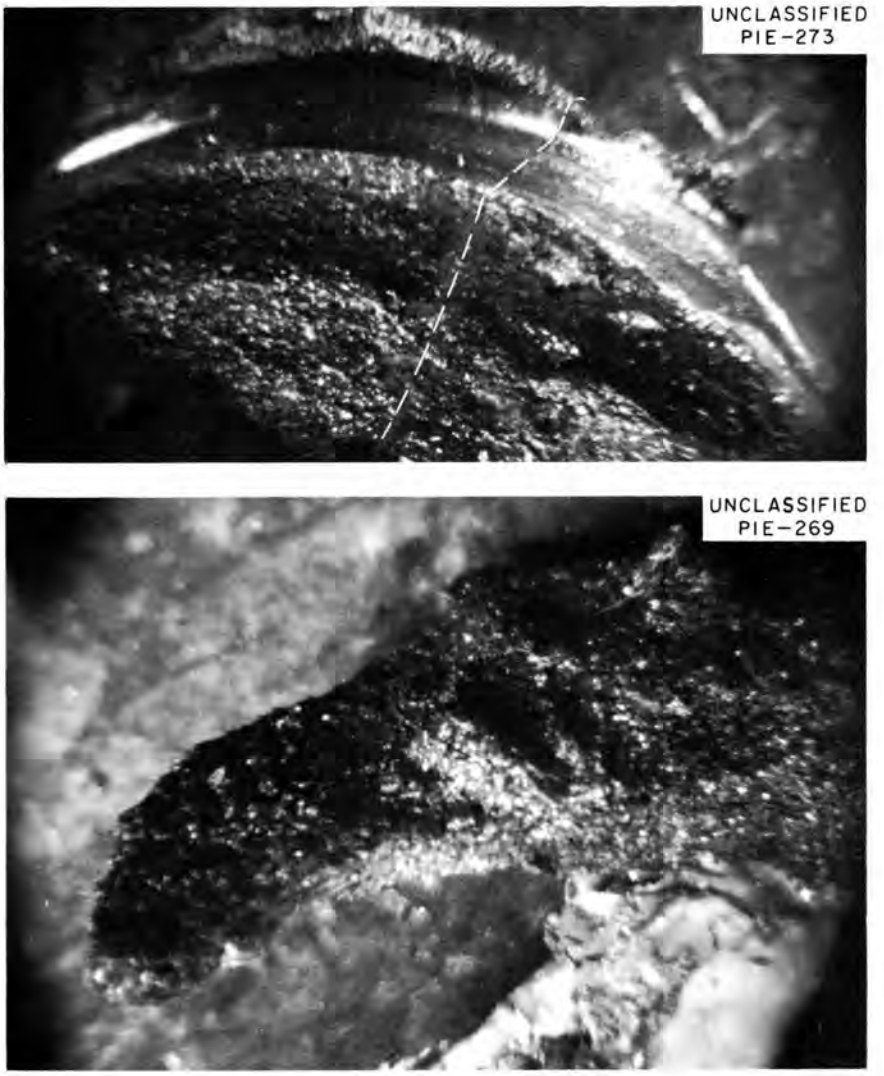

Fig. 1.6. Macrophotograph of Specimen Cut from HRT Core Tank. 3.3X.

in having two very distinctly different needle sizes (as shown in Fig. 1.10, taken at 1000X near the left-hand edge of Fig. 1.8). Such a situation has not been observed in specimens transformed by quenching at an essentially constant cooling rate through the temperature range of transformation (~960 to ~750°C for water-quenched specimens). The duplex needle structure could have been produced by cooling from above 960°C to about 850 to 900°C at one cooling rate, and cooling at a much faster rate from about 850°C to below about 750°C, a sequence which could have occurred by the collapse of a steam blanket at the site.

The microstructure of the burr at the saw kerf (blanket side of specimen), shown in Fig. 1.11, indicates that the temperature at this point was in the neighborhood of 1300 to 1400°C, as shown by the size of the prior beta grains produced in the temperature excursion. The acilular structure is also duplex, as shown in Fig. 1.12.

Fig. 1.7. Composite Cross Section of Metallographic Specimen. Bright field. ~20X. Reduced 11%.

The region of the specimen that experienced the lowest temperature maximum during the temperature excursion is shown in Fig. 1.13 and was located at the saw-cut surface just inside the surface exposed to the core. A photomicrograph at higher magnification is presented in Fig. 1.14 to show the structure existing at the interface between all-beta and alpha-plus-beta structure just inside the specimen from the saw kerf. The temperature at the interface is estimated to have been between 970 and 1000°C. The columnar grain growth of the beta phase, which is barely detectable in the structure of Fig. 1.13, is evidence of a very steep temperature gradient having existed for a very short period of time, and is producible in laboratory experiments only in tapered specimens whose smallest cross sections are melted under water in less than 2 sec.

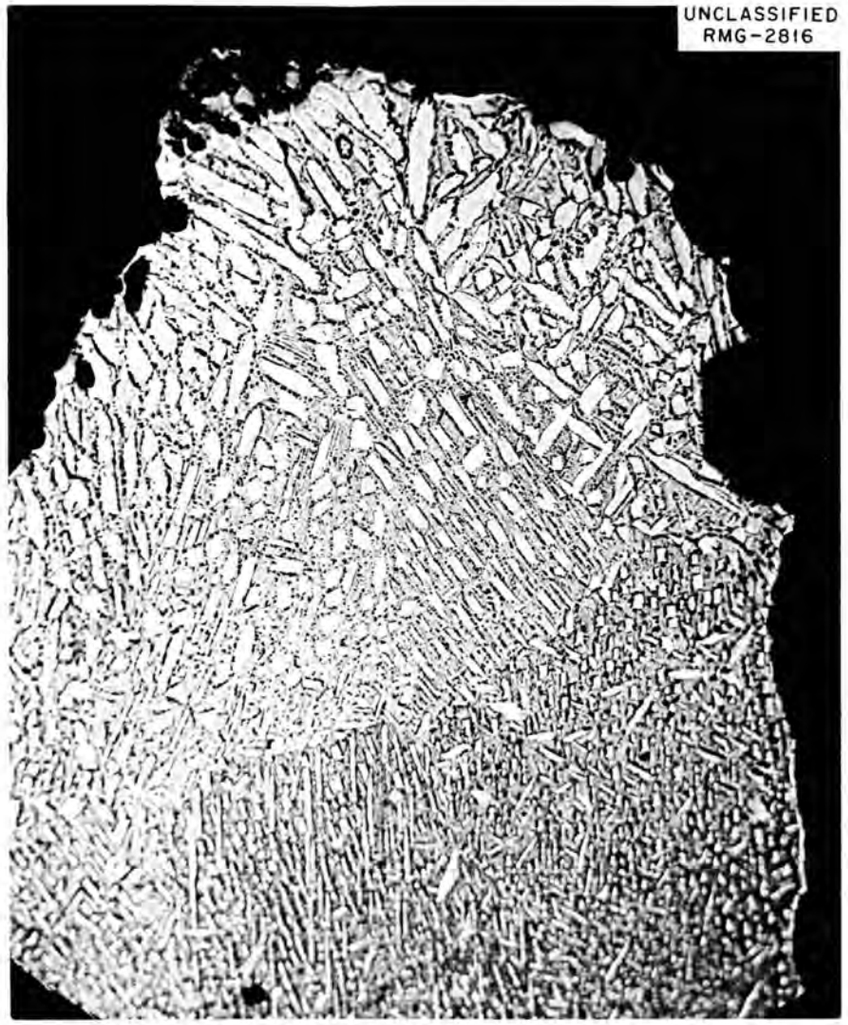

Fig. 1.8. Photomicrograph of Molten Edge. Bright field. 45X.

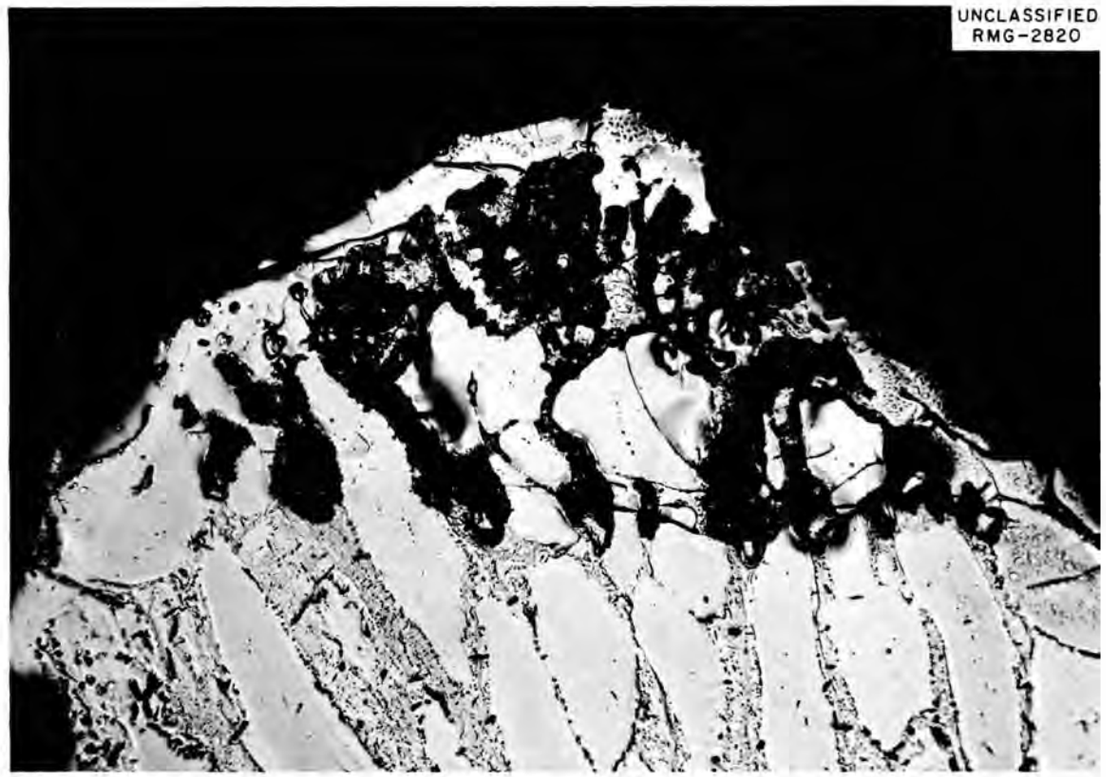

Fig. 1.9. Photomicrograph of Molten Tip. Bright field. 250X. Reduced 7%.

Fig. 1.10. Photomicrograph of Duplex Alpha Needle Structure in Center of Specimen. Bright field. 1000 X.

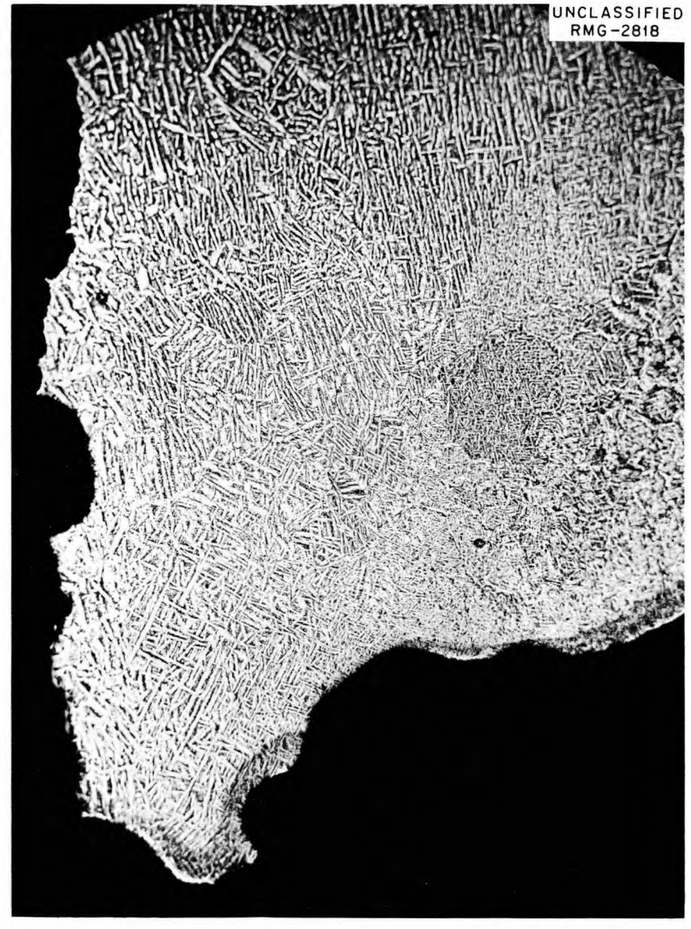

Fig. 1.11. Photomicrograph of Nub at Saw Kerf. Bright field. 45X.

Fig. 1.12. Beta Structure in Nub at Saw Kerf. Bright field. 1000X.

Fig. 1.13. Photomicrograph of Region of Lowest Maximum Temperature in Specimen Examined. Bright field. 45X.

In Fig. 1.15 is shown a structure consisting of an undissolved intermetallic stringer existing in a prior beta matrix at a point near the center of the specimen where the temperature maximum was in the neighborhood of at least 1200 to 1300°C. That the time cycle of the temperature excursion was very short in this region (and over the entire specimen) was shown by laboratory experiments wherein the intermetallic stringers were found to dissolve in the beta matrix in less than 2 min at 1000°C.

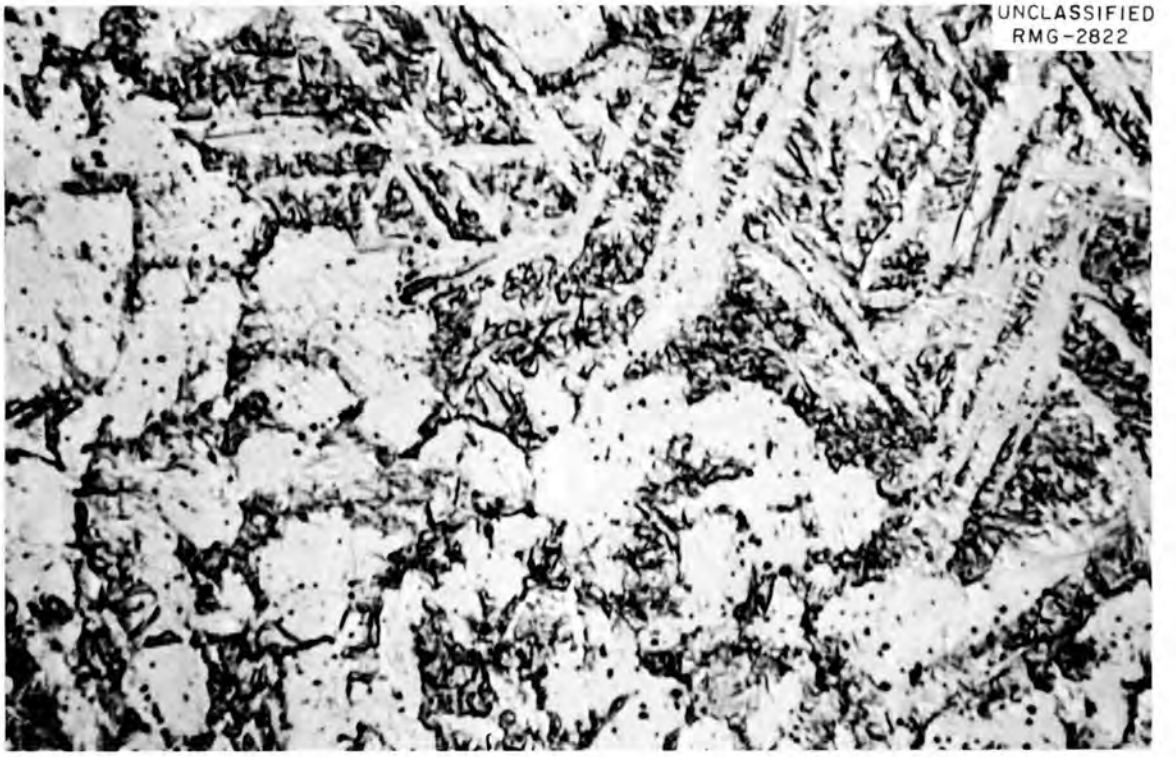

Fig. 1.14. Interface Between All-Beta and Alpha-Plus-Beta Structure. Bright field. 1000X.

Fig. 1.15. Photomicrograph of Undissolved Intermetallic Stringer. Bright field. 1000X.

1.6 MEASUREMENTS OF CORE-VESSEL THICKNESS*

New measurements of the HRT core-vessel thickness were made as part of the remote-maintenance operations following run 21. The remote manipulator, measuring equipment (ultrasonic), and techniques (immerscope) were the same as those used after run 20.[10] The only major change was an improvement in the data processing techniques. The sources of error in the measurements were the same as before and resulted in a total error somewhat less than 4%.

Measurements were made at about 30-deg intervals of longitude and 20-deg intervals of latitude. The relative longitudinal positions of these measurements and those after run 20 and the original measurements made at Newport News[11] are not known. Nevertheless, comparisons made at various latitudes are meaningful since there is little variation in thickness along any one latitude for any particular set of measurements. Figure 1.16 provides such a latitude-by-latitude comparison of thickness between the original measurements and those made after runs 20 and 21. Each point represents the average of 15 to 25 individual measurements.

The thickness of the core tank in the region from the top of the core to 110 deg (20 deg below the equator) has been reduced approximately 14 mils since the core was installed. Between this latitude and that of the top screen (135 deg) the reduction in thickness is greater and increases as the screens are approached. At the latitude 130 deg the thickness has been reduced by about 35

*Contribution by F. W. Cooke and R. W. McClung, Metallurgy Division.

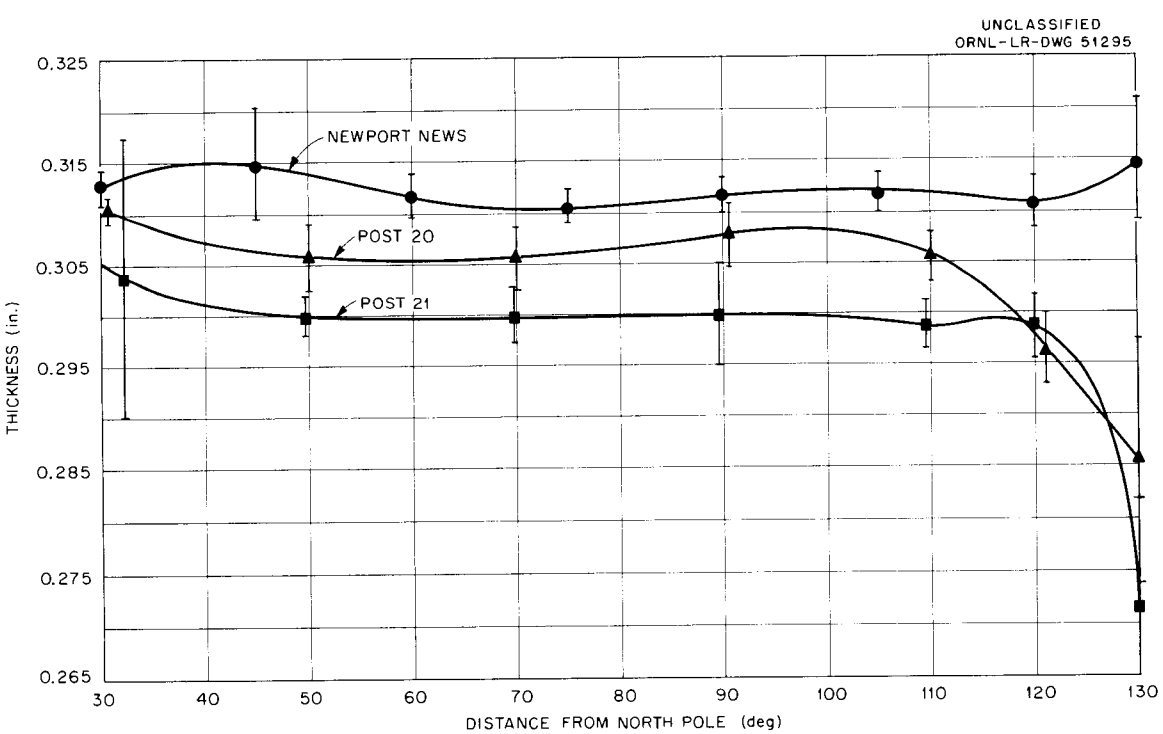

Fig. 1.16. Measurements of HRT Core-Vessel Thickness.

mils. The roughness of the inside of the vessel below 110 deg made measuring very difficult, and only seven interpretable measurements were made at 135 deg.

The thinnest spot measured was 0.250 in. at a point just above the top screen. It was not possible to make measurements at the bottom of pits or in very rough areas.

REFERENCES

1. On loan from the French Atomic Energy Commission.
2. I. Spiewak, F. N. Peebles, et al., HRP Quar. Prog. Rep. Apr. 30, 1960, ORNL-2947, p 3.
3. Ibid., p 9.
4. Ibid., p 8.
5. Ibid., p 8-9.
6. I. Spiewak et al., HRP Quar. Prog. Rep. Apr. 30, 1959, ORNL-2743, p 13-30.
7. I. Spiewak, F. N. Peebles, et al., HRP Prog. Rep. Apr. 30, 1960, ORNL-2947, p 6.
8. R. B. Korsmeyer, F. N. Peebles, et al., HRP Quar. Prog. Rep. Jan. 31, 1959, ORNL-2696, p 28.
9. S. E. Beall et al., HRP Quar. Prog. Rep. Jan. 31, 1960, ORNL-2920, p 3-8.
10. G. M. Adamson et al., HRP Prog. Rep. May 1 through Oct. 31, 1959, p 238.
11. D. E. Tackett, Fabrication History of HRT Core Tank, Appendix E, ORNL CF-58-12-6 (July 1, 1955).

2. HRT PROCESSING PLANT

W. D. Burch P. A. Haas

J. M. Chilton H. B. Whetsel O. O. Yarbro

Improvement in the solids-removal efficiency of the hydroclone system is being sought through use of a revised multiclone.[1] Fabrication and testing of the new unit was completed in preparation for installation prior to the next run. Other, more basic, studies of multiple-hydroclone units were started, with the objective of defining the parameters which affect the performance of such systems.

A study of a proposed fuel-cleanup process based on uranyl peroxide precipitation was started on a laboratory scale. The purpose of the process is to permit on-site removal of fuel contaminants, mainly nickel. Some fission-product decontamination would be achieved, but complete cleanup is not required, since the fuel would be returned to the reactor system.

2.1 MULTICLONE TESTS

2.1.1 Tests of Original Multiclone After Removal from Reactor

The original multiple-hydroclone unit, containing thirteen 0.6-in. hydroclones in parallel, which had been operated for a total of 4500 hr during reactor runs 20 and 21, was removed at the end of run 21. Pressure-drop and mixing-rate tests performed after removal[2] indicated that one to three hydroclone feed ports were partially plugged. An accumulation of solids at this location was also indicated by a radiation survey.

The pressure differentials between feed, overflow, and underflow were determined at flow rates from 3 to 12 gpm and underflow-to-feed ratios of 0, 10, and 15%. The feed-to-overflow and feed-to-underflow pressure drops were 40 and 50%, respectively, above the measurements made prior to installation of the unit in the reactor cell. The induced-underflow rate of the multiclone, determined by adding lithium hydroxide to the underflow pot and noting the decrease in lithium concentration in the overflow with time, was found to be 7 to 10% as compared with an expected 3 to 5% for the unit as-built.

The radiation level adjacent to the multiclone feed port, 90 days after the run 21 shutdown, was 6000 r/hr; the level near the bottom of the underflow pot was noted to be only 500 to 1000 r/hr, which is comparable to most of the reactor high-pressure system piping. By assuming (1) that activity of solids was due only to Zr-95 and Ru-103-106, (2) that fission and corrosion products remaining in the reactor are mixed uniformly, and (3) that the feed chamber was a homogeneous disk source, it was calculated that the 6000 r/hr reading corresponds to an accumulation of 100 g of solids in the feed chamber. The low radiation level indicated the underflow pot to be relatively free of solids other than the expected corrosion film.

2.1.2 Tests of the Replacement Multiclone and Performance of Multiple-Hydroclone Systems

Studies of the performance of multiple-hydroclone units on a single underflow receiver were undertaken, using both a modified Dorr-Oliver TM stage and the new multiclone fabricated for installation in the HRT reactor cell. The results show higher apparent induced-underflow rates and lower efficiencies for the multiclone units than for similar single hydroclones. This phenomenon is believed to indicate unequal flows through the parallel underflow ports. Flow rate vs pressure drop calibrations of the new HRT multiclone were also obtained.

The apparent induced-underflow rates for the HRT multiclone were 3.3 to 3.9% of the feed flow rate, as compared with expected values of 1.3 or 1.4% for single hydroclones of the same dimensions. These values along with experimental values for 3.14- and 2.65-in.-long bakelite hydroclones show apparent induced-underflow rates of multiclones 2.5 to 5 times the values for single hydroclones of the same dimensions.

Values for the feed flow vs feed-to-overflow pressure drop for the new HRT multiclone agree with the values previously obtained for prototype hydroclones of the same dimensions. At 100-ft pressure drop, a flow of 13.4 gpm was measured, compared to the calculated value of 12.4 gpm. The pressure drop vs flow values were not significantly affected by underflow rates up to 10% of the feed rate or by recirculation through the underflow receiver.

The efficiencies of the HRT multiclone were measured with ThO_2 in water at room temperature. They varied with underflow rate in a fashion similar to that previously observed for a TM multiclone (Table 2.1). The efficiencies for an underflow rate of 10% were essentially equal to those of single hydroclones with either continuous or induced underflow. As the underflow rates were decreased, the efficiencies decreased from 40 to 75% for underflow rates of 10%, to 10 to 30% for no underflow (Table 2.1).

Special precautions were taken to ensure that the individual hydroclones in the replacement multiclone were as nearly identical as possible. Underflow ports were machined to tolerances of ±0.0005-in. The reduction in efficiency was still observed, and further studies will be required to obtain a plausible explanation.

2.1.3 Multiclone Solids-Detector Probe

An experimental device for measuring the quantity of solids accumulated in the replacement multiclone underflow pot was built and will be tested in the next run. The principle of the detector is based on the difference in specific gamma activity of solids accumulated in the underflow receiver and reactor fuel. The probe (Fig. 2.1) consists of six 5/8-in. stainless steel disks, 1/4 in. thick, supported in the center of a 1-1/2-in. tube by a 20-mil stainless steel wire. Five-mil thermocouple wires, sheathed in 40-mil tubing, are attached to each disk and brought out through a water-tight terminal box to existing thermocouple connectors. The probe will be inserted into the well provided in the multiclone underflow pot and the tube filled with Santocel made opaque to radiant heat transfer by addition of aluminum powder to insulate the disks from the tube wall.

With the reactor operating at 5 Mw and the multiclone collecting solids at a rate of 1 to 2 g/hr, the gamma field at the center of a settled bed of

Table 2.1. Measurement of Multiclone Efficiencies

Hydroclones:
a. New HRT Multiclone of eighteen 0.40-in.-dia hydroclones, 2.40-in.-length, 0.104-in.-dia underflow port (fabricated from Dwg. D-34004).
b. Modified TM stage with thirty-two 0.40-in.-dia bakelite hydroclones, 3.14-in. length, 0.090-in.-dia underflow port.
c. Modified TM stage with thirty-two 0.40-in.-dia bakelite hydroclones, 2.64-in. length, 0.132-in.-dia underflow port.
d. Single hydroclone of 0.50-in.-dia, 3.00-in. length, 0.125-in.-dia underflow port (fabricated from Dwg. D-21435).

ThO_2 Slurries: Pilot-plant ThO_2 of 1200°C or higher calcination temperatures dispersed in 0.001 *M* $Na_4P_2O_7$.

Underflow Rate (vol % of feed rate)	$P_F - P_o$ (ft)	ThO_2 Mean Dia. (μ)	Calculated Efficiency (%)	Measured Efficiencies, E_o (%)
a. For new HRT multiclone				
10	63	1.6	65	75
5	63	1.6	65	54
2.4	63	1.6	65	35
0.7	63	1.6	65	12
0	63	1.6	65	30
0	63	1.6	65	22
10	28	1.6	55	41
5	28	1.6	55	19
0	28	1.6	55	23
5	63	1.1	45	22
2.4	63	1.1	45	~10
0	63	1.1	45	~10
b. For modified TM stage, 3.14-in.-length hydroclones				
10	63	1.6	65	60
4.7	63	1.6	65	55
0	63	1.6	65	16
13	63	1.3	55	46
7.3	63	1.3	55	40
3.6	63	1.3	55	36
0.9	63	1.3	55	20
0	63	1.3	55	10 to 15
c. For modified TM stage, 2.64-in.-length hydroclones				
4.7	63	1.6	65	15
4.4	63	1.6	65	16
0	63	1.6	65	5
d. For a single 0.50-in.-dia hydroclone				
50	70	1.3	50	82
50	70	1.6	60	89, 96
0	70	1.6	60	31, 56

UNCLASSIFIED
ORNL-LR-DWG 51296

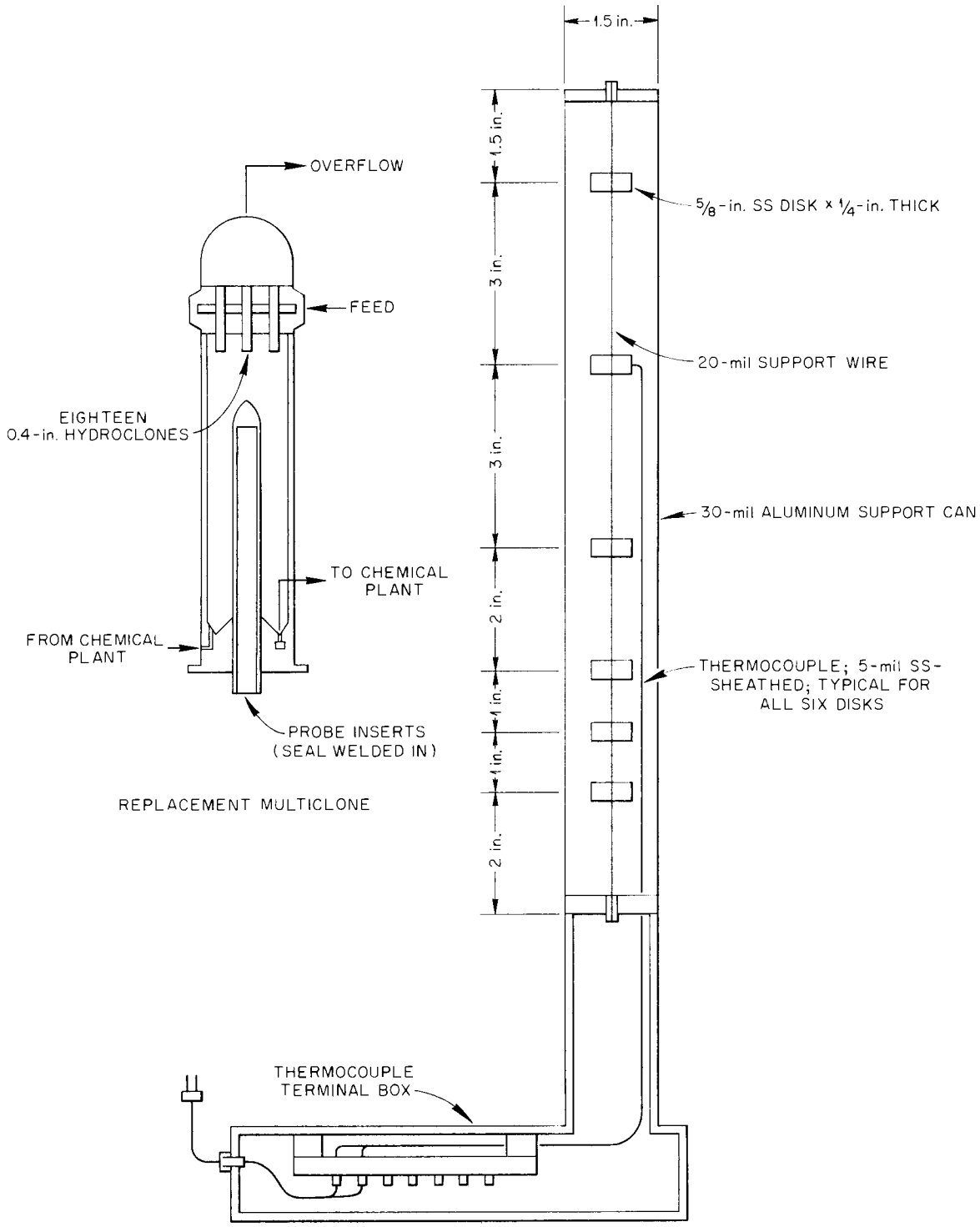

Fig. 2.1. Multiclone Solids-Detector Probe.

500 g of solids has been estimated to be approximately 2 x 10^6 r/hr. The gamma field at the center of the multiclone pot due to fuel solution only will be 20 to 30% of this value. Gamma heating, and therefore temperature, of the probe disks, will be a function of the gamma flux, making it possible to estimate the depth of the settled bed of solids. Bed densities will be determined from solids-removal data obtained from dissolver solution samples in initial runs. The calculations indicate that the probe will permit a reasonable estimate of the solids accumulation on the underflow pot, provided that the solids settle to bed densities exceeding 300 to 500 g/liter.

The probe was tested in a 2.5 x 10^6 r/hr field in a Co-60 storage vault. Temperature differences between the outside can and probe disks ranged from 7 to 13°C due to gamma heating of the disks. Damage to the support can during assembly, which reduced the insulating thickness around some of the disks, accounts for most of the spread in disk temperatures. Heat losses from the disks were two to three times the values expected. The support can will be repaired and an attempt made to reduce the heat losses prior to installation of the probe in the multiclone unit.

2.2 PROPOSED FUEL PROCESSING BY PEROXIDE PRECIPITATION

Purging of soluble fission and corrosion products by removal of 10 liters of fuel solution with accumulated solids at the end of each run would maintain acceptable soluble-containment levels in the reactor fuel if the hydroclone system were operated on a weekly cycle as originally designed. Since it has proved more convenient to operate the solids-removal system on a two- to three-week cycle, the entire fuel batch must be processed infrequently to remove the accumulated soluble contaminants, mainly corrosion-product nickel. The first fuel batch was removed following run 13, in which very high stainless steel corrosion rates were noted, and processed by solvent extraction. The second batch, in use since March 1958, has now accumulated nickel to the point where processing may be required. Since the solvent-extraction plants are inoperative at this time, alternatives, such as on-site storage or processing by other methods, have been investigated. One such attractive alternative is a process based on precipitation of uranyl peroxide, UO_4, separation of the filtrate containing the contaminants, and regeneration of the fuel by destroying the peroxide and by addition of acid and copper in the required amounts. The process as envisioned could be installed in the present processing cell and operated in a D_2O system. Use of existing storage tanks and sampling facilities would greatly simplify the installation.

2.2.1 Laboratory Studies

Laboratory investigations were undertaken to study the variables affecting the process and to determine the most practical way to carry out the operation. The requirements that the process should meet are as follows:

1. uranium recovery, greater than 90%;

2. decontamination from soluble impurities, greater than a factor of 10;

3. filtration rate, greater than 20 liters/hr-ft^2.

The 90% uranium recovery is acceptable because the "loss" may be transferred to the decay storage tanks for recovery at a later date. The filtration-

rate requirement is not rigid, but a process which is capable of handling an 8-kg batch of uranium in one or two days' operating time is desirable; the filtration step appears to be the most time-consuming operation.

A synthetic solution, containing the uranium, copper, nickel, acid, manganese, iron, and rare earths in the same ratio as in the present fuel batch, at a uranium concentration of 150 g/liter, was used for most of the studies. Scouting tests revealed no advantages in the use of more dilute solutions, and the entire 8 kg may be processed in one batch in a 6-in.-dia critically safe vessel at the 150-g/liter concentration. Precipitations were made in a 1-1/2-in.-dia glass column, with a glass "M" frit in the bottom for vacuum filtration.

A literature study revealed that pH and temperature are the two most important variables affecting UO_4 precipitates. In general, yields are higher when the pH is high (>2) and the temperature is low. As UO_4 is precipitated from the fuel, additional acid is released, giving a final acidity of 0.95 *M* and a pH of approximately 0.0. The effect of partial neutralization on uranium recovery was investigated by using Na_2O_2 solutions containing various amounts of sulfuric acid as the precipitation reagent. The following results were obtained:

Precipitant	% U Loss
H_2O_2	3.1
Na_2O_2 in 0.025 *M* H_2SO_4	20
Na_2O_2 in 0.2 *M* H_2SO_4	19

Since acceptable yields were obtained with H_2O_2 only (the lower yields with partial neutralization are not understood, but pH levels were still below 2) and the addition of sodium would result in much more stringent precipitate washing requirements, subsequent work was restricted to precipitations with H_2O_2 only.

The effect of the order of reagent addition on filtration rates was checked, using three different precipitation reagents. As the following results show, the addition of the peroxide to the uranium gave better filtration rates than the addition of uranium to the peroxide:

Reagent	Filtration Rate, in./hr*	
	Peroxide Added to Uranium	Uranium Added to Peroxide
3% H_2O_2	5-1/4	1-1/2
6% Na_2O_2	2-5/8	3-1/4
1-1/2% H_2O_2 - 3% Na_2O_2	2-1/8	1-5/8

*1 in./hr = 2.5 liters/hr-ft^2.

The effect of excess peroxide on uranium recovery and decontamination from nickel was investigated for a uranium solution of 150 g/liter, with the following results:

Mole Ratio H_2O_2:U	% U Loss	% Ni in Precipitate
2:1	6.9	13.7
2-1/2:1	5.1	10.4
3:1	2.4	9.5
4:1	2.2	0.6*

*After one wash of precipitate.

The stability of peroxide in this specific fuel solution was determined as a function of temperature by measurement of the rate of oxygen evolution. In previous work,[3,4] decomposition was found to be catalyzed by iron and further promoted if copper is present. The catalytic effect of iron was linear with iron concentration up to 65 ppm. Typical iron concentrations in periods when all the fuel was collected in the low-pressure system were in the range of 200 to 400 ppm (at U concentrations of 150 g/liter). The decomposition was measured at concentrations of 200 and 1100 ppm over the temperature range of 25 to 50°C. The results, plotted in Fig. 2.2, confirm the catalytic effect of iron

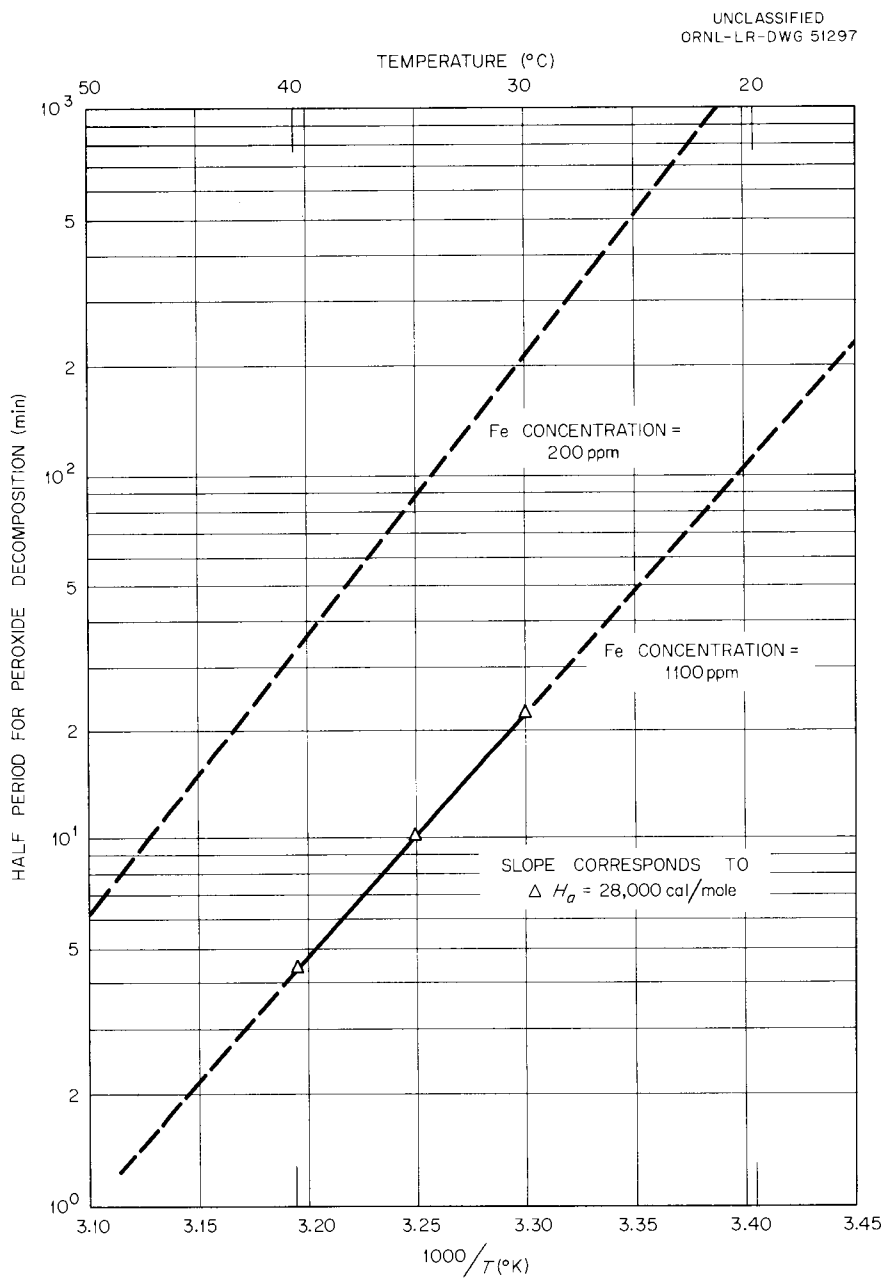

Fig. 2.2. Peroxide Decomposition vs Temperature for Two Iron Concentrations.

at these concentrations and show approximately the same temperature dependence. At the expected iron concentration of 300 ppm, the precipitation and filtration must be carried out below 25 °C to give acceptable peroxide decomposition rates.

2.3 SHIELD-WATER DECONTAMINATION

Water from the reactor containment tank, containing 70 curies of activity, predominantly strontium-89, was drained to the waste pond on May 16, 1960. After only 90% of the activity was scavenged by the normal calcium phosphate precipitation treatment and after additional treatments proved ineffective, 250 lb of diatomaceous earth, in two different batches, was spread on the pond surface and allowed to settle. This, in conjunction with further phosphate treatment, gave an additional decontamination factor of 20, leaving residual activity of 0.3 curie in the pond water, which was drained.

In the six-week period following the draining, strontium activity in the Melton Branch, to which the pond drains, slowly rose until slightly more activity was accounted for than was known to have been drained. It appears that some leakage into the ground water system occurred while activity levels in the pond were high and that the activity is slowly seeping into Melton Branch. Strontium-90 discharged in this six-week period was estimated at 60 millicuries, based on measured total strontium activity, estimates of water flow, and calculated Sr-89/Sr-90 ratios.

REFERENCES

1. W. D. Burch et al., HRP Quar. Prog. Rep. Apr. 30, 1960, ORNL-2947, p 15.

2. O. O. Yarbro, Test of HRT-CP Multiclone No. 1 Following Removal from Reactor Cell, (To be issued as CF memo 60-6-105).

3. M. J. Kelly et al., HRP Quar. Prog. Rep. Apr. 30, 1960, ORNL-2947, p 47-54.

4. H. F. McDuffie et al., HRP Quar. Prog. Rep. Apr. 30 and July 31, 1958, ORNL-2561, p 313-316.

3. HRT COMPONENT TESTING AND DEVELOPMENT

I. Spiewak F. N. Peebles

C. H. Gabbard C. G. Lawson J. C. Moyers
P. H. Harley M. Richardson

3.1 TEST OF THE HRT REPLACEMENT FUEL-CIRCULATION PUMP

The suction and discharge piping on a 450-gpm canned-motor fuel-circulation pump was modified for the purpose of reversing the flow direction in the HRT. After assembly and installation in a test loop, the pump was pretreated with trisodium phosphate and dilute nitric acid rinses at 85°C and then operated for 110 hr in oxygenated water at 250°C.

Complete hydraulic data were obtained over the operating range of the pump while it was circulating cold water at low pressure. The pump was then transferred to the HRT for future operations of the reactor.

3.2 HRT RECOMBINER TEST

The design of the primary and secondary recombiners has been modified[1] to permit adequate heating, more convenient reactivation, and simpler installation in the reactor system. Recombiners with the new design features were fabricated for use in the HRT.

Prior to installation in the reactor the new recombiners were tested with cylinder gas. The results showed the recombination efficiency of these units to be satisfactory. The primary recombiner had an efficiency,

$$100\left(1 - \frac{H_2 \text{ out}}{H_2 \text{ in}}\right),$$

of 99.6% at a hydrogen flow rate of 80 liters/min; the secondary recombiner had an efficiency of more than 98% using 26 liters of O_2 per minute and 1 liter of H_2 per minute.

3.3 HRT FEED-PUMP TEST

Two HRT feed-pump assemblies (No. 24 and No. 25), which had been decontaminated and reclaimed after reactor use, were tested to ensure proper pump operation and constancy of feed rate over an extended period. A final check on operation of these pumps will be made at the HRT.

During the test, simulated fuel solution containing 9 g of UO_2SO_4 per liter was pumped for 2810 hr with a discharge pressure of 1500 psi. For the final 2472 hr of the test, the heads operated at 1.62 gpm without phase adjustment and with no loss in flow rate.

3.4 TEMPERATURE DISTRIBUTION FOR REVERSE FLOW IN THE HRT

An experimental technique was developed for measuring the local fluid age at a point within a reactor core model. The temperature distribution throughout the volume of the HRT reversed-flow core can be inferred from such measurements.

The fluid-age measurement involves the determination of the local concentration of a tracer salt (by conductivity probes) as a function of time after a step function change in the salt concentration in the inlet fluid. The mean age of fluid within the vessel for the position of measurement can then be calculated from the relationship,

$$\tau_m = \frac{\int_0^\infty t \frac{\partial F}{\partial t}\, dt}{\int_0^\infty \frac{\partial F}{\partial t}\, dt},$$

where τ_m = age of fluid within vessel for fluid located at position of measurement,

$C(t)$ = concentration of salt at any time, t, for fluid located at position of measurement,

$C(\infty)$ = concentration of salt as $t \rightarrow \infty$ for fluid located at position of measurement = concentration of salt at inlet for $t > 0$.

$$F = \frac{C(\infty) - C(t)}{C(\infty)},$$

t = time in seconds measured from instant step change was seen at the vessel inlet.

From such measurements for many places within the vessel, the spatial distribution of the fluid age can be obtained.

The temperature in the HRT with reversed flow is essentially directly proportional to the fluid age because of the flat power-density distribution (over 90% of the volume is within 20% of the mean thermal flux) and because of the large amount of mixing that occurs within the vessel. The proportionality constant is the mean power density divided by the volumetric heat capacity of the fluid. Hence,

$$T = \frac{P.D.}{\rho C}\, \tau_m,$$

where T = fluid temperature at location where mean fluid age is τ_m,

P.D. = mean power density,

ρC = volumetric heat capacity of the fluid.

The spatial distribution of fluid age was measured using the HRT core mockup with reversed flow and an inlet flow rate of 425 gpm. The estimated temperature distribution calculated from the fluid-age measurements is shown in Fig. 3.1. For comparison, the temperature distribution obtained from qualitative observations of dye behavior[2], and from free-jet theory to obtain the circulation ratio within the vessel, is shown in Fig. 3.2. Neither method takes into account the effect of changing physical properties upon the flow distribution or heat-source distribution.

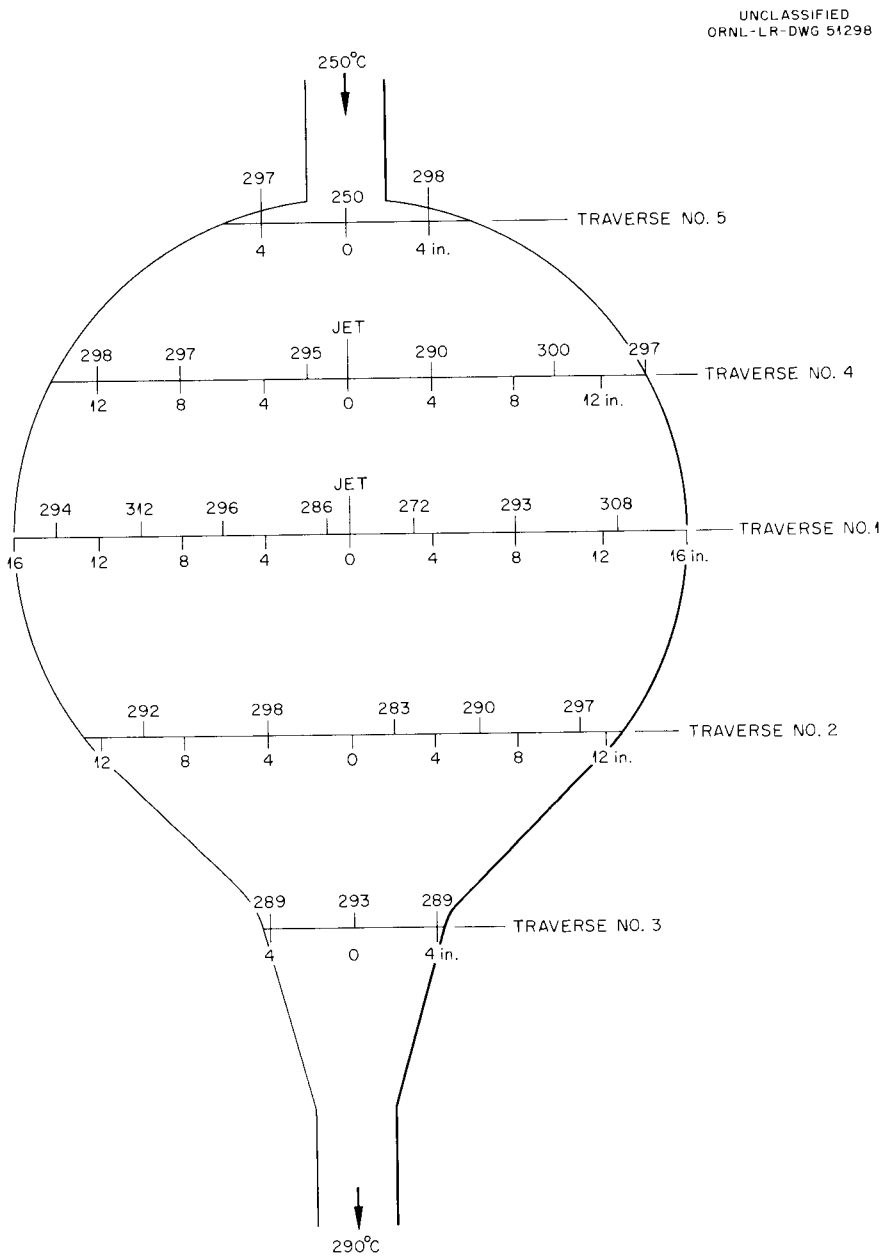

Fig. 3.1. Estimated Temperature Distribution in HRE-2 Reverse Flow at 5 MwT with 250°C Core Inlet.

UNCLASSIFIED
ORNL-LR-DWG 48839

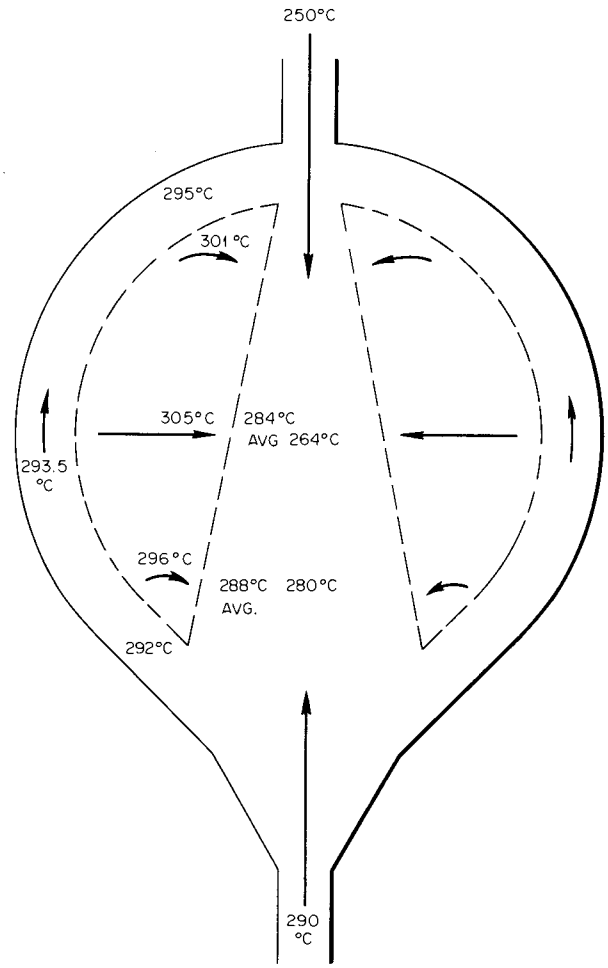

Fig. 3.2. Steady-State Temperature Distribution for Revised HRT at 5-Mw Core Power.

The two temperature distributions are in excellent agreement, except for the following points:

1. The maximum fluid temperature in the bulk volume is about 60°C above the inlet temperature rather than 55°C above the inlet.

2. The maximum ambient fluid temperature near the wall is about 58°C above inlet temperature rather than 45°C and is located in the upper hemisphere. This is due to an asymmetry in the flow pattern.

3. The temperature distribution at the intersection between the 30° and 90° cones is within 4°C of the outlet temperature. The temperature distribution at this elevation is flatter than predicted by free-jet theory.

If the blanket and core inlet temperatures are kept at 250°C, then the maximum wall temperature is calculated to be 301°C. If the core inlet is at 250°C and the blanket inlet is at 200°C, then the maximum core wall temperature should be 294°C.

REFERENCES

1. W. R. Gall et al., HRP Prog. Rep. Oct. 31, 1959, ORNL-2879, p 35-38.

2. I. Spiewak, F. N. Peebles, et al., HRP Quar. Prog. Rep. Apr. 30, 1960, ORNL-2947, p 19-20.

4. HRT REACTOR ANALYSIS

P. R. Kasten

L. L. Bennett S. Jaye

4.1 PRESSURE RISE FOLLOWING A COLD-WATER ACCIDENT WITH REVERSED FLUID FLOW

Modifications[1] to reverse the direction of flow through the HRT core are presently being made. With reversed flow the HRT will have a flow distribution described ideally as a free jet passing through a sphere along the polar axis from north to south.[2] Core fluid is entrained into and mixes with the jet during its passage. In order to satisfy continuity in the jet, fluid is shed from the jet at the bottom of the sphere and flows back up along the walls of the vessel. This flow pattern causes the incoming fluid to pass more rapidly into the important central region of the reactor than does fluid under upward-slug-flow conditions. Therefore, with reverse flow, a cold-water accident would add reactivity at a higher initial rate than with upward flow. It would be expected that this greater rate of reactivity addition would cause a more rapid rise in reactor power and a larger increase in core pressure.

In order to estimate the maximum pressure rise in the core, it was first necessary to calculate the rate of reactivity addition associated with cold fluid entering the core. This calculation was made by using a two-group, two-dimensional reactor code, Equipoise.[3] The HRT was approximated in cylindrical geometry. A series of calculations was made with various fuel concentrations and a uniform temperature of 260°C, to establish the critical concentration. It was then considered that fuel solution of this critical concentration was cooled to 100°C and introduced into the core at 150 gpm (one-third the normal flow rate). With upward flow it was assumed that the cold fluid rose through the core without mixing and with no nuclear heating of the fluid. In reversed flow the cold fluid passed down through the core in the central jet. Hot fluid was entrained in the jet[2] and increased the average temperature of fluid in the jet by about 30°C per foot traveled. Again it was considered that no nuclear heating took place.

Time increments were chosen such that individual regions of the core were successively filled with the cold fluid and the corresponding values of k_e were calculated. Time zero was taken with cold fluid entering the top of the core region in reversed flow and entering the bottom of the core region in upward flow. The curve of k_e versus time was approximated by a series of ramp additions of reactivity in a kinetics code, PET-I.[4] This code was modified to include a calculation of the core pressure rise as a function of time, on the basis that the pressure rise was that required for free expansion of the fluid.[5]

The results[6] of the reactor power and pressure rise calculations are summarized in Table 4.1. Some calculations were made with only the core pressurizer available for fluid expansion (V_p = 2.5 ft^3) while others considered the core and blanket pressurizers to be connected (V_p = 5 ft^3). Each condition was calculated with two different values for the temperature coefficient of reactivity in order to determine if this had a significant influence on the core pressure rise. As

shown in the table, the change in temperature coefficient had a negligible effect. Thus, although the reactivity compensation for a given temperature rise was less with a less-negative coefficient, there was less reactivity present, and these effects balanced each other.

With the core and blanket pressurizers directly connected, the maximum calculated pressure rise with reversed flow was about 380 psi. This is only slightly below the value calculated for upward flow and only one pressurizer available.

Table 4.1. Results of HRT Pressure-Rise Calculations

Flow Direction	Temperature Coefficient, $\Delta k_e/°C$	Effective Volume* of Pressurizers, V_p (ft^3)	Maximum Pressure Rise During Power Surge (psi)
Up	-1.85×10^{-3}	2.5	400
Up	-1.70×10^{-3}	2.5	400
Up	-1.70×10^{-3}	5.0	210
Up	-1.85×10^{-3}	5.0	210
Reverse	-1.85×10^{-3}	2.5	545
Reverse	-1.70×10^{-3}	2.5	545
Reverse	-1.70×10^{-3}	5.0	380
Reverse	-1.85×10^{-3}	5.0	375

*The effective volume of one pressurizer (either core or blanket) is 2.5 ft^3.

4.2 CRITICALITY CONDITIONS IN THE HRT FUEL-TRANSFER VESSEL

One hundred liters of irradiated fuel solution are to be transferred from the HRT area in a large shielded vessel. The solution contains 8 kg of enriched uranium (83.4% U^{235}) in an aqueous solution (25% D_2O - 75% H_2O); 250 g of gadolinium will be present for neutron poisoning. The vessel is a right-circular cylinder with dished heads, an inside diameter of 19-1/4 in., and a height of 30-1/2 in. This cavity is completely surrounded by a 3/8-in. stainless steel liner, 9-1/8 in. of lead shielding, and a 3/8-in. stainless steel skin. The quantity of solution is sufficient to fill the vessel to a height of 21 in.[7]

A uniform dispersion of 8 kg of enriched uranium and 250 g of gadolinium in 100 liters of water has an infinite multiplication constant of 0.59. However, if the uranium settles uniformly while the gadolinium remains dispersed, the infinite multiplication constant will exceed unity when the uranium concentration is approximately 180 g/liter. On the other hand, since the neutron leakage increases as the uranium settles, the effective multiplication constant will exhibit a maximum value.

To determine whether the solution will achieve criticality as the uranium settles, two-group, two-dimensional calculations were performed[8] with the

Equipoise[3] program on the IBM-704 computer. Effective fast-group constants for the fuel-bearing region and the water reflector above it were determined with the GNU[9] 34-group program.

The effective multiplication constant as a function of the height of fuel-bearing region is shown in Fig. 4.1. As the concentration of uranium increases and approaches 400 g/liter, the effective multiplication constant increases to a maximum value of 0.86. When the uranium settles further, the increased leakage causes the multiplication constant to decrease.

The effect of increasing the D_2O concentration is also shown in Fig. 4.1. Again the maximum multiplication constant occurred at a concentration of approximately 400 g/liter; as shown, an increase in D_2O concentration was accompanied by a decrease in the effective multiplication constant.

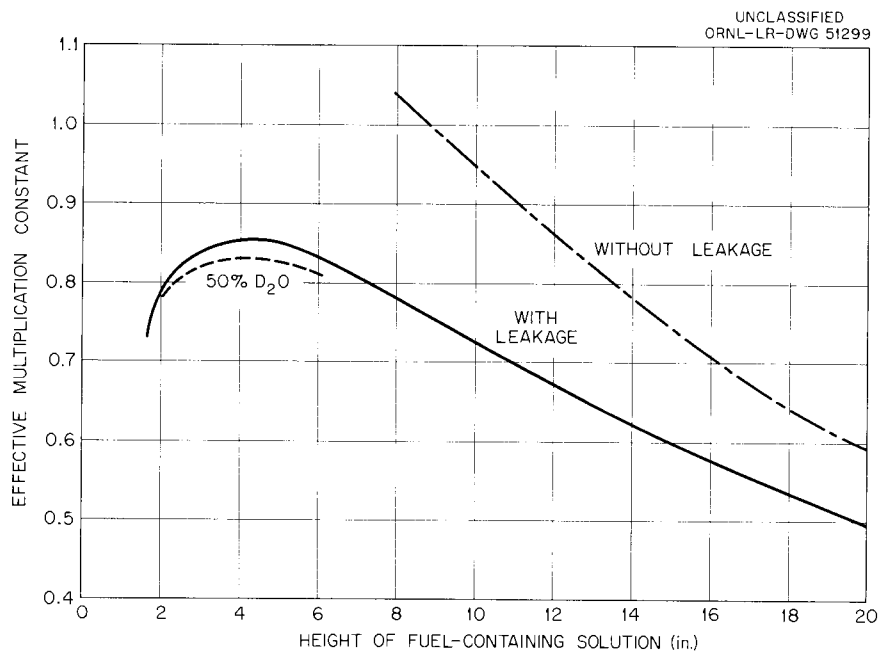

Fig. 4.1. Effect of Uranium Settling on Multiplication Constant.

If the uranium settles, it would not do so in a uniform manner. The concentration would probably be greater near the bottom and decrease with height. Since this configuration places more fuel closer to the vessel boundaries, the leakage would be increased and the effective multiplication constant would be decreased. To show that this was indeed the case, calculations were performed with the uranium distributed in a nonuniform manner. The upper 87-1/2% of the solution volume contained 34 g/liter, while the lower 12-1/2% contained 400 g/liter. The effective multiplication constant under these conditions was 0.73, which is well below the multiplication constant associated with all fuel contained in the 400-g/liter region.

REFERENCES

1. C. G. Lawson, Proposed Revisions to the HRT Core, ORNL CF-60-1-20 (Jan. 12, 1960).

2. C. G. Lawson, Fuel Transport Lag Time and Temperature Distribution for Reversed Flow HRE-2, HRP-60-41 (Apr. 4, 1960).

3. M. L. Tobias and T. B. Fowler, Equipoise, an IBM-704 Code for the Solution of Two-Group, Two-Dimensional Neutron Diffusion Equations in Cylindrical Geometry, ORNL-2967 (in press).

4. S. Jaye and M. P. Lietzke, Power Response Following Reactivity Additions to the HRT, ORNL CF-58-12-106 (Dec. 30, 1958).

5. P. R. Kasten, Homogeneous Reactor Safety, ORNL CF-55-5-51 (May 9, 1955).

6. L. L. Bennett and S. Jaye, Pressure Rise in the Reversed-Flow HRT Following a Cold Fluid Accident During Startup, ORNL CF-60-7-61 (July 1960).

7. Personal communication from W. D. Burch and P. N. Haubenreich of ORNL, June 1960.

8. S. Jaye and L. L. Bennett, Criticality in the HRT Transfer Vessel, ORNL CF-60-7-81 (July 26, 1960).

9. C. L. Davis, J. M. Bookston, B. E. Smith, GNU - A Multigroup One-Dimension - Diffusion Program, GMR-101 (Nov. 12, 1957).

PART II. ENGINEERING DEVELOPMENT

5. DEVELOPMENT OF REACTOR COMPONENTS AND SYSTEMS

I. Spiewak F. N. Peebles

D. M. Eissenberg C. G. Lawson H. R. Payne
C. H. Gabbard J. C. Moyers M. Richardson
P. H. Harley L. F. Parsly A. N. Smith
R. J. Kedl R. P. Wichner

5.1 DEVELOPMENT OF CYLINDRICAL RE-ENTRANT CORE VESSEL

Detailed velocity-distribution measurements were obtained previously[1] in a vertical cylindrical test core vessel, 2 ft in diameter and 6 ft long, which is a full-scale model of a 40-Mw reactor (half linear scale for a 400-Mw reactor). These results showed that with a vaned annular entry at the top of the vessel and with the main outlet at the top of the vessel about 50% of the inlet fluid short-circuited the major fraction of the core volume.

During the report period, attempts were made to decrease the fraction of inlet fluid which short-circuits the core: the inlet velocity was increased, the inclination of the inlet swirl-vanes was altered, and outlet-pipe baffles were used. The attempts were not successful. A flow rate of approximately 200 gpm per thermal megawatt would be required within this type core to operate an aqueous homogeneous reactor with a 250°C inlet, without exceeding temperature limitations set by corrosion rates and fuel stability.

Other flow concepts requiring a lower throughput per megawatt than the vaned-inlet, re-entrant cylindrical core are being investigated. These include:

1. straight-through cylindrical cores containing either nested-conical diffuser vanes or vortex generators followed by a conical diffuser, to distribute the inlet fluid;

2. re-entrant cylindrical cores with a scroll-case vortex generator located at the entrance of the vessel;

3. re-entrant cylindrical cores with a distributed inlet running the length of the core with the fluid introduced tangentially into the core.

5.2 THORIA BREEDER REACTORS WITH PELLET BLANKETS

The essential features of a proposed breeder reactor with a thoria pellet blanket were described previously.[2] In order to define more clearly the mechanical details of this type reactor, a general arrangement layout was made for a 400-MwT reactor vessel (Fig. 5.1). The reactor vessel contains a 4-ft-dia

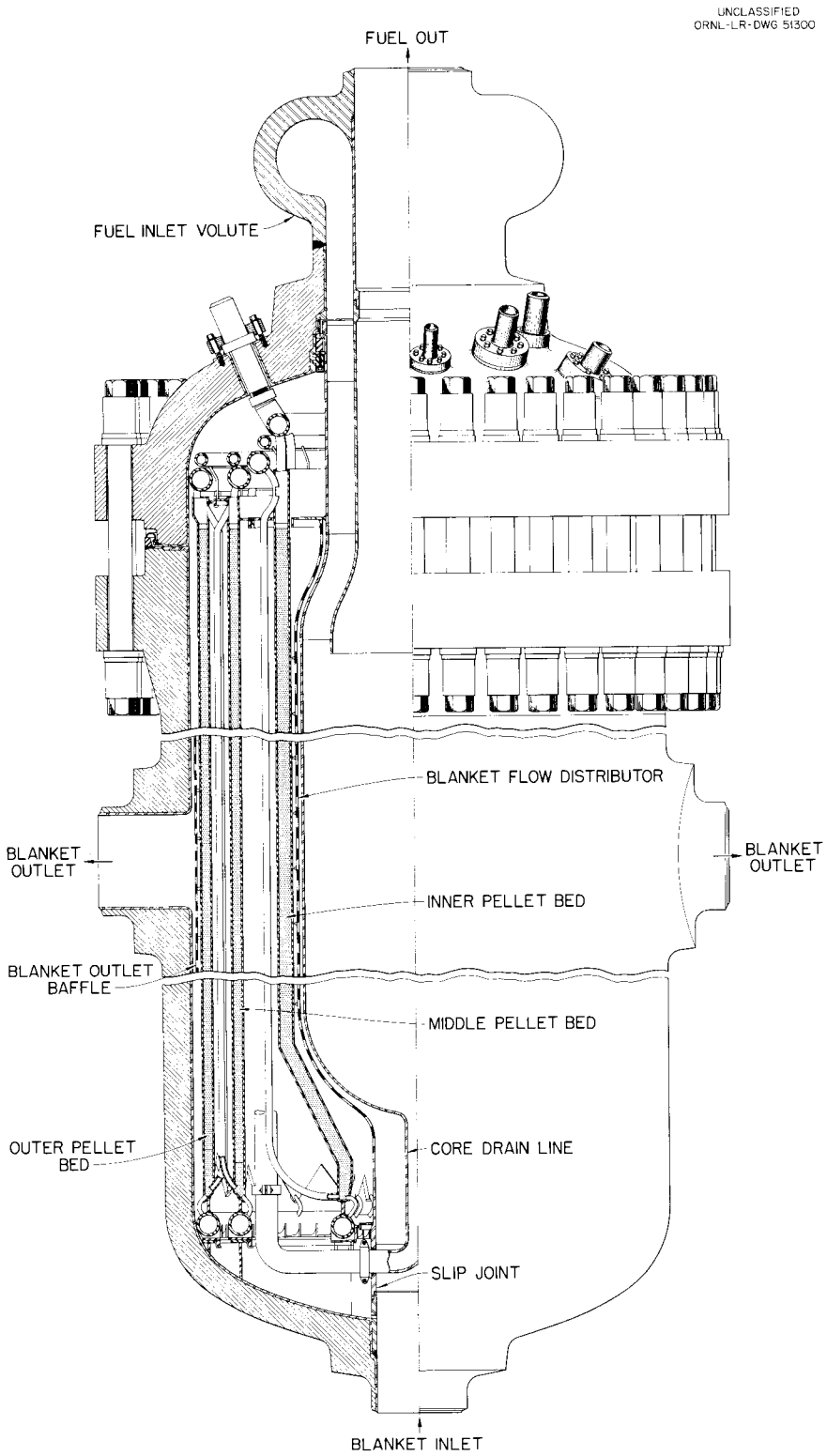

Fig. 5.1. 400-MwT Pebble-Blanket Reactor-Vessel Arrangement.

12-ft-long cylindrical core, with concentric annular beds of thoria pellets in the blanket region. Means for rearranging, removing, and recharging pellets in the innermost bed are provided. Pellets in the two outer beds can be removed from the blanket and recharged, but not recirculated within the beds or from one bed to another. A PWR-type seal-welded closure is provided in the pressure vessel to permit removal and replacement of the core tank or pebble baskets.

5.2.1 Pellet-Blanket Test Model

The design of a low-temperature pellet-blanket test model was essentially completed. The model, which simulates a sector of an annular pellet bed, is a flat section containing three vertical pellet channels. This equipment will be used to develop techniques for transporting pellets and for controlling the cross-flow distribution through the pellet beds. Development of these techniques will proceed on a low-priority basis.

5.3 CIRCULATION-PUMP DEVELOPMENT

5.3.1 200Z Pump and Loop

The 200Z canned-motor pump, which has a motor similar to that used in the HRT circulation pumps but which contains parts more suitable for use in circulating thoria slurries, continued to operate in high-temperature water in a test of its alumina radial bearings. The pump has operated satisfactorily for 4200 hr.

5.3.2 Stator Irradiation Test

A report was prepared[3] which describes the effects of irradiation of a test stator in a Co^{60} source for an accumulated dosage of about 5.4×10^9 rads.

5.4 FEED PUMPS

5.4.1 Oxygen Compressor

The three-stage diaphragm compressor, designed to recycle radioactive oxygen, was not operated in the report period. Further tests are planned for FY-1961 to determine the cause of the failure of third-stage diaphragms, reported previously.[4]

5.4.2 Increased-Capacity Solution Feed Pumps

Endurance testing of the 10-3/4-in. double-diaphragm head and the 12-in. single-diaphragm head was terminated after they had operated satisfactorily for 16,690 and 12,070 hr, respectively. No further testing of these heads is planned.

5.5 THE 300-SM SLURRY SYSTEM

A series of runs to demonstrate reliable handling of thoria slurry in a system approaching a reactor in complexity was successfully completed in the 300-SM slurry system. A full-flow shell-and-tube exchanger installed in the high-pressure loop performed well; aluminum-oxide-trimmed ball valves in the feed lines showed that such valves are capable of shutting-off flowing slurry

repeatedly; the available slurry feed and letdown equipment permitted regulation of the slurry concentration in the high-pressure system from less than 0.1 to 1000 g of Th per liter; and a modified pressurizer inlet reduced the tendency for slurry accumulation in the pressurizer during normal operation. During the final run, completed on June 10, the system was operated for 1962 hr at 1500 psi and temperatures up to 300°C. The run time represented approximately 83% of the total elapsed time during the test period.

To demonstrate a system for handling slurry, the high-pressure loop was concentrated three times, starting with less than 0.1 g of Th per liter, to 950, 955, and 1017 g/liter and was then diluted to the original low concentration. The concentrations were effected by pumping slurry having densities of 2.0 to 2.4 g/cc from the low- to the high-pressure system, and letting down dilute slurry. Approximately 12 hr were required to concentrate the system to 900 g/liter. In order to attain concentrations in the high-pressure loop greater than 900 g/liter, it was necessary to drain supernatant water from the pressurizer while slurry was being added to the loop.

Throughout the run, the low-pressure system gave good performance. The feed pump was connected directly to the dump tank by means of a 10-ft suction line and cooler, and was located about 4 ft above the bottom of the tank. Slurry having a density up to 2.4 g/cc could be pumped satisfactorily when the dump-tank pressure was 35 to 40 psia. In some instances, loss of pump suction was observed to occur when the dump-tank pressure was reduced to below 25 psia or when the slurry volume in the dump tank was less than 50 to 70 liters. After such stoppages in suction flow, flushing the suction line with water and increasing the dump-tank pressure or the slurry volume in the dump tank opened the feed-pump suction line.

The aluminum-oxide-trimmed ball valves were closed against flowing slurry approximately 40 times during the final period of 300-SM operation. Inspection of the valves after the run revealed the valve seats to be in generally good condition and some detectable out-of-roundness of the balls. The slurry leakage rate through two ball valves in series changed from 2 cc/min at the start of the run to about 7 cc/min at the end of the run. The corresponding water leakage rates at the beginning and end of the run were about 10 and 20 cc/min, respectively.

The modified pressurizer inlet[5] installed prior to the run eliminated slurry accumulation in the pressurizer during normal operation of the high-pressure loop. Slurry was transferred into the pressurizer during feed operation at high concentrations when supernatant water was being drained from the pressurizer, and also when the feed pump was being used to increase the pressurizer level. None of these instances of slurry entry into the pressurizer resulted in immobile slurry plugs. The mixing rate between the pressurizer liquid and the loop circulating stream with the modified pressurizer was approximately 30% lower than with the standard reducing-tee inlet on the pressurizer. These relative mixing rates were indicated by the pressurizer heat load.

Flow characteristics of the horizontal 18-tube full-flow heat exchanger were good during the 300-SM test. There were no indications of plug formation or scale buildup in the tubes. Examination of the exchanger after the run showed no observable attack on the tubes or tube sheets.

Slurry-film heat transfer coefficients were determined from measurements of the over-all coefficients with slurry and with water for the same shell-side

conditions. Data obtained at 8.1 and 21.6 fps in the tubes at temperatures over the range 200 to 300°C are shown in Fig. 5.2 as a j-factor versus Reynolds number plot. The laminar-flow and transition-flow regimes, shown for the two slurries tested, were located according to the recommendations of Thomas and Hayes.[6] In spite of the wide scatter of experimental points, the data are not inconsistent with the turbulent-flow heat transfer correlation recommended in reference 6. Two factors contributed to the poor precision of the experimental slurry-film heat transfer coefficients: in the high-pressure heat transfer system the temperature difference across the slurry film was a minor fraction of the total temperature difference between hot slurry in the tubes and boiling water in the shell; there was a possible variation in effective heat transfer area due to nonuniform vapor removal rate from the shell side of the exchanger.

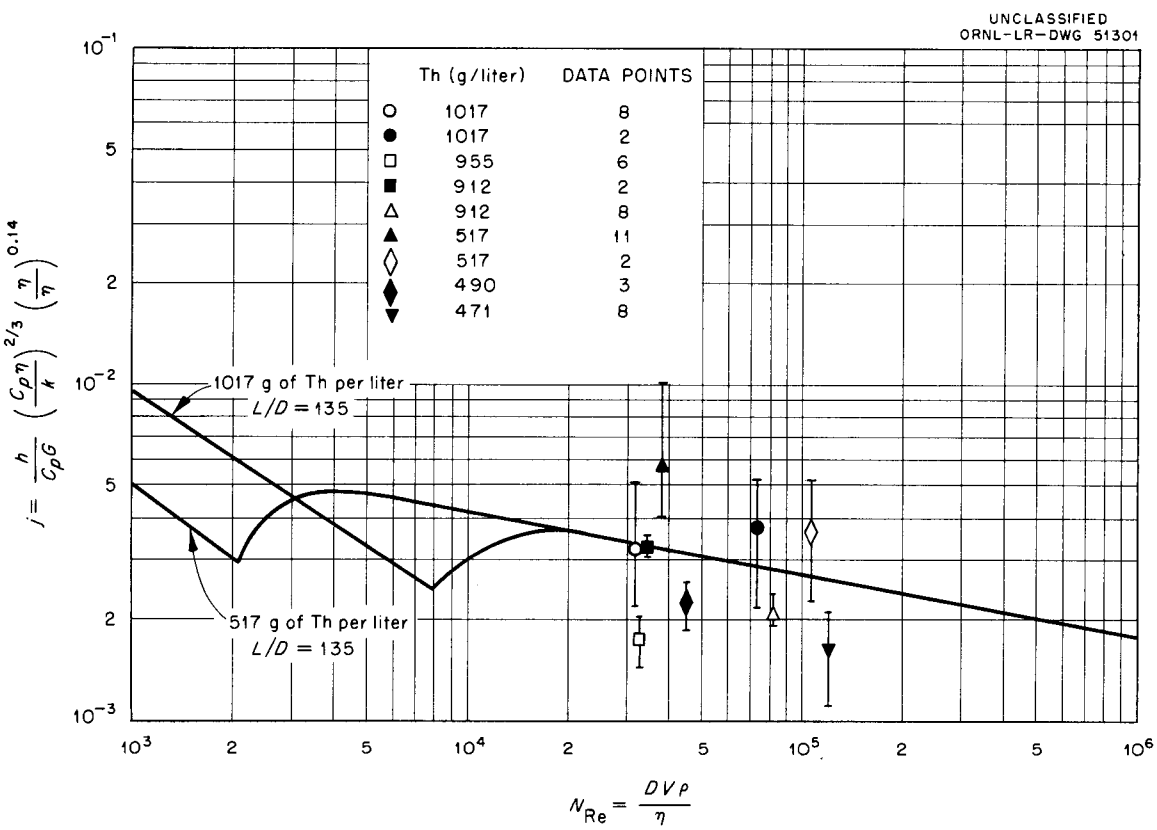

Fig. 5.2. Slurry-Film Heat Transfer Correlation, 300-SM Run 10.

Two equipment failures caused shutdown of the high-pressure system during the run. One was the failure of letdown valves reported previously,[7] and the other was caused by plugging of the letdown line. The ceramic-trimmed ball valves have since proved to be more reliable for this service and probably are suitable for slurry-reactor applications. Operation of the 300-SM system has also shown that flocculated-slurry plug formation in stagnant lines, such as that which occurred in the letdown line, can be eliminated by effective flushing following periods of slurry flow. The run was terminated by the failure of the lower radial bearing of the circulating pump.

Slurry has now been removed from the 300-SM system, and the equipment has been placed in standby condition. No slurry tests with this facility are planned for FY-1961.

5.6 SLURRY LOOP EXPERIMENTS

5.6.1 200B Loop Operation, Run 4B

During the course of run 4B, in which a 1600°C-fired 1.8-μ-dia thoria slurry (DT-12 and -13) was pumped in the 200B loop at temperatures between 170 and 280°C, it was noted that there was a significant increase in heat transfer resistance with time.[8] At 3216 hr of slurry circulation, the measured slurry heat transfer coefficient had been reduced by a factor of 3, and the loop was shut down in order to examine the copper-disc heat meter.[9] Inspection revealed no buildup of slurry on the heat transfer surface. The observed reduction in heat transfer rates was apparently due to a rough, black copper oxide scale which had formed on the heat transfer surface. Nickel plating on the surface to prevent corrosion of the copper-disc heat meter had been eroded away during the run.

The run will be continued with the same slurry after the heat meter is repaired and replated. A gamma densitometer also will be installed in the heat-meter pipeline in order to provide data on slurry concentration when heat transfer measurements are being obtained.

5.6.2 200A Loop Operation, Run 22A

Run 22A, in the 200A loop, was begun on July 22, 1960. The purpose of the run is to observe the high-temperature dropout behavior of a 1600°C-fired 3.65-μ-dia thoria slurry and to compare the behavior with that of the slurry used in run 21A (800°C-fired long-digested, 1.7-μ-dia thoria).[10]

REFERENCES

1. I. Spiewak, F. N. Peebles, et al., HRP Quar. Prog. Rep. Apr. 30, 1960, ORNL-2947, p 29-32.
2. Ibid., p 32.
3. H. R. Payne, Investigation of the Effect of Radiation on the Electrical Resistance of Class H Motor Insulation (in press).
4. I. Spiewak, F. N. Peebles, et al., HRP Quar. Prog. Rep. Jan. 31, 1960, ORNL-2920, p 24-25.
5. Ibid., p 44.
6. D. G. Thomas and P. H. Hayes, Heat- and Momentum-Transport Characteristics of Non-Newtonian Aqueous Thorium Oxide Suspensions, HRP-59-133 (July 1, 1959).
7. I. Spiewak, F. N. Peebles, et al., HRP Quar. Prog. Rep. Apr. 30, 1960, ORNL-2947, p 37.
8. Ibid., p 37-39.
9. R. B. Korsmeyer, F. N. Peebles, et al., HRP Quar. Prog. Rep. Jan. 31, 1959, ORNL-2696, p 61-62.
10. I. Spiewak, F. N. Peebles, et al., HRP Quar. Prog. Rep. Jan. 31, 1960, ORNL-2920, p 37-38; I. Spiewak, F. N. Peebles, et al., HRP Quar. Prog. Rep. Apr. 30, 1960, ORNL-2947, p 39-40.

6. INSTRUMENT AND VALVE DEVELOPMENT

A. M. Billings R. L. Moore

6.1 VALVE TRIM FOR THORIUM OXIDE SLURRY APPLICATIONS

6.1.1 Trim for 300-SM Loop Valve

Four sets each of Kennametal grade KH (tungsten carbide) and Kentanium 162B (titanium carbide) valve trim, fabricated by Kennametal, Inc., were received and will be tested in slurry service. These sets of trim are the conventional plug and seat type for use in standard Annin split-body valves.

One set of grade KH was installed in the lower letdown valve (HCV-1281) in the 300-SM loop on March 22, 1960, and from all indications, the valve operated satisfactorily to the conclusion of loop operation.

After approximately 4-1/2 months of service, two Annin valves modified for aluminum oxide ball-plugs and seats,[1] were found to have almost identical individual leak rates of 20 cc of water per minute with 2000 psi differential pressure across the valve seat (see Sec. 5.5). The feed-pump discharge block valve (HCV-1211), a typical valve, was removed for inspection. As can be seen in Fig. 6.1, no visible wear occurred to the valve seat; the ball-plug, however, exhibits a seating line with a depth less than 0.001 in. This localized wear appears to have been caused by nonrotation of the ball-plug during valve actuation, possibly the result of too high friction between the internal fail-closed spring and the ball-plug. To minimize the friction and permit rotation of the ball-plug to distribute the wear, a weaker fail-closed spring will be installed in future valves of this type.

6.2 HRT VALVES

6.2.1 Isolation-Chamber Stem-Sealing Bellows

Owing to premature failure of the 0.007-in.-thickness single-ply stem-sealing bellows in the HRT sampler isolation chambers, replacement bellows were fabricated for this application. The new bellows, made by the Fulton Sylphon Division, have the same over-all dimensions as the original, but are two-ply, with a 0.005-in. ply thickness, and have seamless construction.

Life tests were made on five of the Fulton Sylphon bellows test assemblies with 1000 psig applied externally at 225°C and with the interior pressure at atmospheric. Four of the units were strokes 1/8 in., with 50% of the stroke in extension and 50% in compression. The cycling rate was 10 per minute. Average life of the four units was 3950 strokes. The fifth assembly was tested in a similar manner with a stroke of 1/16 in., approximately the stroke which is required in the isolation chamber. This unit exhibited a life of 55,160 strokes.

UNCLASSIFIED
PHOTO 35919

Fig. 6.1. Aluminum Oxide Valve Trim from 300-SM Loop Valve HCV-1211, After 4½ Months of Service.

All failures occurred in convolutions adjacent to the seal weld at the plug end of the test assembly. Lighter seal welds would probably improve the life expectancy.[2]

REFERENCES

1. R. L. Moore et al., HRP Quar. Prog. Rep. Jan. 31, 1960, ORNL-2920, p 51, Fig. 9.5.

2. A. M. Billings, Life Test of Stem-Sealing Bellows for HRT Valves, ORNL CF-58-3-39, pp 3, 6, 7, 18.

PART III. SOLUTION FUELS

7. REACTIONS IN AQUEOUS SOLUTIONS

M. J. Kelly

D. R. Cuneo L. O. Gilpatrick M. D. Silverman

7.1 DISSOLUTION OF INORGANIC SOLIDS IN HRT FUEL

A study was undertaken to determine the dissolution rate of solids in simulated HRT fuel in well-stirred autoclaves at ~250°C. This study was limited to those solids which could conceivably have existed within the HRT core as a consequence of off-design operation. The solids tested were UO_3, UO_2, U_3O_8, $CuO \cdot 3UO_3$, and reactor-solution solids prepared by drying and calcining simulated fuel solution at 500°C. Under the test conditions these solids dissolved rapidly, generally following apparently first-order kinetics.

7.1.1 Experimental Procedure

A 1-liter stirred autoclave was used for all the experiments. The temperature of the autoclave was controlled at 250 ± 5°C. Special features of the apparatus were a thin-walled glass bulb containing the test solid and a fritted stainless steel filter stick used as a sampling tube.

The glass bulb, filled with the desired amount of solid, and the filter stick were installed on tubing connections through the autoclave head. A tubing connection was available to control the gas atmosphere in the autoclave. A sampling tube without the filter frit was also present. Simulated fuel solution, sometimes with added acid, was put into the autoclave and all fittings were closed. The temperature was raised to 250°C, after a suitable gas atmosphere was provided. To initiate the solid addition, a high gas pressure was suddenly applied to the interior of the glass bulb containing the solid sample. The bursting of the bulb was established as zero time; thereafter, serial samples were withdrawn through the filter frit until the solid had dissolved. Analysis of these samples enabled the experimenter to follow the rate of solution of the solid. When the rate of solution was extremely rapid, the precision of the results was affected by the time required to draw individual samples.

7.1.2 Results and Discussion

In every experiment the rate of solution of the solid was fast. The apparent half life for solution varied from less than 0.5 min to 2.5 min.

The first experiments, using UO_3 and solids prepared by evaporating simulated reactor fuel to dryness and calcining these solids overnight at 500°C, showed rates of solution so rapid that calculation of the rate constant was impractical. The apparent half life of the reaction was less than 0.5 min.

Experiments using material (prepared by W. L. Marshall's group) with the reported composition $CuO \cdot 3UO_3$ also dissolved rapidly. The results of these experiments were clouded by corrosion of the stainless steel filter frit which caused some anomalous results. In spite of these experimental difficulties, the data seemed to indicate that the uranium and copper dissolved at different rates. The apparent half life was less than 2.0 min for both components, with the uranium returning to solution somewhat the more rapidly.

A more thorough investigation was made of the rate of solution of U_3O_8 and UO_2, since they represent probably the most refractory components in this group of solids. The experimental results are shown in Figs. 7.1 and 7.2. Figure 7.3 shows a plot of the results, assuming a first-order process. The half lives of the reactions, shown in Table 7.1, were calculated from this graph. Table 7.1 also shows the chemical conditions for the individual experiments. In experiments 1 and 2 the U_3O_8 was prepared by firing, at 800°C, UO_2 which had been prepared by precipitation from molten salts. In experiments 3 and 4 the UO_2, from another source, was found by analysis to contain 28% of U_3O_8 and, while its preparation technique was unknown, it appears likely that it was made by hydrogen reduction. If so, its state of subdivision was the probable cause of the short half life. Experiments 5, 6, and 7 used UO_2 prepared by precipitation with water vapor from molten-salt melts at 800°C. This was stoichiometric material with a high density and low specific surface area--probably the most refractory UO_2 available.

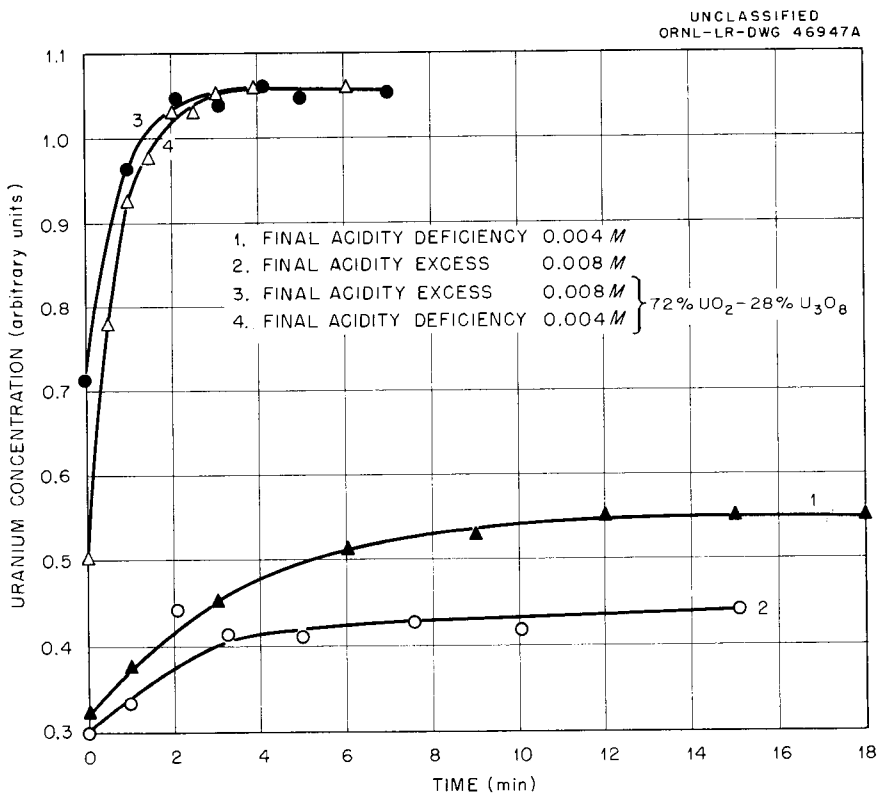

Fig. 7.1. Dissolution of U_3O_8 in 0.034 M UO_2SO_4 + 0.023 M H_2SO_4.

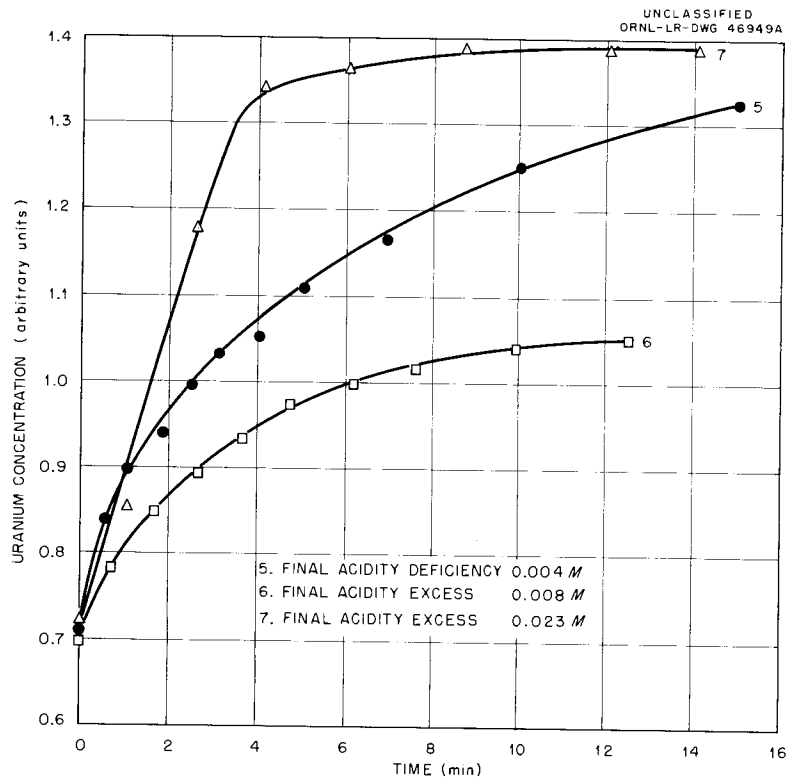

Fig. 7.2. Dissolution of UO_2 in 0.034 M UO_2 + 0.023 M H_2SO_4.

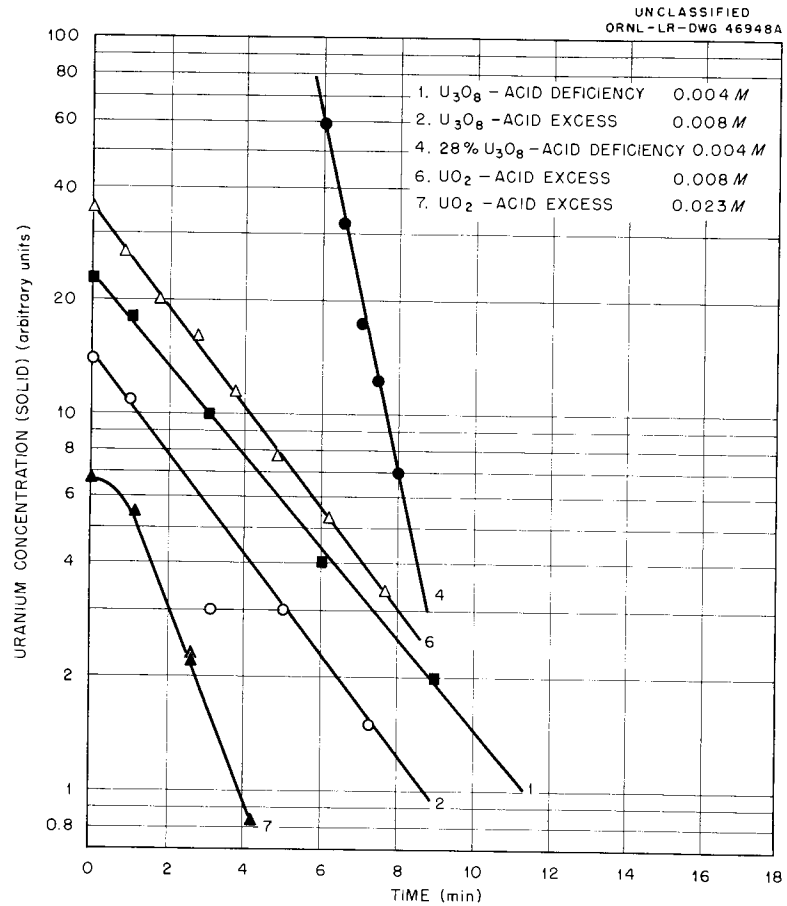

Fig. 7.3. Dissolution of Solids U_3O_8 and UO_2 in 0.003 M UO_2SO_4 + Excess H_2SO_4.

Table 7.1. Dissolution of U_3O_8 and UO_2 in Uranyl Sulfate Solutions

Solution: 0.03 *M* UO_2SO_4, 0.015 *M* $CuSO_4$, 0.023 *M* H_2SO_4 (initial)
Oxygen overpressure: 200 psi at room temperature
Temperature: 250 ± 5 °C

Run No.	Dissolved Component	Final Acid (*M*)	Increase in U Conc.	Time Required for Complete Dissolution (min)	t 1/2 (min)
1	U_3O_8	-0.004*	0.019	12	2.5
2	U_3O_8	+0.008	0.01	2-3	2.2
3	UO_2 - 72% U_3O_8 - 28%	+0.008	0.01	3	~0.5
4	UO_2 - 72% U_3O_8 - 28%	-0.004*	0.019	5	0.5
5	UO_2	-0.003*	0.019	15	~2.4
6	UO_2	+0.008	0.01	10-12	2.4
7**	UO_2	+0.023	0.019	8	1.2

*Indicated original excess-acid concentration of 0.023 *M* has been exceeded by this amount equivalent to dissolved uranium.

**Initial acid 0.053 *M*; half-life value estimated, since run did not show first-order kinetics.

7.1.3 Conclusions

The results reported here suggest that the solids tested, if formed in the reactor, should redissolve promptly under conditions of good agitation such as are being provided by the present modifications to the HRT. This conclusion is predicated upon the availability of excess acid and oxygen at the reaction site. Since all these solids are rich in uranium, the local area of high fission density and, therefore, high temperature created by the solid could result in an inability of the solution to contact the solid particle as long as it remained in a high-intensity neutron flux.

8. HETEROGENEOUS EQUILIBRIA IN AQUEOUS SYSTEMS

W. L. Marshall

E. U. Franck
J. S. Gill
E. V. Jones
J. E. Savolainen
R. Slusher
F. J. Smith

8.1 LIQUID-LIQUID EQUILIBRIA IN THE SYSTEM UO_3-SO_3-D_2O

Previous investigations,[1,2] defined liquid-liquid equilibrium temperature boundaries in the system UO_3-SO_3-H_2O. The present investigation extended this work to the UO_3-SO_3-D_2O system, using the same experimental methods and covering a range of SO_3 concentrations from 0.05 *m* to 1.0 *m*. Other studies[2] have shown the nature and composition of the heavy-liquid phases in equilibrium with the light-liquid phases for both H_2O and D_2O systems at 285, 300, 325, and 350°C.

The results of the present study are shown in Fig. 8.1. Each series of tests was made at a constant SO_3 concentration, and the results are displayed as plots of temperature vs the mole ratio UO_3:SO_3 (R). This procedure was used since, in previous work, R values for any such series appeared to be nearly linear with temperature. Critical curves are also shown on the figure, representing the temperatures at which the vapor composition became identical with the liquid composition (i.e., the meniscus between the two phases disappeared).

Comparison of these results with those previously obtained for the light-water system[2] revealed that the value for R at the appearance of the second-liquid phase was approximately 10% lower for the D_2O system. This difference corresponds approximately to the 10% lower specific volume for solutions in the D_2O system.

The results in Fig. 8.1 show also that the solubility of UO_3 in the supercritical fluid is considerable, as was previously observed in the analogous H_2O system.[2] In 0.80 *m* SO_3 solution, for example, as much as 0.2 *m* UO_3 was soluble in the supercritical fluid.

This investigation is being continued until a sufficient amount information is attained to define the UO_3-SO_3-D_2O edge of the phase diagram for the system UO_3-CuO-NiO-SO_3-D_2O above 300°C.

8.2 CRITICAL CURVES AND SOLID-LIQUID EQUILIBRIA IN THE SYSTEM NiO-SO_3-H_2O ABOVE 300°C

In addition to the subsystems UO_3-SO_3-H_2O and CuO-SO_3-H_2O, the other important subsystem of the multicomponent system UO_3-CuO-NiO-SO_3-H_2O is NiO-SO_3-H_2O. Solid-liquid equilibria were investigated[3] from 10^{-4} to 3 *m* SO_3 at temperatures as high as 300°C. No second-liquid phase was found. In view of the existence of heavy-liquid phases in the UO_3-SO_3-H_2O and CuO-SO_3-H_2O systems, it was desirable to know whether, under saturation vapor pressure, and at higher temperatures, a second-liquid phase might be found in the NiO-SO_3-H_2O system.

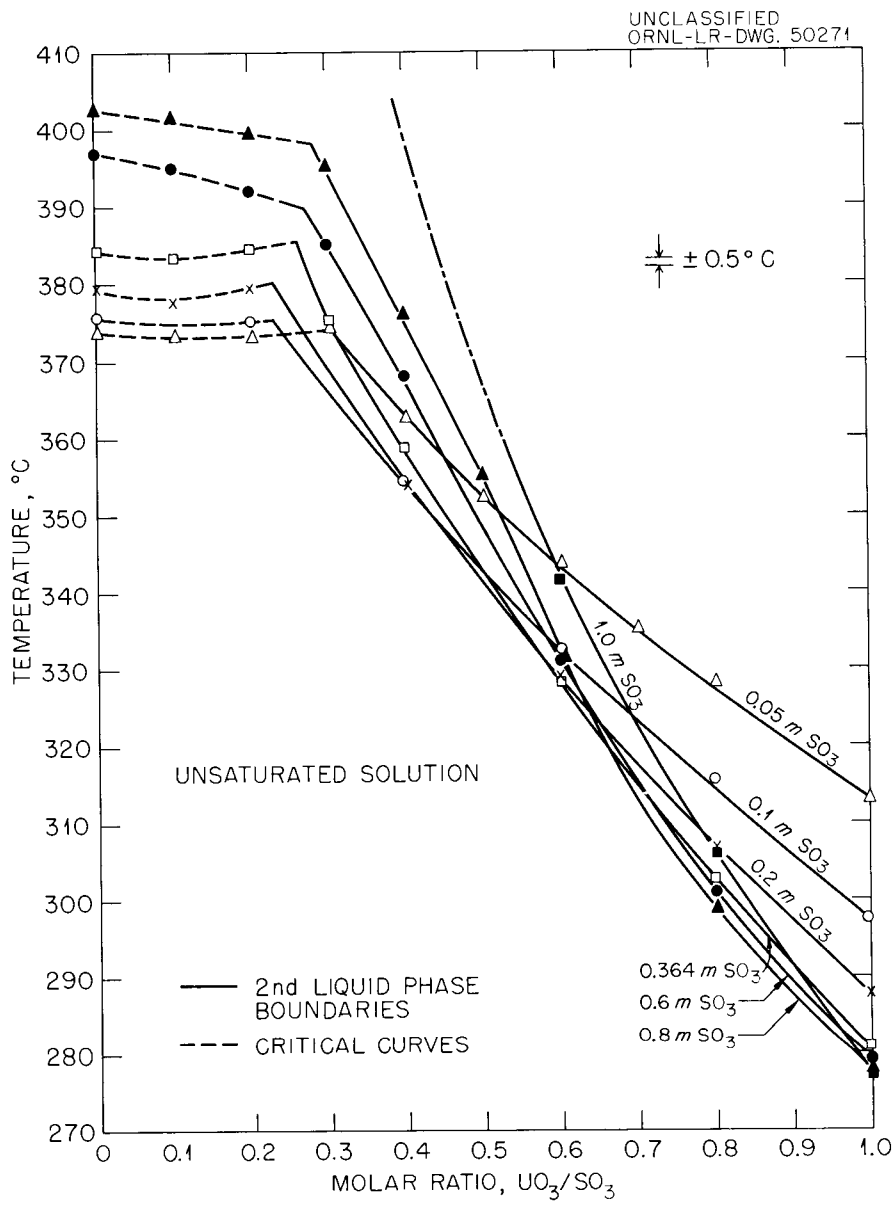

Fig. 8.1. Second-Liquid Phases and Critical Temperatures for the System UO_3-SO_3-D_2O.

The experimental approach used for this study was the same as that discussed in the preceding section for the system UO_3-SO_3-D_2O. The results of the earlier study of the nickel system suggested that the mole ratio, NiO/SO_3, would have to be kept below approximately 0.3 in order to achieve stability above 300°C. The over-all experimental results are shown in Fig. 8.2, plotted as saturation mole ratio, NiO/SO_3, vs temperature for several concentrations of SO_3. The data show that no two-liquid-phase region was found. It was found that the solubility of NiO in the supercritical fluid extended to mole ratios, NiO/SO_3, somewhat greater than 0.1, at least for solutions from 0.5 to 2 *m* in SO_3. The location of the point of intersection of the critical curve with the

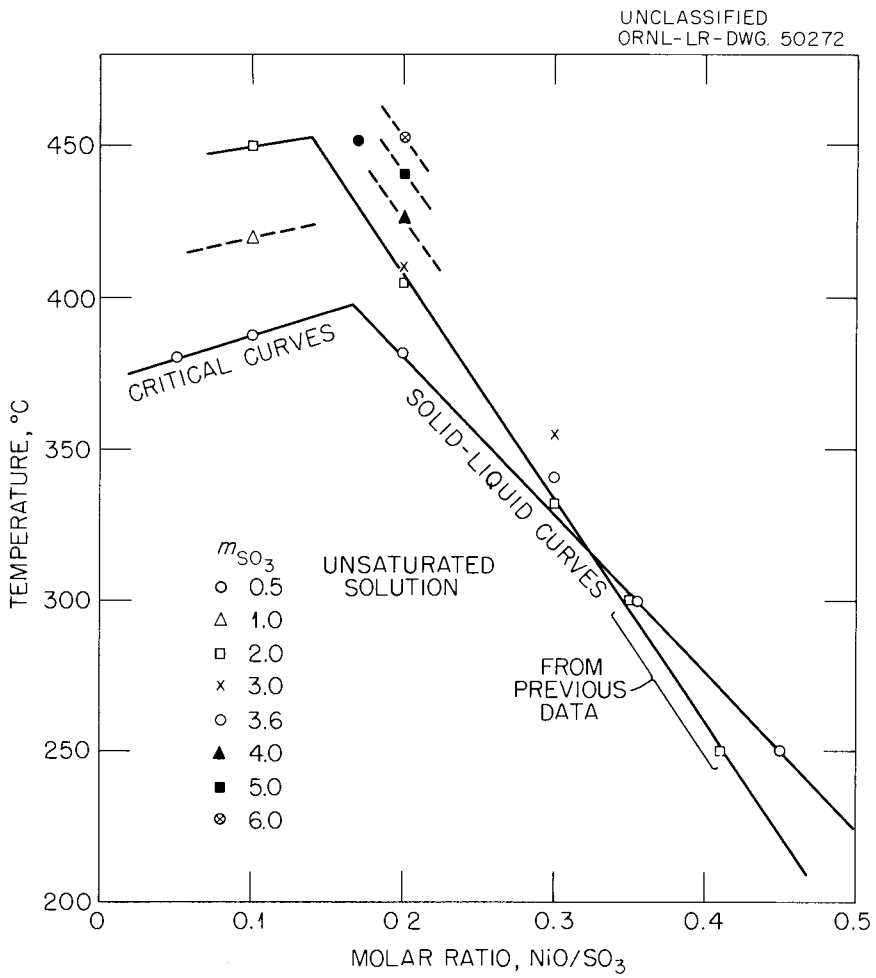

Fig. 8.2. System $NiO-SO_3-H_2O$ Above 250°C; Solubility in Supercritical Fluid and Solid-Liquid Equilibria.

solid-liquid curve suggests that NiO is more soluble than 0.2 *m* but less soluble than 0.34 *m* in a 2 *m* SO_3 supercritical fluid.

Application of these findings to the multicomponent system $UO_3-CuO-NiO-SO_3-H_2O$ suggests that there must be a portion of the system, adjacent to the $NiO-SO_3-H_2O$ edge, which is saturated with a nickel-containing solid phase; consequently, no complete definition of the five-component system at saturation vapor pressure in terms of liquid-liquid-vapor equilibria appears possible.

8.3 THE SYSTEM $ThO_2-HNO_3-H_2O$ AT 200 AND 300°C

Investigations of the thermal and hydrolytic stability of $Th(NO_3)_4$ in H_2O solution at elevated temperature were among the first solubility studies to be made on the AHR project.[4] These earlier investigations were carried out in sealed tubes using the synthetic method. The renewed interest in $Th(NO_3)_4-DNO_3-D_2O$ solutions as breeder blanket solutions suggested that the earlier investigations of the $ThO_2-HNO_3-H_2O$ system be extended.

Pressure vessels used for the study of solution-solid equilibria in other systems were employed.[2] These vessels were equipped with capillary tubes for direct sampling to permit analysis of the liquid. The vessels were charged with selected levels of nitrate and an excess of thorium, either by the use of $Th(NO_3)_4$ solutions or mixtures of ThO_2 and nitric acid solutions. The vessels were then sealed and rocked at 200 or 300°C for appropriate periods of time, after which the rocker was stopped, the excess solid allowed to settle, and the solution sampled. The solution sample was analyzed for its Th^{+4} and NO_3^- content. The experimental results are given in Table 8.1 and are shown graphically in Fig. 8.3. The solid ThO_2 used in these experiments was selected from three different batches of the oxide, each prepared by precipitation from thorium nitrate solution as the oxalate and then calcined at a different temperature:

ThO_2 Product	ORNL Pilot Plant No.	Calcination Temp. (°C)
A	DT-58-650	650
B	DT-58-1100	1100
C	DT-15-1600	1600

Three batches of oxide, having different surface areas and chemical reactivities as a result of the differences in calcination temperatures, were tested to establish whether equilibrium conditions were truly being established in the

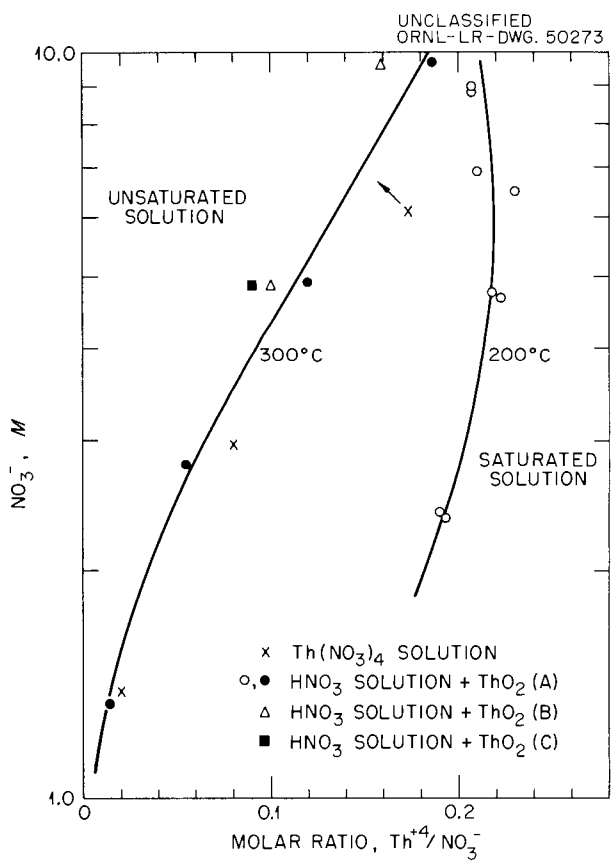

Fig. 8.3. Solubility Equilibria in System ThO_2-HNO_3-H_2O at 200 and 300°C.

Table 8.1. Solubility of ThO_2 in HNO_3-H_2O Solutions at 200 and 300°C

Temp. (°C)	Initial Mix	Rocking Time: After 2.5 hr NO_3^- (*M*)	After 2.5 hr Molar Ratio Th^{+4}/NO_3^-	After 24 hr NO_3^- (*M*)	After 24 hr Molar Ratio Th^{+4}/NO_3^-	After 48 hr NO_3^- (*M*)	After 48 hr Molar Ratio Th^{+4}/NO_3^-
200	ThO_2 (A) + HNO_3 soln	8.45	0.180	9.40	0.198	8.89	0.209
	"	6.92	.160	7.08	.205	6.90	.210
	"	4.57	.148	4.72	.207	4.76	.217
	"	2.35	.154	2.38	.183	2.39	.191
	"	8.95	.172	9.23	.213	9.20	.203
	"	6.64	.170	7.12	.212	6.50	.232
	"	4.52	.165	4.70	.211	4.70	.223
	"	2.40	.146	2.36	.189	2.35	.194
				After 2 hr		After 20 hr	
300	$Th(NO_3)_4$ soln			10.13	0.235	-	-
	$Th(NO_3)_4$ soln + ThO_2 (A)			10.12	.189	10.13	0.186
	ThO_2 (A) + HNO_3 soln			9.63	.180	9.68	.186
	ThO_2 (B) + HNO_3 soln			9.59	.146	9.68	.159
	ThO_2 (C) + HNO_3 soln			9.58	.097	-	-
	ThO_2 (A) + HNO_3 soln			4.91	.136	4.88	.121
	ThO_2 (B) + HNO_3 soln			4.88	.091	4.86	.099
	ThO_2 (C) + HNO_3 soln			4.81	.054	4.87	.091
	$Th(NO_3)$ soln			6.19	.197	6.14	.173
	"			3.04	.112	2.96	.080
	"			1.40	.041	1.39	.020
	ThO_2 (A) + HNO_3 soln			2.85	.069	2.80	.054
	"			1.32	.020	1.32	.016
	"			0.656	.0021	0.660	.0018
	"			.214	.0001	.217	.00008
	"			.061	.00014	.064	.00013

solubility experiments. The results in Table 8.1 show that, at 300°C, the HNO_3-H_2O solutions were saturated at the end of the runs to approximately the same extent by all three different preparations of ThO_2 solid. Moreover, the rates at which the solutions saturated were rapid, both at 200 and 300°C.

Examination of the solubility data for ThO_2 in HNO_3-H_2O showed a sharp decrease in the saturation molar ratio, Th^{+4}/NO_3^-, at concentrations of NO_3^- below 10.0 *M*, whereas for the analogous UO_3 system the decrease was very much less.[5] At 200°C, this very sharp decrease in saturation mole ratio was not evident, but the studies have not been extended to very low concentrations of NO_3^-. The analogous D_2O systems should show relatively little difference in solubility relationships from the H_2O systems.

The rapid rate at which the various forms of refractory ThO_2 dissolved in HNO_3-H_2O solution at 200 and 300°C (Table 8.1) may be of considerable interest. At temperatures up to 100°C the dissolving rate is very low; consequently, in the chemical reprocessing of ThO_2 fuel elements, a small amount of HF is customarily added to HNO_3 to promote the dissolution. In these studies, however, no HF or other complexing agent was present, but the rates of solution were fast. Methods by which refractory ThO_2 or other refractory oxides can be rapidly dissolved in pressure vessels at 200°C, 300°C, or higher should be of general interest in chemical processing.

8.4 THE SYSTEM UO_3-HNO_3-H_2O AT 25 TO 350°C

Investigation of the system UO_3-HNO_3-H_2O was essentially completed.[2] Figures 8.4 and 8.5 show the over-all collection of data for this system. Both figures include new data at 325 and 350°C at very low and very high concentrations. In Fig. 8.5, the curves taken from the data in Fig. 8.4 are shown on the same scale for saturation mole ratio, UO_3/HNO_3, vs log HNO_3 at the various temperatures. It is of interest to note that the curves at the various temperatures may be extrapolated to an intersection at a hypothetical 35 *m* nitrate concentration with a mole ratio, $UO_3/HNO_3 = 0.5$ (i.e., at the approximate composition, $UO_2(NO_3)_2 \cdot 3H_2O$).

8.5 CONDUCTIVITY OF AQUEOUS SOLUTIONS AT ELEVATED TEMPERATURES

Measurements of electrical conductivity of aqueous solutions give information which contributes greatly to an understanding of the ionic species present. Such information can be combined with the results of solubility and acidity determinations to provide an over-all understanding of the characteristics of aqueous systems. In earlier AHR studies,[6] the conductivities of aqueous solutions of uranyl sulfate and uranyl fluoride were measured over the temperature range of 0 to 200°C and the concentration range of 10^{-4} to 7.25 N. The data for uranyl sulfate were interpreted in terms of a dissociation constant, and the heat, free energy, and entropy of dissociation were calculated. Many investigations have been made of the dissociation of sulfuric acid at various temperatures.[7] In an ORNL-sponsored solubility study,[8] Stuckey determined the critical temperatures as a function of composition in the system SO_3-H_2O; critical temperatures as high as 650°C were measured.

In order to extend further both our knowledge of sulfate systems and our capacity to study the other systems, a program for the measurement of electrical conductivity in aqueous systems at high temperatures and high pressures has been

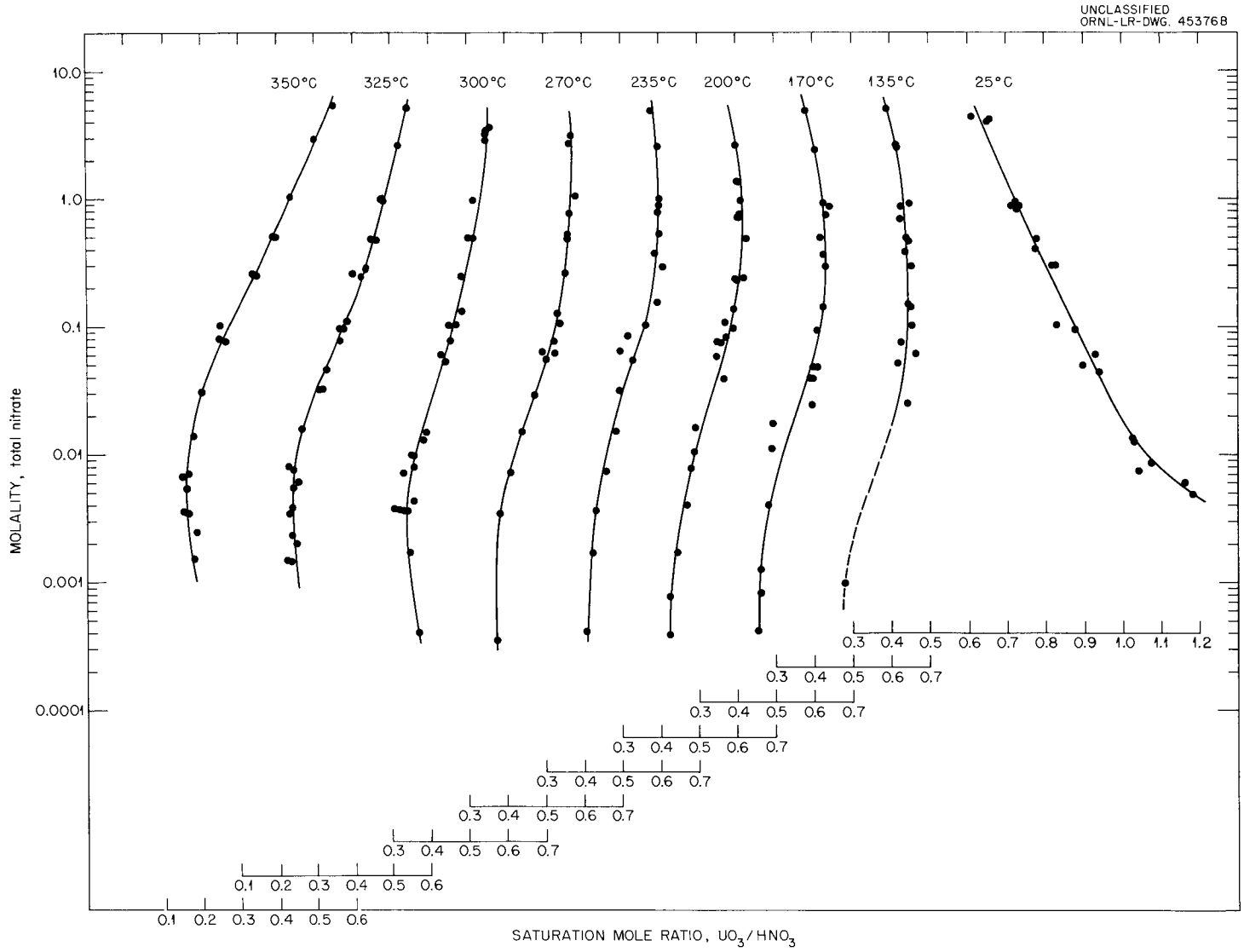

Fig. 8.4. The Solubility of $UO_3 \cdot H_2O$ in HNO_3-H_2O Solutions, 25 to 350°C.

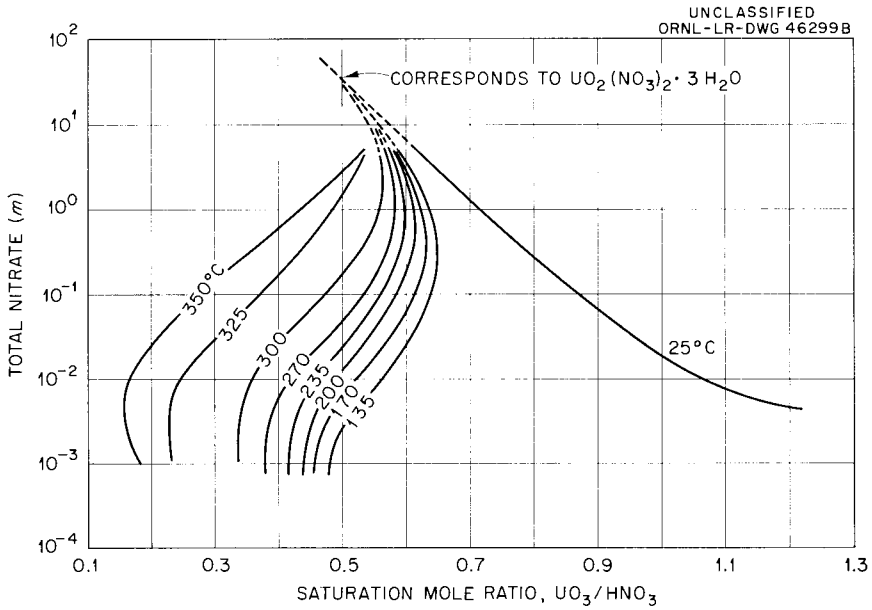

Fig. 8.5. The Solubility of $UO_3 \cdot H_2O$ in HNO_3-H_2O Solutions, 135 to 350°C.

initiated. Dr. E. U. Franck, on leave from the University of Göttingen and an expert in this field, is directing the establishment of the program. The initial objective will be the measurement of the conductivity of aqueous H_2SO_4 from 300 to 600°C and to several thousand atmospheres of pressure in order to provide thermodynamic information concerning H_2SO_4 in the neighborhood of and above the critical temperatures. A photograph of the high-pressure bench and associated apparatus is shown in Fig. 8.6.

8.6 CHEMICAL STABILITY OF VERY DILUTE SYSTEMS*

It is possible that the patches used to repair the Zircaloy-2 core tank in the HRT may not be completely sealed to the tank wall; if the patches are not leak-tight, the possibility exists that fuel solution in the core may leak into the water in the blanket. Such leakage would result in a large dilution of the fuel solution. It was the purpose of the studies reported here to determine the stability of several dilute solutions so that reasonable estimates can be made regarding the fate of uranium and copper that might find its way into the blanket.

The basic composition of the fuel solution was assumed to be 0.04 *m* UO_2SO_4, 0.025 *m* $CuSO_4$, and 0.035 *m* H_2SO_4; and the solutions tested were made by appropriate dilution of this solution, except in one case to be discussed later. In circulating dilute, highly oxygenated uranyl sulfate solutions in stainless steel systems, some of the chromium of the steel is oxidized to the hexavalent state with a resultant increase in acidity of the solution. With very dilute solutions the acid formed from this reaction is often greater than that present in the diluted fuel solution, and thus the actual stability of the solution is obscured. To circumvent this difficulty, the runs were made as follows: 180 liters of the solution to be tested was saturated with oxygen at room temperature

*This section contributed by J. C. Griess and H. C. Savage, REED.

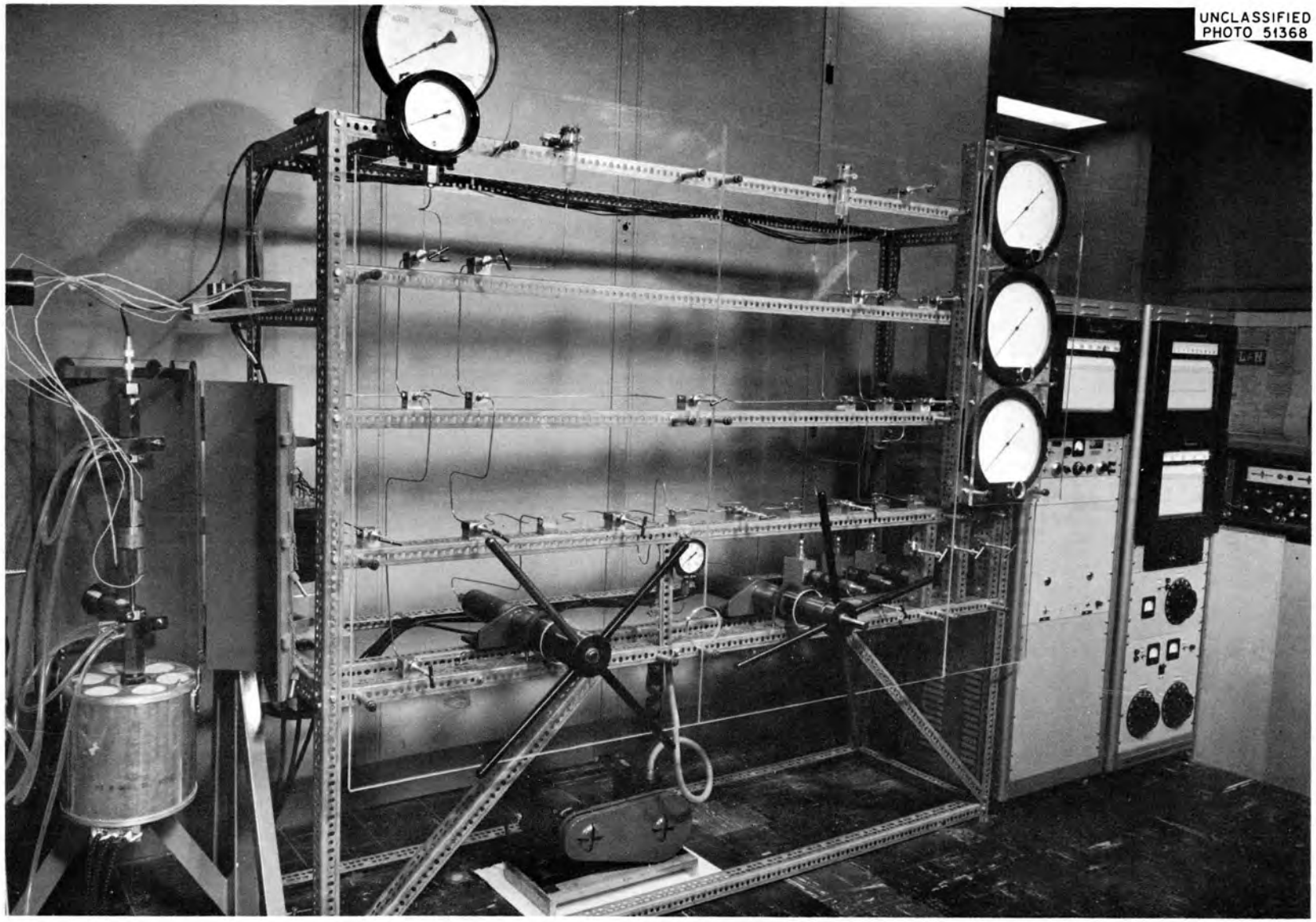

Fig. 8.6. Apparatus for Electrical Conductivity Studies at Elevated Temperatures and Pressures.

by bubbling gaseous oxygen through the solution. The loop was then filled with this solution, brought to temperature, and the oxygen-containing solution was fed to, and let down from, the loop at a rate of about 3 liters/hr. By this means, sufficient oxygen was maintained in the loop to prevent reduction and precipitation of uranium and not enough to cause significant quantities of hexavalent chromium to form. When the last of the solution had been fed to the loop, the pump was stopped and sufficient nitric acid was added to the loop to make its concentration about 1%. With this amount of nitric acid, all uranium and copper compounds precipitated or adsorbed in the loop were dissolved, and an analysis of the resulting solution, with appropriate volume corrections, yielded a measure of the stability of the solution. Periodically, samples of the letdown stream were analyzed chemically to determine the uranium and copper content.

Tests were conducted at temperatures of 200 to 325°C with a solution containing about 0.0002 *m* UO_2SO_4 (55 to 60 ppm U), 0.00013 *m* $CuSO_4$ (8 to 9 ppm Cu), and 0.00018 *m* H_2SO_4 (pH 3.5), which represents a 200-fold dilution of the fuel solution. Figure 8.7 shows the uranium concentration of the letdown stream during the run. The copper concentration followed the uranium concentration; i.e., the percentage of loss of uranium and copper were the same in all cases. It should be noted that the approach to constant concentration was temperature-dependent and that at 200 and 225°C there did not appear to be a significant loss of uranium based on analysis of the letdown stream. In all cases the sulfate concentration remained constant. When uranium and copper were lost, the pH decreased as expected if both elements were assumed to be completely hydrolyzed.

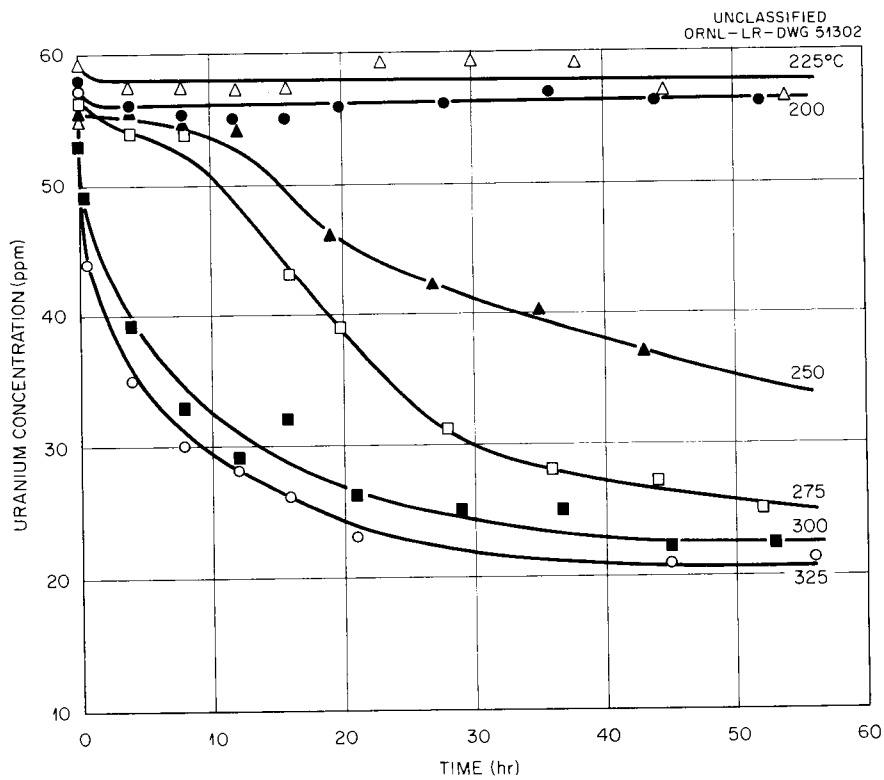

Fig. 8.7. Uranium Concentration in the Letdown Stream of a Loop in Which the Feed Solution Contained 0.00020 *m* UO_2SO_4, 0.00013 *m* $CuSO_4$, and 0.00018 *m* H_2SO_4.

Table 8.2 shows the per cent of the total uranium and copper that precipitated upon passage through the loop. Material balances between 90 and 103% were obtained. No fundamental significance should be attached to the values listed in Table 8.2 since this was a once-through system, and as shown in Fig. 8.7 the time required to reach a steady-state value was a function of the temperature. Had the solutions been recycled through the loop until no further change in concentration was observed, the values listed in Table 8.2 would have been higher. However, the values reported in Table 8.2 show that at temperatures as low as 200°C some uranium, at least 3%, was lost from solution when the assumed fuel solution was diluted 200-fold.

Table 8.2. Effect of Temperature on the Precipitation of Uranium and Copper from a Solution Originally Containing 0.00020 *m* UO_2SO_4, 0.00013 *m* $CuSO_4$, and 0.00018 *m* H_2SO_4

Temperature (°C)	Per Cent of Total Precipitated	
	Uranium	Copper
325	45	45
300	41	40
275	30	38
250	17	21
225	6	7
200	3	10

At 325°C the letdown stream near the end of the run contained 21 ppm U, 3 to 4 ppm Cu, and had a pH between 3.1 and 3.2. To see if any loss would occur from a starting solution of the above composition, such a solution was prepared and passed through the loop at 325°C. In this case there was no apparent change in solution composition based on analysis of the letdown stream. However, at the conclusion of the run it was found that 7% of the uranium and 23% of the copper had deposited in the loop, indicating that even with the lower pH the solution was not completely stable. Whether the loss represented hydrolysis or adsorption on the loop walls could not be determined.

In addition to the results reported above in which the fuel solution was diluted 200-fold, two other runs were made at 325°C in which other dilutions were employed; in one case the solution was diluted by a factor of 50 and in the other case by a factor of 10. The results of these runs, along with the results for the 200-fold dilution at 325°C, are presented in Table 8.3, from which it is apparent that the amount of uranium lost depended on the dilution factor. At a 10-fold dilution detectable amounts of uranium and copper were not lost from solution at 325°C.

The data presented in the above paragraphs indicate that leakage of fuel solution around the patches in the core-tank wall to the blanket will probably result in the formation of insoluble uranium and copper compounds in the blanket unless the leakage is sufficient to result in a concentration of about 1 g of uranium per liter (0.004 *m*). It would seem reasonable to assume that at least much of the uranium and copper would deposit on the core-tank wall since this

will be the hottest surface in contact with the solution. The lower the temperature of the blanket fluid and the cooler the core-tank wall, the less the likelihood of deposition from the blanket fluid. The addition of more than 0.035 *m* H_2SO_4 to the fuel solution would also reduce the amount of uranium and copper deposited. However, from the data obtained in the above series of runs, the acid concentration of the fuel solution would have to be at least 0.07 *m* to produce a stable solution at 325°C when diluted 200-fold and 0.055 *m* at 250°C at the same dilution. Both acid concentrations are probably impractical, from a corrosion point of view, in the fuel solution.

Table 8.3 Loss of Uranium and Copper from Diluted Fuel Solution at 325°C

Solution Composition	Dilution Factor	Per Cent of Total Precipitated	
		Uranium	Copper
0.00020 *m* UO_2SO_4 0.00013 *m* $CuSO_4$ 0.00018 *m* H_2SO_4	200	45	45
0.00080 *m* UO_2SO_4 0.00050 *m* $CuSO_4$ 0.00070 *m* H_2SO_4	50	40	32
0.0040 *m* UO_2SO_4 0.0025 *m* $CuSO_4$ 0.0035 *m* H_2SO_4	10	<0.5	<0.5

REFERENCES

1. H. W. Wright et al., HRP Quar. Prog. Rep. Oct. 1, 1952, ORNL-1424, p 108.

2. W. L. Marshall et al., HRP Quar. Prog. Rep. Jan. 31, 1960, ORNL-2920, p 62-75.

3. W. L. Marshall et al., HRP Quar. Prog. Rep. July 31, 1958, ORNL-2561, p 307-312.

4. W. L. Marshall, J. S. Gill, and C. H. Secoy, HRP Quar. Prog. Rep. Nov. 30, 1950, ORNL-925, p 279-290.

5. See Sec. 8.4, this report.

6. R. D. Brown et al., "The Electrical Conductivity of Uranyl Sulfate and Uranyl Fluoride in Aqueous Solution," J. Am. Chem. Soc. 76 1532, 1580 (1954); R. D. Brown et al., AECD-3488 (rev.) (Dec. 1952).

7. A partial review by T. F. Young, L. F. Maranville, and H. M. Smith is given in "The Structure of Electrolytic Solutions," p 35-63, W. J. Hamer (ed.), Wiley, New York, 1959.

8. J. E. Stuckey, Critical Phenomena in Binary Aqueous Solutions, The System SO_3-H_2O, Ph.D. dissertation, 1957, the University of Oklahoma; studies made at Oak Ridge National Laboratory, 1955-1957.

9. SOLUTION CORROSION

J. C. Griess H. C. Savage
J. L. English

9.1 DYNAMIC TESTS WITH HIGH-ACID UO_2SO_4 SOLUTIONS

Generally speaking, the higher the acid concentration of the fuel solution in the HRT, the greater its chemical stability. Since it was originally believed that 0.025 *m* H_2SO_4 in the fuel solution would be adequate to stabilize the solution, most previous corrosion tests were conducted with solutions containing about this concentration of free acid. However, the results obtained from chemical analysis of the HRT fuel solution during run 21 indicated that increased acidity of the solution might be desirable. Therefore, corrosion tests with type 347 stainless steel were conducted at 250 and 300°C in a solution containing 0.04 *m* UO_2SO_4, 0.025 *m* $CuSO_4$, and 0.05 *m* H_2SO_4. Since type CD4MCu stainless steel appeared to have reasonably good corrosion resistance at lower acid concentrations, and since it has other desirable properties, specimens of this alloy were included in some of the runs. The specimens of CD4MCu were machined from a single casting. With both alloys an attempt was made to determine the critical velocity and the amount of metal that corroded during the formation of a protective coating when below the critical velocity.

Type 347 stainless steel specimens, when exposed to the above solution at 250°C, showed a critical velocity of about 10 fps. Even at velocities slightly below 10 fps, about 0.002 in. of metal corroded before a protective oxide film formed. Exposure of specimens to oxygenated water at 280°C for 48 hr prior to exposure to the uranyl sulfate solution at 250°C for 270 hr resulted in a critical velocity of 15 to 20 fps; at flow rates less than the critical velocity, about 0.001 in. of metal corroded during formation of the protective film. When the specimens were given the above pretreatment in high-temperature water and exposed to the uranyl sulfate solution at 300°C for 319 hr, a critical velocity of 45 to 50 fps was observed and only 0.0001 to 0.0003 in. of metal corroded at flow rates less than the critical velocity. The same specimens that were exposed at 300°C (without descaling) were then exposed to the uranyl sulfate solution at 250°C for 560 hr, during which time no further corrosion occurred up to 50 fps.

Less extensive tests were carried out with CD4MCu, and to date none of the specimens have been prefilmed before exposure. With specimens of type CD4MCu stainless steel a critical velocity of less than 10 fps was observed at 250°C. In the velocity range of 10 to 14 fps the metal corroded to an average depth of 0.005 in. during a 275-hr run. At 300°C the critical velocity was about 30 fps, and 0.0005 to 0.001 in. of metal was removed during the formation of a protective oxide film. At both temperatures an unusual form of localized attack was observed. At 250°C preferential attack occurred on the grains themselves. The grain boundaries were raised, giving the specimen a very rough surface. At 300°C a similar attack was observed although the grain boundaries were less well defined. In addition, relatively large areas showed very minor attack. Specimens are being examined metallographically to determine what phase or phases in the alloy appear to have the greatest resistance to attack by highly acidic uranyl sulfate solution.

It is clear that the cast CD4MCu stainless steel has a lower critical velocity than the wrought type 347 stainless steel. This result is consonant with previous data which showed that cast type 347 stainless steel usually has a lower critical velocity in a given environment than does the wrought material.[1]

The experiments with type 347 stainless steel indicate that pretreatment of the specimens can be beneficial, at least for relatively short periods of time, and in some previous cases pretreatment films have lasted for many hundreds of hours.[2] However, it must be realized that films developed below the critical velocity have been demonstrated to be metastable when exposed at flow rates above the critical velocity. Thus, although the specimens exposed at 300°C resisted attack when exposed above the critical velocity at 250°C, the protective film probably would eventually deteriorate at velocities much above 10 fps, with a resultant high corrosion rate of the steel. How long the temporary protection would last cannot be predicted.

9.2 LABORATORY CORROSION STUDIES

9.2.1 Aluminum Oxide Corrosion Tests

Specimens of aluminum oxide of two different purities were corrosion tested in the following environments: (1) 1500 hr in oxygenated distilled water at atmospheric boiling; (2) 1500 hr in oxygenated distilled water at 300°C; and (3) 1000 hr at atmospheric boiling in an air-aerated, simulated fuel solution containing 0.04 *m* UO_2SO_4, 0.02 *m* H_2SO_4, and 0.005 *m* $CuSO_4$. The tests were run to determine if either of the two materials had suitable corrosion resistance for use as a nonconducting liner in a magnetic flowmeter. The four specimens were supplied by the Coors Porcelain Company; two were 93 to 95% aluminum oxide, and the other two contained a minimum of 98% aluminum oxide. Prior to the corrosion tests, water absorption tests (ASTM:C67-57) were run on single specimens having different alumina content at room temperature and at atmospheric boiling. In all cases the water absorption was 0.01% or less.

Table 9.1 summarizes the results of the corrosion tests. In distilled water the corrosion resistance of both grades of alumina was excellent at 100°C and entirely satisfactory at 300°C. Attack in the boiling, simulated reactor fuel solution was much more severe than in water, and there might be some question as to whether rates of 21 or 31 mpy could be tolerated. It was observed in all the tests that the rate of attack on the specimens decreased with increased exposure time.

9.2.2 Brazed Aluminum Oxide - Titanium Tests

Recently a program was initiated in the Metallurgy Division to determine the feasibility of brazing aluminum oxide to stainless steel. Such materials would be useful in valve and flowmeter construction. Four brazing alloys of the following composition in weight per cent were investigated: (1) 95 Zr, 5 Be; (2) 80 Zr, 15 Fe, 5 Be; (3) 48 Ti, 48 Zr, 4 Be; and (4) 47 Ti, 47 Zr, 3 V, 3 Be. For the initial tests, the aluminum oxide samples were brazed to titanium-75A, which has a linear coefficient of thermal expansion much closer to that of aluminum oxide than does stainless steel. All specimens were brazed in a vacuum at approximately 1000°C.

Table 9.1. Corrosion of Aluminum Oxide by Various Media

Medium	Specimen Identity	Alumina Content (%)	Temp. (°C)	Total Time (hr)	Weight Loss (mg/cm^2)	Corrosion Rate (mpy)
Oxygenated distilled water	AV30-1	98	100	1500	0.2	0.1
	B890-1	93-95	100	1500	0.5	0.3
Oxygenated distilled water	AV30-2	98	300	1500	4.5	2.7
	B890-2	93-95	300	1500	1.7	1.0
Simulated reactor fuel solution*	AV30-1**	98	100	1000	21.2	20.8
	B890-1**	93-95	100	1000	32.5	31.3

*Air-aerated 0.04 *m* UO_2SO_4 - 0.02 *m* H_2SO_4 - 0.005 *m* $CuSO_4$ solution.
**Same specimens as used for tests in water at atmospheric boiling.

Corrosion tests were run for 1500 hr in oxygenated distilled water at 300°C and in an aerated simulated reactor fuel solution (0.04 *m* UO_2SO_4 - 0.02 *m* H_2SO_4 - 0.005 *m* $CuSO_4$) at atmospheric boiling. Weight-loss data are given in Table 9.2. The reported weight losses are based upon the combined area of the aluminum oxide and the brazing alloy only, since attack on titanium is negligible in the two environments. The approximate combined areas of the aluminum oxide and the exposed braze metal on the eight specimens varied between 3.5 and 7.0 cm^2, of which 20 to 50% represented braze-metal area.

Table 9.2. Observed Weight Losses on Brazed Aluminum Oxide - Titanium Specimens Exposed for 1500 hr in Various Media

Medium	Temperature (°C)	Brazing-Alloy Composition (wt %)	Weight Loss (mg/cm^2)*
Oxygenated distilled water	300	95 Zr, 5 Be	7.1
		80 Zr, 15 Fe, 5 Be	7.5
		48 Zr, 48 Ti, 4 Be	9.0
		47 Zr, 47 Ti, 3 V, 3 Be	5.3
Reactor fuel solution**	100	95 Zr, 5 Be	15.2
		80 Zr, 15 Fe, 5 Be	6.7
		48 Zr, 48 Ti, 4 Be	38.8
		47 Zr, 47 Ti, 3 V, 3 Be	11.8

*Based upon combined areas of aluminum oxide and braze alloy only.
**An air-aerated, simulated reactor fuel solution containing 0.04 *m* UO_2SO_4 - 0.02 *m* H_2SO_4 - 0.005 *m* $CuSO_4$.

No conclusive statements can be made regarding the corrosion behavior of the four brazing alloys in view of the type of specimen employed. For example, an unknown portion of the observed weight losses was due to attack on the aluminum oxide member of each specimen. In the boiling reactor fuel solution, there was no visual indication of attack on any of the four braze alloys; the brazed areas were metallic and shiny. At 300°C in water, the braze alloys were dull and were covered with black corrosion products.

Over-all, the results of the tests were encouraging. Neither corrosion nor thermal cycling resulted in the aluminum oxide being detached from the titanium.

REFERENCES

1. J. C. Griess et al., HRP Quar. Prog. Rep. Jan. 31, 1955, ORNL-1853, p 83.

2. J. C. Griess et al., HRP Quar. Prog. Rep. Jan. 31, 1957, ORNL-2272, p 80-81.

10. RADIATION CORROSION

G. H. Jenks H. C. Savage

A. L. Bacarella S. E. Bolt
J. E. Baker V. A. DeCarlo
S. H. Wheeler

10.1 IN-PILE LOOPS

10.1.1 Introduction

An in-pile loop experiment, 0-1-25, was carried out in continuation of the program of studies to determine the in-pile corrosion of possible materials of construction for aqueous homogeneous reactors.

Zirconium alloys comprised most of the materials tested as specimens in this experiment. These specimens have been examined for weight loss, induced activity, and composition of materials retained on surfaces. The results of the measurements are being reported elsewhere and are summarized here.[1] Some chemical, metallurgical, and visual examinations of the experiment are still in progress, and the experiment will be reported in detail when all data have been received.

The solution for the experiment was 0.04 *m* UO_2SO_4, 0.016-0.035 *m* H_2SO_4, and 0.006 *m* $CuSO_4$ in D_2O, and the main-stream temperature was 280°C. As indicated by the loop number (0-1-25), the exposure was carried out in beam-hole HN-1 of the ORR. The loop was constructed of type 347 stainless steel; the design was similar to that of the LITR loops and has been described previously.[2] One of the major design changes was in the provisions for exposing specimens in the loop core. The core contained two tapered-channel coupon holders instead of one as in the LITR loops. The velocities of solution past the channel specimens ranged from about 10 to 23 fps, and the included angles in the channels ranged from about ±4° to 0°. Specimens (called annulus specimens) were arrayed in the regions around the core channels as in previous loops. The average velocity of solution past annulus specimens was about 1.5 fps. The objectives of the tests with the different zirconium alloys are listed below.

Zircaloy-2.--Correlation and analysis of previous in-pile loop and autoclave data for the corrosion of Zircaloy-2 have indicated that the relationship between corrosion rates, R (mpy), and fission power density in solution, P (w/ml), is:

$$1/R = \frac{2.3}{P\alpha} + 1/K \ , \qquad (1)$$

where α represents the factor by which the effective power density at a corroding surface is greater than that in solution due to uranium sorption on the surface, and K is a constant for a given temperature and solution and is evaluated by extrapolation of the corrosion data to infinite power density. The value of α depends upon solution composition and velocity of solution flow past a test surface. In solutions containing uranium and acid at concentrations near

those in the present experiment, the apparent values of α were appreciably greater than unity (6-7) at low solution velocities (~1 fps) but were nearer unity at the higher velocities in the channel holders. Nearly all the results upon which the above equation is based and from which the constants have been evaluated were obtained in experiments which employed H_2O solutions, specimen material from stock fabricated to give preferred grain orientations, and Zircaloy-2 specimens with machined surfaces. Also, all the specimens exposed to high solution velocities in these past experiments were mounted in holders in such a manner that about 35% of the area of a specimen was covered by the holder or by adjacent specimens. The covered surfaces were not sealed from the solution and were probably exposed to a thin layer of essentially static solution. Analyses of the past corrosion results have led to the suggestion that the covered surfaces corrode at rates near those expected at low solution velocities while the surfaces exposed to appreciable solution velocities corrode at lower rates.

One objective of the present test was to determine whether the covered and exposed surfaces do, indeed, corrode at different rates, and to evaluate, as closely as possible, the rates on each of the surfaces of given specimens. This information is considered of importance for the proper evaluation of the results of this and of past in-pile experiments and for the prediction of corrosion rates under given sets of conditions in reactors. To accomplish this objective, coupons having different ratios of exposed to total areas were employed in the core-annulus and in the channel specimen arrays. It was anticipated that the rates on the covered and exposed surfaces of these and other specimens could be obtained from comparisons of the average corrosion rates observed for these specimens.

Another objective of the test with Zircaloy-2 was to gain some information as to whether the method of fabrication of the Zircaloy-2 stock material or the surface preparation of specimens affect the value of K. Most of the specimens were made of stock fabricated to give random grain orientation, and most of the specimens were chemically polished. The value of K for machined specimens of other stock material has been established in past experiments as noted above.

To permit an evaluation of the effects of additional surface preparations or pretreatment on the Zircaloy-2 corrosion results, Zircaloy-2 specimens that had been sandblasted, overground, and sandblasted followed by chemical polishing, and specimens of chemically polished weld and air-contaminated weld materials were also included in a channel array. These specimens were suggested and supplied by the HRP Metallurgy Section.

Crystal-Bar Zirconium.--Two chemically polished specimens of crystal-bar zirconium were included in the core annulus arrays for comparisons between the corrosion rate of this material and that of Zircaloy-2 and for estimation of the value of K for the crystal-bar zirconium in this experiment. Previous results obtained with crystal-bar zirconium at 280°C, and in solutions in which the effect of sorbed uranium was negligible, have indicated that the relation between corrosion rate and power density is the same as that for Zircaloy-2 except that the value of K for the crystal bar is about one-half that for the alloy.[3]

Zr-Nb Alloys.--Two specimens each of Zr-15Nb, Zr-15Nb-2Mo, and of Zr-15Nb-1Cu in the beta-quenched and in the heat-treated conditions (400 to 500°C for one to two weeks) were included in the core annulus. Specimens of some of these materials were also included in a core channel array. The numbers and locations of specimens of the different alloys were such that inter-comparisons could be

made between their corrosion rates, and an indication obtained of the effects of velocity on the corrosion rates. It was not known whether the corrosion-rate - power-density relationship for these alloys is of the same general form as that for Zircaloy-2, and it was not anticipated that the number of specimens of a given material in this experiment would be sufficient to establish a relationship. These specimens were suggested and supplied by the HRP Metallurgy Group as part of their alloy development program.

Zr-1Cr Alloy.--Three chemically polished specimens of Zr-1Cr (heat treated at 750°C and air-cooled) were included in a channel array in order to determine the corrosion rates of this material in comparison with those of similarly located Zircaloy-2 specimens. Zr-1Cr shows better corrosion resistance than Zircaloy-2 in 500°C steam, and it might resist radiation-induced corrosion better than Zircaloy-2. The results of an in-pile autoclave test with this material indicated no difference between the alloys.[4] However, it was considered worth while to compare the materials under the dynamic conditions in the loop.

10.1.2 Experimental Methods and Procedures

The experimental methods and procedures were similar to those described for previous experiments.[5] Coupons with higher than usual ratios of exposed to total area were provided by beveling or by scalloping the coupon edges. The beveled-edge coupons were exposed in a channel array, and the scalloped coupons in annulus arrays. The loop was operated in-pile for 2741 hr, during which time the reactor energy was 36,895 Mw-hr. The experiment was operated for several periods in the fully or partially retracted positions and, as a result, was exposed to a calculated amount of radiation equivalent to that prevailing during 30,598 Mw-hr of reactor energy with the loop in the fully inserted position. About 90% of the reactor energy was accumulated at the 16- and 20-Mw levels.

10.1.3 Results and Discussion

In presenting the results, reference will be made to average, covered-surface, and exposed-surface corrosion rates (abbreviated as AR, CSR, and ESR, respectively). The AR values were calculated from the results of weight measurements using radiation time and assuming that the corrosion attack on a specimen was uniform over the entire surface. As noted above, the experiment was exposed to several reactor power levels and, as a result, a specimen corroded at different rates during exposure. The AR values reported are those normalized to the rate at the 16-Mw power level. The solution-power-density values employed are those calculated for the 16-Mw power level also. The CSR and ESR values were calculated from the AR values for specimens having different ratios of exposed to total areas.

(a) Chemically Polished Specimens of Commercially Annealed Zircaloy-2 Stock Material, in Annulus and Channel.--The AR values for these specimens are shown in Fig. 10.1 in a plot of reciprocal corrosion rate vs reciprocal power density. Information on the size and type of a given specimen, whether or not a specimen was cathodically defilmed, and on the ranges of solution velocities and included angles for channel specimens is included in the figure. In general, some weight loss was noted upon defilming specimens exposed to power densities below about 1.2 w/ml, but no significant loss occurred upon defilming specimens exposed to higher power densities.

UNCLASSIFIED
ORNL-LR-DWG 51303

	CORROSION RATES TOTAL AREA		AREA (cm^2)		
	CC	CA	TOTAL	EXPOSED	% EXPOSED AREA
1/2 x 1/2 in., 4 BEVELED EDGES	●		3.47	3.22	92.4
1/2 x 1/2 in., 3 BEVELED EDGES	▲		3.44	3.05	88.6
1/4 x 1/2 in., OVERSIZED	■		2.39	1.58	66.1
1/4 x 1/2 in.	♦	◊	2.19	1.42	64.8
1/4 x 1/2 in.		□	2.19	1.54	70.3
1/2 x 1/2 in., SCALLOPED EDGES		△	3.44	3.25	94.4

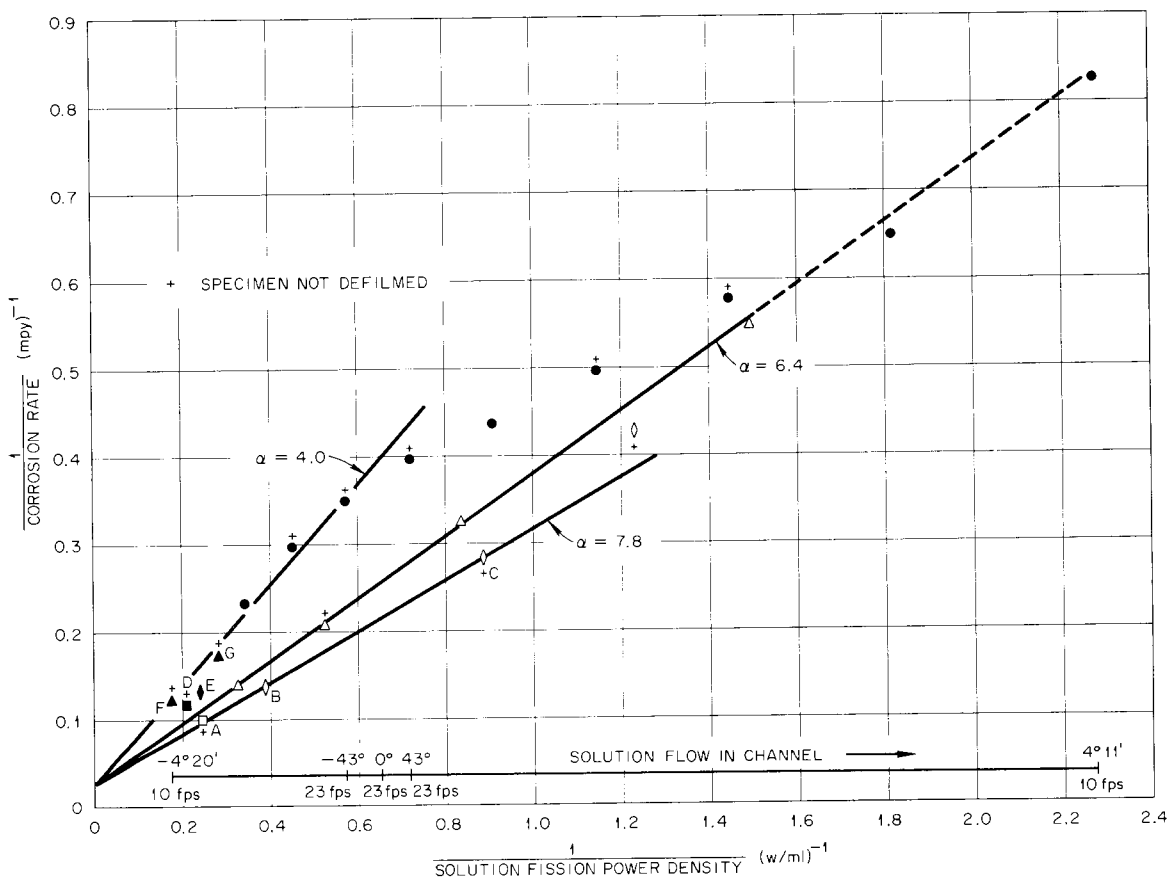

Fig. 10.1. Average Corrosion Rates of Chemically Polished Zircaloy-2 Core Coupons.

The results for the annulus specimens of both types are consistent with a K value (determined by extrapolation of lines through the points to infinite power density) of 40 mpy, the same value as that determined for Zircaloy-2 in the previous loop and autoclave experiments.[6] At a given power density, the indicated AR value for a scalloped specimen was less than that for a specimen having a smaller ratio of exposed to total area. This difference is ascribed to the occurrence of appreciable corrosion on the covered surfaces. Assuming that the ESR and CSR values for these annulus specimens were independent of specimen size, the values for these quantities calculated from the AR values indicate that the α values for the exposed and covered surfaces were 6.2 and 10.9, respectively. These calculated values are illustrated by the dotted lines in Fig. 10.2. The actual values, calculated from the AR values for specimens A,

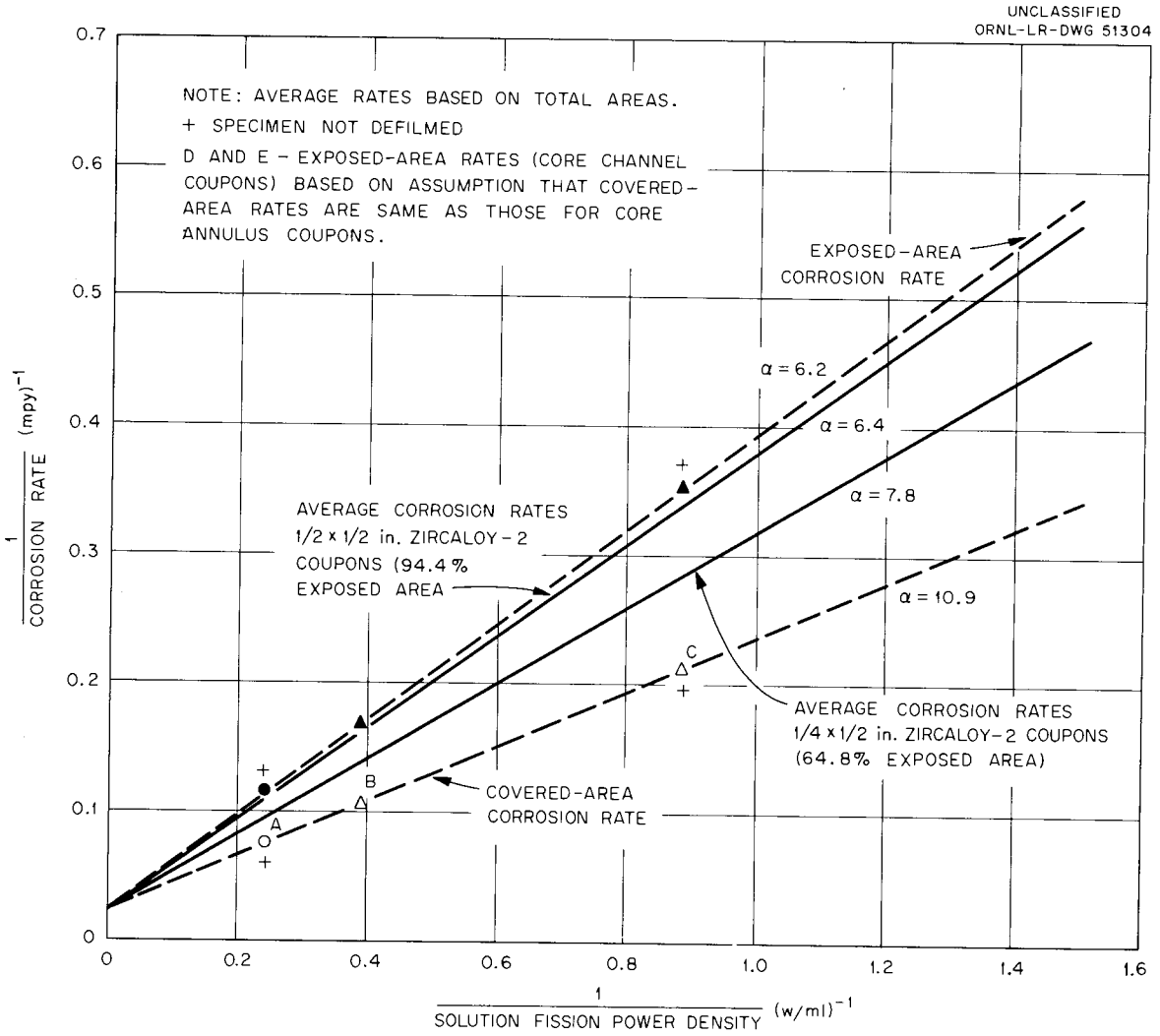

Fig. 10.2. Corrosion Rates of Chemically Polished Zircaloy-2 Core-Annulus Coupons.

B, and C and from the AR values taken from the line for α equals 6.4 in Fig. 10.1, are plotted in Fig. 10.2 to illustrate the fit of the lines with the calculated values.

The specimens exposed to higher solution velocities in the channel exhibited, in general, lower AR values than those exposed in the annulus. However, the data indicate that there was little reduction in corrosion due to an increase in velocity in the range 10 to 23 fps in the convergent section of the channel, and that the beneficial effect of a given solution velocity was less in the divergent section than in the convergent section. In fact, at the largest divergent angles there was little or no difference between the AR values for the channel specimens and those of the similarly shaped annulus specimens. The AR values for the two rectangular 1/4 x 1/2 in. channel specimens, D and E (Fig. 10.1), are greater than those found for the adjacent beveled-edge specimens, F and G. This difference is again ascribed to appreciable corrosion on the covered surfaces of the channel specimens. An estimate of the CSR values for these four channel specimens, made using the AR values for specimens D and E and AR values for beveled-edge specimens taken from a line drawn between the

points for the two adjacent specimens (F and G), indicates an α value of 8.0 for these covered surfaces. The corresponding ESR values for these four specimens correspond to an α value of about 4.0.

Analyses for surface uranium and some other elements were made on many of the undefilmed channel and annulus specimens. In general, the results indicate that significant amounts of uranium were present, along with iron and nickel oxides in amounts which would not affect the weight-loss results appreciably but which, for some of the specimens, would be of importance in considerations of the contributions of the surface uranium to the fission-recoil irradiation of the surfaces. Because of this and because of the erratic nature of the analytical results, a direct correlation does not appear feasible between the results for the amounts of sorbed uranium and the α values determined from the corrosion data.

The general relationships between solution velocity, position in the channel, and AR values for the channel specimens which are indicated by the data are in qualitative agreement with those observed in previous loop experiments and discussed elsewhere.[7]

The α value of 8.0 corresponding to the CSR values calculated for the channel specimens is not considered very reliable because of the strong possibility that portions of the beveled edges of a specimen were exposed to lower solution velocities than those prevailing on the central portions. If this were the case, in fact, the α value of 8.0 is lower than the true value. If certain, apparently reasonable, assumptions are made as to the fraction of the beveled surfaces which was exposed to essentially static solution, it can be estimated that the α value for the covered surfaces may have been as great as 15. Assuming this value for the covered surfaces, the calculated ESR values for the specimens exposed in the convergent section of the channel correspond to α values which range from about 2 to 1.5, with the lower value prevailing at the highest velocity.

Similar considerations of the flow past annulus-specimen surfaces suggest that those specimen edges which were perpendicular to the direction of flow were exposed to lower solution velocities than the flat exposed surfaces and, hence, that the α value for the covered surfaces was greater than the calculated value of 10.8. Assuming that the α value of 15 for the covered surfaces also applies to these vertical surfaces, the calculated α value prevailing on the exposed flat surfaces in the annulus was about 3.6.

The α values of 2 to 1.5 for the channel specimens at velocities of 10 to 20 fps are within the range of values deduced from the results of previous experiments with 0.04 *m* UO_2SO_4 solution in H_2O. These previous results showed probable values at 10 and 18 fps, and at the included channel angle of -3°40', of between 2 and 3 and 1 and 1.7, respectively. The α value for covered surfaces in the present experiment was probably substantially greater than the values of 6 to 8 estimated from the previous results. The explanation for the increased uranium sorption which is implied by the higher α value is uncertain. However, it is considered possible that it was associated with the use of D_2O rather than H_2O as the solvent.[8] It is also possible that the α value in this experiment was affected by a low hydrogen-ion concentration during portions of the exposure (a result of a greater than usual rate of steel corrosion).

(b) Zircaloy-2 Specimens with Various Surface Preparations and Zircaloy-2 Weldments.--AR results obtained with channel-type specimens of weldments and of alpha-annealed material with various surface preparations are shown in Fig. 10.3.

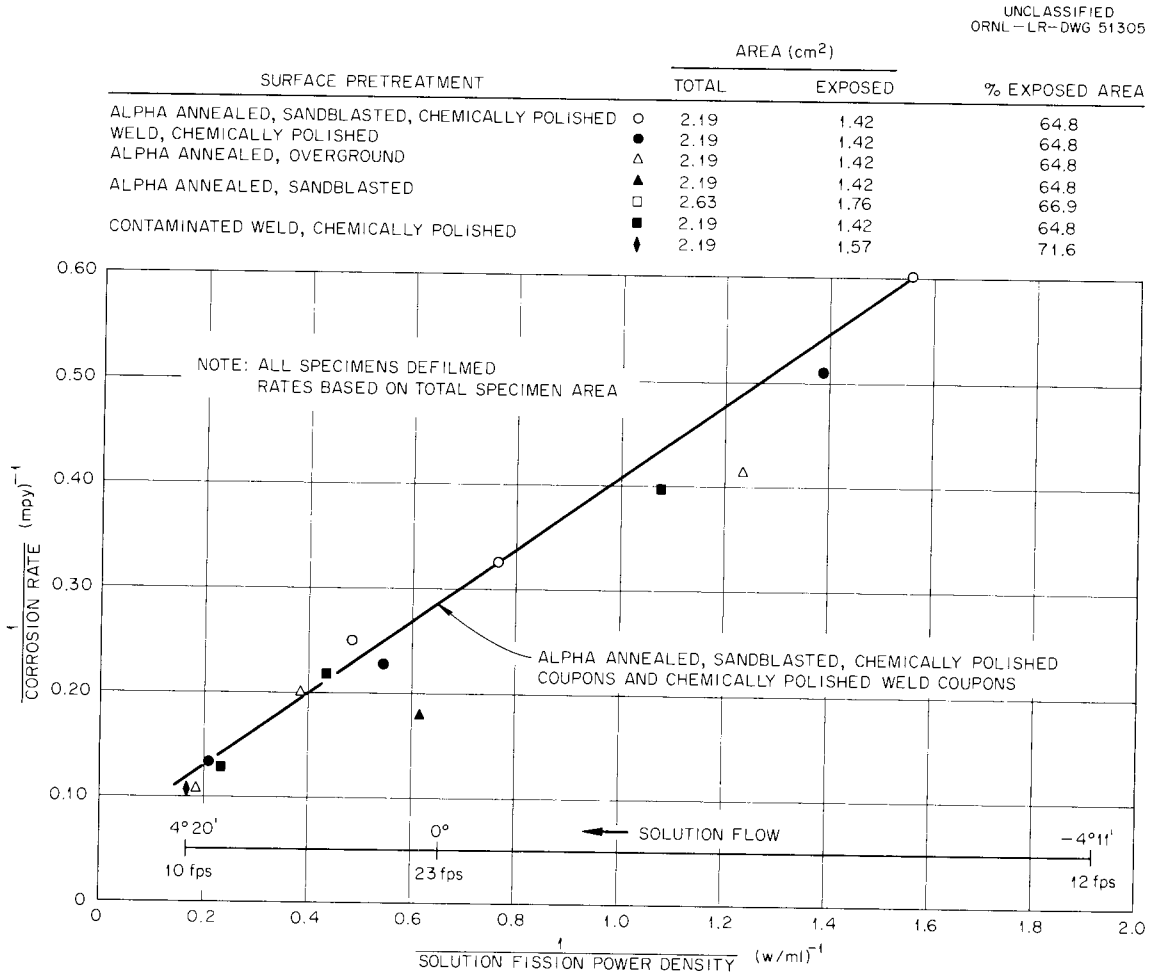

Fig. 10.3. Average Corrosion Rates of Zircaloy-2 Core-Channel Coupons (Various Pretreatments).

Except for the sandblasted specimens, little difference is apparent between the corrosion rates found for the different surface preparations and materials. The sandblasted specimens which were exposed at power densities of about 0.5 and 1.7 w/ml corroded at appreciably greater rates than the other specimens. However, the rate for the other sandblasted specimen, which was exposed at a power density of about 4.5 w/ml, was about the same as that for the specimens with the other pretreatments.

The results for a given type of material or surface preparation in this group are insufficient to permit an analysis for CSR and ESR values. However, comparisons between the AR values for the specimens exposed at power densities of about 4 to 5 w/ml and those for the 1/4 x 1/2 in. specimens of chemically polished Zircaloy-2 exposed at about the same velocities and power densities in the other channel holder (specimens D and E, Fig. 10.1) indicate that, at these power densities at least, the different pretreatments did not change the corrosion rate appreciably from that for the chemically polished specimens of stock Zircaloy-2.

Crystal-Bar Zirconium.--The AR values obtained with two annulus specimens of crystal-bar zirconium are shown in Fig. 10.4 together with a line which illustrates the AR results obtained with Zircaloy-2 specimens of similar type. It is apparent that the crystal-bar specimens suffered more corrosion than the similarly located Zircaloy-2 specimens. However, an extrapolation of the line through the two points indicates a K value which is less than that for Zircaloy-2 and which is in near agreement with the value of 20 mpy determined in the previous experiments mentioned in the introduction. Assuming that the relationship between corrosion rate and power density is of the form of Eq. (1), as indicated by previous results, the average value of α for the crystal-bar zirconium specimens was 12.3 whereas that for the Zircaloy-2 was 7.8.

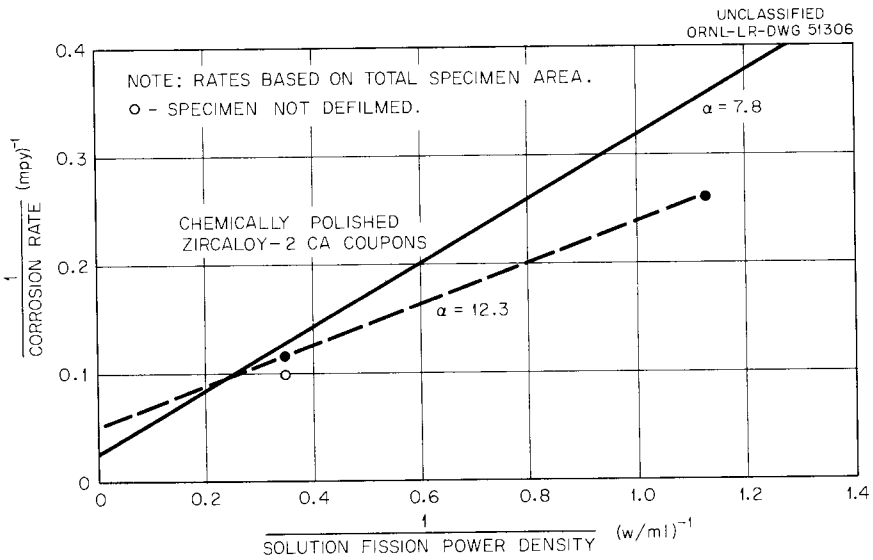

Fig. 10.4. Average Corrosion Rates of Chemically Polished Crystal-Bar-Zirconium Core-Annulus Coupons ($\frac{1}{4} \times \frac{1}{2}$ in. Coupons, 64.8% Exposed Area).

Zr-Nb Alloys.--The AR results obtained with annulus specimens of Zr-15Nb, Zr-15Nb-2Mo, and Zr-15Nb-1Cu are shown in Fig. 10.5, and those for channel coupons of Zr-15Nb-1Cu and Zr-15Nb-2Mo in the beta-quenched condition are shown in Fig. 10.6. In each plot, the AR results for similarly shaped and located specimens of Zircaloy-2 are illustrated for comparisons. As can be seen in the plots, the corrosion rates for the alloys in the beta-quenched condition were substantially less than those for Zircaloy-2. However, in the heat-treated conditions, the alloys corroded at higher rates than the Zircaloy-2. The results in Fig. 10.6 show that the corrosion rates of the alloys exposed to high solution velocities in the channel were substantially less than those exposed to lower velocities in the annulus.

As mentioned in the introduction, it is not known whether the corrosion-rate - power-density relationship for these niobium alloys is of the same general form as that for Zircaloy-2. However, it is worth noting that if this relationship is valid for these niobium alloys, the values of K for beta-quenched materials indicated by the results in Fig. 10.5 were much less than those for Zircaloy-2 (5 to 10 mpy vs 40 mpy for Zircaloy-2). The K values for the heat-treated materials, on the other hand, were probably not substantially different from those for Zircaloy-2. The results obtained with the channel specimens are

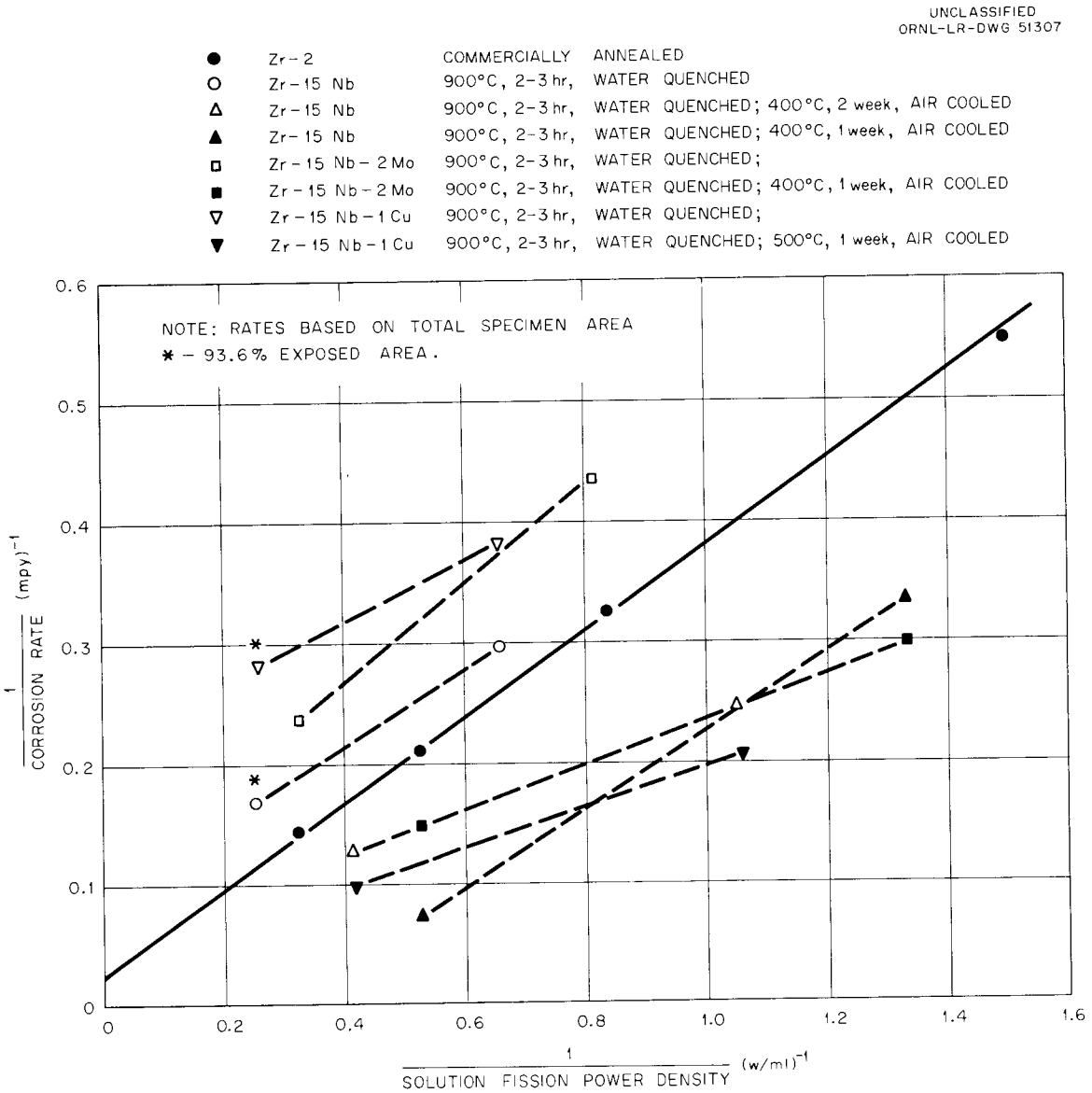

Fig. 10.5. Average Corrosion Rates of Chemically Polished Zirconium-Alloy Core-Annulus Coupons ($\frac{1}{2} \times \frac{1}{2}$ in. Coupons, 94.4% Exposed Area).

considered as evidence that uranium sorption plays an important role in the in-pile corrosion of these alloys just as it does for Zircaloy-2 specimens.

The observations in this experiment that the corrosion resistance of the beta-quenched materials was better than that of Zircaloy-2 and that the resistance decreased substantially upon heat treatment are in line with results in previous loop experiments.[9]

Zr-1Cr Alloy.--The AR results obtained with three specimens of Zr-1Cr alloy are plotted in Fig. 10.6. There was little difference between the corrosion resistance of this material and that of Zircaloy-2, and in this respect the results agree with the previous autoclave test of this material.[4]

UNCLASSIFIED
ORNL-LR-DWG 51308

MATERIAL	TREATMENT		AREA (cm^2) TOTAL	EXPOSED	% EXPOSED AREA
Zr-15Nb-1 Cu	900°C, 2 hr, WATER QUENCHED	●	2.19	1.42	64.8
	900°C, 2 hr, WATER QUENCHED	▲	2.19	1.57	71.6
Zr-15Nb-2 Mo	900°C, 3 hr WATER QUENCHED	■	2.19	1.42	64.8
Zr-1Cr	750°C, 1 hr, AIR COOLED	♦	2.19	1.42	64.8

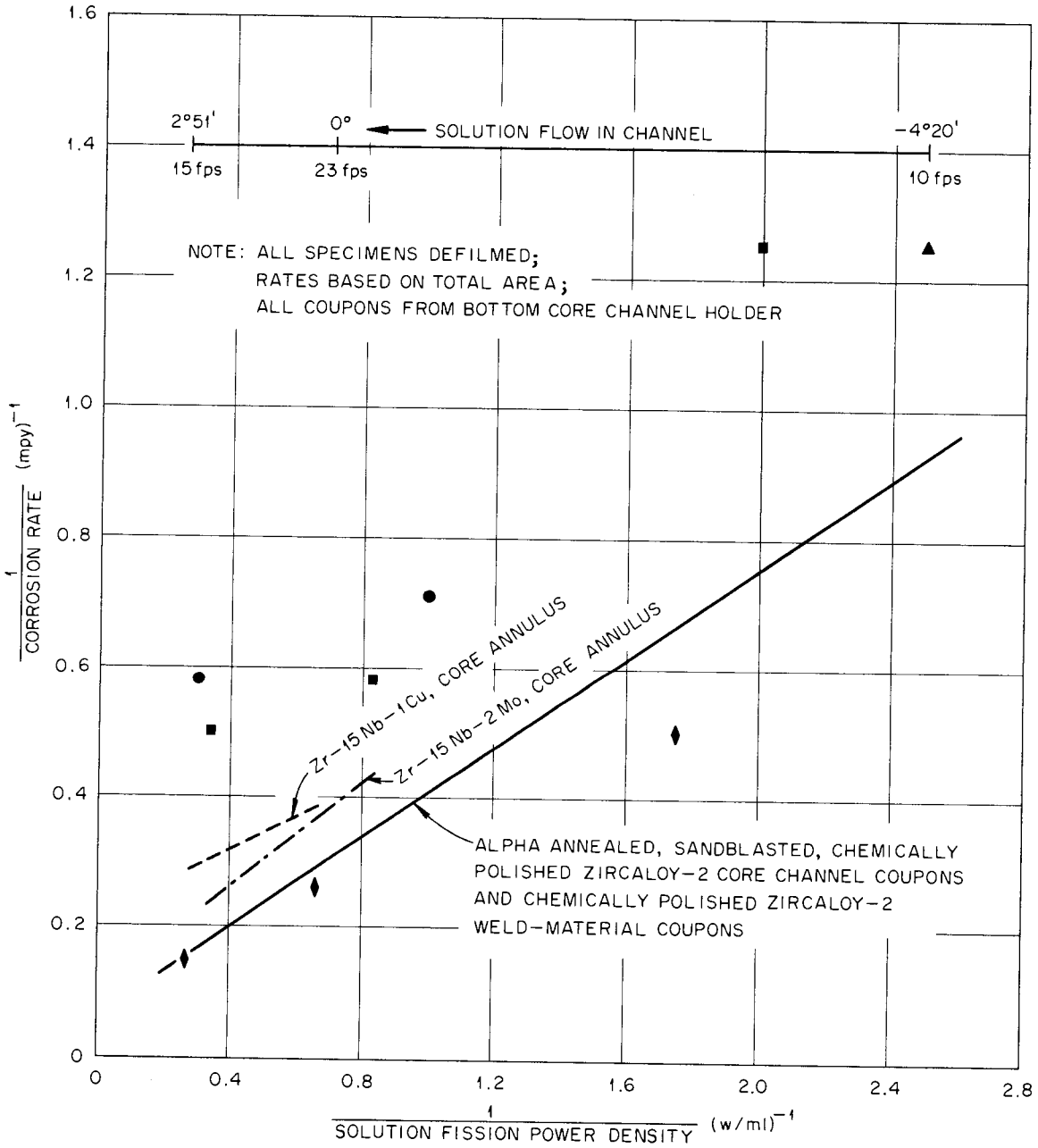

Fig. 10.6. Average Corrosion Rates of Chemically Polished and Heat-Treated Zirconium-Alloy Core-Channel Coupons (¼- by ½-in. Coupons).

10.1.4 Conclusions

1. At 280°C at least, the value of the factor K in Eq. (1) is probably the same for machined as for chemically polished Zircaloy-2 surfaces, for Zircaloy-2 fabricated to given random grain orientations as for material having preferred grain orientations, and for D_2O solutions of uranyl sulfate as for solutions employing H_2O solvent.

2. Under a given set of conditions in this experiment, surfaces which were chemically polished, overground, or sandblasted followed by chemical polishing corroded to about equal extents. Sandblasting alone had a deleterious effect on the corrosion resistance of Zircaloy-2 at some power-density levels.

3. Specimens of weld and air-contaminated weld materials corroded at about the same rate as stock Zircaloy-2.

4. The corrosion on covered Zircaloy-2 surfaces was substantially greater than that on surfaces exposed to flowing solution. The value of α on the covered surfaces may have been as high as 15; that on the exposed surfaces was as low as 1.5 to 2 under some flow conditions.

5. The value of α for the covered surfaces was probably greater than the value of 6 to 8 deduced from the results of previous experiments which employed H_2O solutions of UO_2SO_4.

6. The results for two specimens of crystal-bar zirconium indicate a K value of about 20 mpy for this material, a value in near agreement with that determined in previous experiments. Uranium sorption on crystal-bar zirconium, as measured by the value of α, was greater than that on Zircaloy-2.

7. Specimens of Zr-15Nb, Zr-15Nb-2Mo, and Zr-15Nb-1Cu in the beta-quenched condition showed better corrosion resistance than Zircaloy-2. However, specimens of these materials heat-treated at 400 to 500°C for one to two weeks showed poorer corrosion resistance than Zircaloy-2. The results provide evidence that uranium sorption plays an important role in the in-pile corrosion of these materials just as it does for Zircaloy-2 and zirconium. It is possible that the performance of some of the heat-treated alloys was poorer than that of Zircaloy-2 because of a difference in the uranium sorption.

8. The Zr-1Cr alloy suffered radiation-induced corrosion in about the same amount as Zircaloy-2.

10.2 SUPPORTING RESEARCH

10.2.1 Electrochemical Studies of Zircaloy-2 Corrosion

The measurement of corrosion rates by the linear polarization technique[10] was extended to temperatures above 250°C. The apparatus was modified to permit the temperature of the Teflon seals to be held near 25°C while the system operated at the higher test temperature. This modification required that a new method be developed for attaching the test sample to the external measuring instruments. In one method the test sample was threaded on to a zirconium wire. This proved unsatisfactory because electrical contact was lost, probably due to oxide growth between the threads on the wire and test sample. Several other experiments were performed with the test sample discharge-welded to the zirconium

wire. This technique was unreliable because the samples were lost during exposure or upon removal from the reaction cell. The best results, reported here, were obtained when the zirconium wire was Heliarc-welded to a machined tip on the test sample. However, there is still some question in the interpretation of the results obtained with this method of attachment, because the rate on the welded areas was apparently higher than on the other areas (white oxide was formed).

In the experiment reported, rate-time measurements were performed on a machined Zircaloy-2 specimen (obtained from Allegheny-Ludlum) in 0.05 *m* H_2SO_4, 300 ppm O_2 (25°C), at 258°C. The results for the first 1600 min can be satisfactorily expressed by an equation of the form:

$$1/R = 1/A + Bt \ , \qquad (2)$$

where R is the corrosion rate in μg of oxygen per cm^2 per min; A is a constant, 0.57, B is a constant equal to 0.37 cm^2 per μg of oxygen; and t is the time in minutes. From 1600 to 3600 min the rate decreased to a steady-state rate of 0.14 mpy (0.0014 μg of oxygen per cm^2 per min) and remained constant at this rate until the experiment was terminated at 18,000 min. The value of A is not reliable (as an initial rate) because of uncertainty in the initial exposure time.

The area of the welded section which exhibited the white oxide was estimated to be 0.06 cm^2 or about 1% of the total area. Its contribution to the corrosion current for the major portion of the experiment was probably negligible. However, at the steady state, it is conceivable that the welded section could have been generating a significant part of the measured corrosion current.

The potential-time behavior for this specimen at 258°C was similar to that previously observed[10] for the Firth-Sterling alloy at 208°C. However, at these higher temperatures, the observed potential changes occur in a much shorter time interval, and the steady-state potential was observed to be -1.150 ± 0.100 v, compared to -0.550 ± 0.100 v at 208°C.

The current-potential behavior for the anodic and cathodic reactions on the Zircaloy-2 specimen is presented in Fig. 10.7. The Tafel slope for oxygen reduction is 0.220 v, and the calculated $\alpha_c Z_c = 0.48$. A one-point estimate for the anodic Tafel slope was performed, and gave a value of $b_a = 1.060$ v, with $\alpha_a Z_a = 0.1$. An extrapolation of the cathodic curve to the open-circuit potential, E_o, gave a value for the corrosion current of 3.3×10^{-7} amp/cm^2 (0.13 mpy). About the same value, 3.6×10^{-7} amp/cm^2 (0.14 mpy), was obtained for the corrosion current from a small current polarization measurement, $(dn/dI)_{n \to o}$, and using the equation

$$I_{corr} = \frac{RT/F}{(\alpha_a Z_a + \alpha_c Z_c)\ (dn/dI)_{n \to o}} \ ,$$

where $(\alpha_a Z_a + \alpha_c Z_c) = 0.58$ (see Fig. 10.7).

It can be concluded that this modification of the equipment yields satisfactory results. The welded junction, which led to some question in the interpretation of the results, will be eliminated in future measurements.

The observed rate-time behavior furnished further evidence for the logarithmic oxidation kinetics.

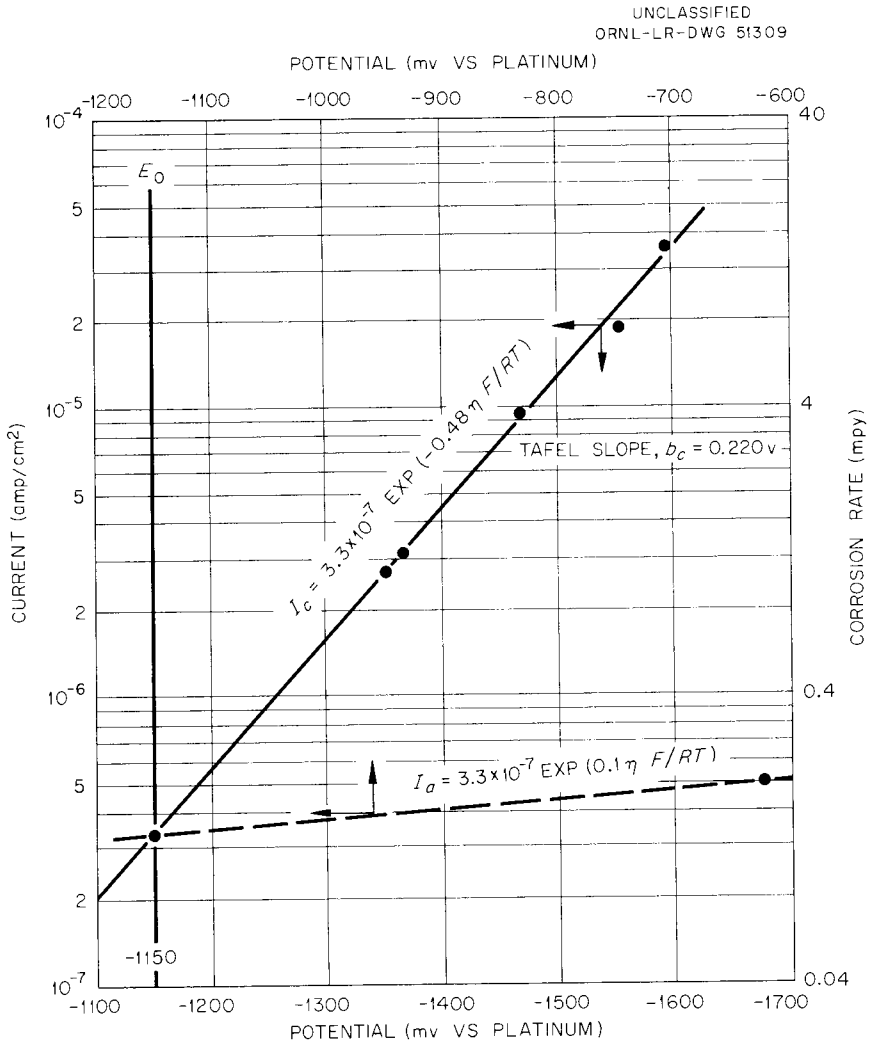

Fig. 10.7. Experimental Current-Potential Plot for Machined Zircaloy-2 Specimen in 0.05 m H_2SO_4, 250 psi O_2 (25°C), 258°C, Time = 10,000 min.

At these higher temperatures the rate of film growth is greatly accelerated, and since the potential is a function of the oxide thickness, the potential changes would be expected to occur in a much shorter time interval as observed. Furthermore, the lower steady-state potential observed at 258°C is consistent with the greater amount of oxide formed.

REFERENCES

1. J. E. Baker, Preliminary Results from In-Pile Loop Experiment 0-1-25 (in preparation).

2. G. H. Jenks et al., HRP Prog. Rep. Oct. 31, 1959, ORNL-2879, p 130-132.

3. G. H. Jenks et al., HRP Prog. Rep. July 31, 1958, ORNL-2561, p 221-224.

4. G. H. Jenks et al., HRP Prog. Rep. Oct. 31, 1959, ORNL-2879, p 143-144.

5. J. E. Baker and G. H. Jenks, HRP Radiation Corrosion Studies: In-Pile Loop L-4-8, ORNL-2042.

6. G. H. Jenks et al., HRP Prog. Rep. Oct. 31, 1959, ORNL-2879, p 138.

7. G. H. Jenks, A Model for the Effects of Irradiation on Zircaloy-2 Corrosion and a Review and Correlation of In-Pile Zircaloy-2 Corrosion Data (in press).

8. G. H. Jenks et al., HRP Prog. Rep. Oct. 31, 1956, ORNL-2222, p 109.

9. G. H. Jenks et al., HRP Prog. Rep. Oct. 31, 1958, ORNL-2654, p 159-160.

10. G. H. Jenks and A. L. Bacarella, HRP Prog. Rep. Jan. 31, 1959, ORNL-2696, p 144-146.

PART IV. SLURRY FUELS

11. ENGINEERING AND PHYSICAL PROPERTIES

H. W. Hoffman
D. G. Thomas

11.1 EFFECT OF pH ON THE RHEOLOGICAL CHARACTERISTICS OF ThO_2 SUSPENSIONS

In previous experiments[1,2] with flocculated ThO_2 suspensions, shear diagrams were obtained with as-received materials for which the pH varied between 4 and 10. Since it was believed that the yield stress and the coefficient of rigidity of the suspensions should not be independent of the acidity level, a systematic study of the influence of pH on these laminar-flow properties was undertaken.

Glass and calomel electrodes immersed in the suspension were used to indicate the pH. While no entirely satisfactory theoretical interpretation[3,4] of the results so obtained is possible, this technique was adopted in the interest of simplicity and expediency. The suspension pH was varied from 1.6 to 12 by additions of sulfuric acid, chromic acid, or sodium hydroxide. In the absence of additives, the suspension pH was 8.1 for concentrations ranging from 0.069 to 0.154 volume-fraction solids. The acid suspensions contrasted a second effect in that the HSO_4^- ion is strongly adsorbed by ThO_2, while the chromate ion is virtually unabsorbed.[5] The mean particle diameter of the thorium oxide was 1.35 microns.

The results are shown in Fig. 11.1 for a constant volume-fraction solids of 0.090. It was observed that the ratio of the coefficient of rigidity of the suspension to the absolute viscosity of the suspending medium (η/μ) was relatively constant (2.6 minimum to 3.9 maximum) over the full pH range. This lack of dependency of η/μ on pH seems to be characteristic of almost all ThO_2 suspensions studied[1,2] regardless of the physical parameters of the particles. In contrast, the yield stress, τ_y, varied nearly fivefold within the same pH limits. The effect of the anion (HSO_4^- or $CrO_3^=$), which is quite marked at pH = 1.6, diminishes rapidly and is of little significance at pH levels above 4.

The ±20% variation in the yield stress (in the range pH = 4 to 10) as the result of pH changes may explain part of the scatter in the previously reported correlations.[1,2]

REFERENCES

1. H. W. Hoffman et al., HRP Prog. Rep. Oct. 31, 1959, ORNL-2879, p 159-61.

2. P. R. Kasten et al., HRP Prog. Rep. July 31, 1958, ORNL-2561, p 86-87.

3. H. R. Kruyt (ed.), Colloid Science, Vol I, Elsevier Publishing Co., Amsterdam, 1952.

4. J. Th. G. Overbeek, J. Colloid Sci. 8, 593-605 (1953).

5. M. E. Wadsworth et al., Progress Reports, Institute for the Study of Rate Processes, University of Utah, Salt Lake City, Utah (Feb. 15, 1958 to Jan. 11, 1960).

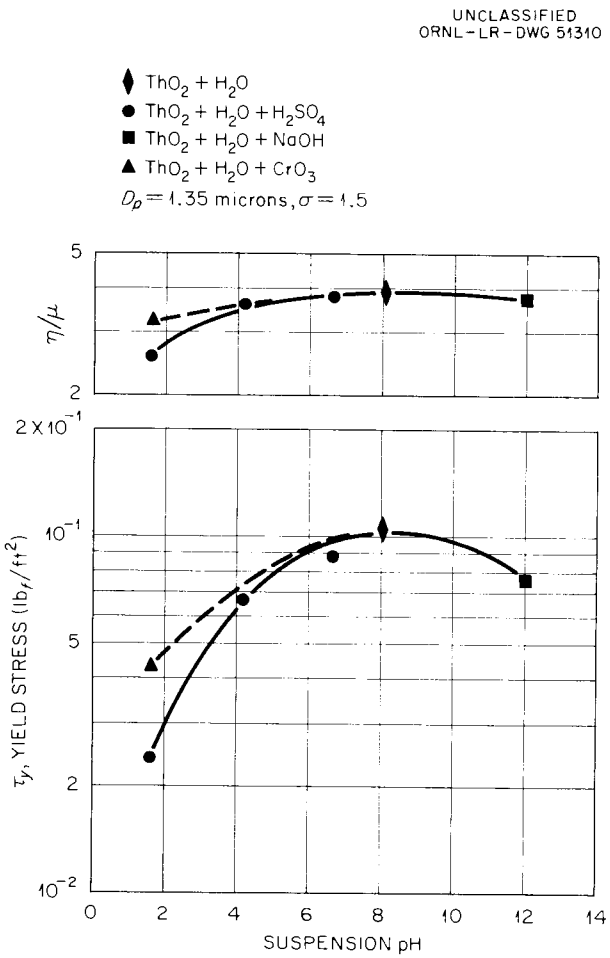

Fig. 11.1. Effect of Suspension pH on Yield Stress and Coefficient of Rigidity. Volume-fraction solids = 0.090.

12. THORIUM OXIDE IRRADIATIONS

J. P. McBride

Work on the effect of reactor irradiation on the properties of thorium oxide continued with the examination of the second series of dry thoria powders irradiated in aluminum capsules in a lattice position of the LITR and the slurry of 18-μ Houdry spheres irradiated in a settled condition in hole C-43 of the LITR.

12.1 THORIA-POWDER IRRADIATION

Examination of the C-series of dry thoria powders fired at 650, 800, 900, 1100, and 1500°C (starting material 650°C-fired D-16 ThO_2)[1] and irradiated for 22 months in the LITR was completed.[2] Sixteen months of the irradiation was in the C-52 lattice position and the remainder in the C-21 lattice position. As with the D series of oxides (irradiated 16 months),[2] the 650, 800, and 900°C-fired samples were red and had agglomerated into hard, glossy clinkers. Similarly, the 1100 and 1500°C-fired oxides were powders of off-white and blue colorations. Specific surface areas for all series C and D oxides except the 1500°C-fired materials were markedly decreased by the irradiation (Table 12.1). Estimated maximum temperatures of the powders during irradiation were less than 300°C. The marked decrease in specific surface areas with all except the high-fired oxides indicate again that irradiation produces about the same sintering effect as firing the oxide to 1500°C.

The series C irradiated powders were poured from the aluminum irradiation capsules, and the material remaining in the capsules was submitted for neutron-activation - sedimentation particle-size analysis. An attempt was made to obtain a representative sample of powder poured from the D-series tubes. The particle-size distribution data, obtained after 8 months or more cooling and using the gross induced activity, showed a general reduction in average particle size of as much as a factor of 2 in some cases (Table 12.1) and a substantial production of fines less than 0.6 μ in size (Table 12.2). The fraction of particles or agglomerates larger than 7.1 μ was also decreased. Substantial changes in fraction of material in the oxide particles in the size range 0.6 to 7.1 μ did not occur. Hence, the radiation effect of probably most concern is the production of fines which might lead to cake formation or other undesirable changes in slurry properties. The particle-size data for series C do not reflect the obvious "clinker" formation observed in the lower fired oxides,[2] since the only material submitted for analysis was that which clung to the walls of the irradiation container when the bulk of the irradiated material was poured out.

The results of irradiating oxides fired at different temperatures indicate the desirability of using a high-fired oxide in a blanket slurry (Table 12.2). The production of fines of <0.6 μ in the low-fired oxide was large compared to that of the 1500°C-fired material. The choice of the D-16 oxide for the irradiation experiments makes the data difficult to interpret because of its broad size distribution and plate-like particle shape. Dry-powder irradiations with carefully classified oxides of more cubic shape will be carried out.

Table 12.1. LITR Thoria Powder Irradiations

Maximum Temperature <300°C

Oxide Firing Temp. (°C)	Thermal-Neutron Flux x 10^{-13}		Average Particle Size (μ)			Specific Surface Area (m^2/g)		
	Series D	Series C	Before Irradiation	After 489 days (Series D)	After 659 days (Series C)	Before Irradiation	After 489 days (Series D)	After 659 days (Series C)
650	2.6		2.4		1.3	28	1.0	<0.5
800	1.6	1.1	2.7		3.5	15	<0.5	<0.5
900	1.7	1.0	2.4		1.7	8	<0.5	<0.5
1100	1.5	1.1	3.1	2.9	1.4	3.3	1.9	0.6
1500	1.4	1.1	4.7	3.3	2.4	0.8	0.8	0.8

Table 12.2. Particle Size Distribution of Irradiated Thoria Powders

Irradiation condition: 489 days at 1.6 x 10^{13} neutrons/cm^2·sec
659 days at 1.1 x 10^{13} neutrons/cm^2·sec
Dispersant: 0.001 *M* $Na_4P_2O_7$

Particle-Size Increment (μ)	Weight Per Cent of Material Within Indicated Size Increment											
	650°C-Fired		800°C-Fired		900°C-Fired		1100°C-Fired			1500°C-Fired		
	Before Irradiation	After 659 days	Before Irradiation	After 659 days	Before Irradiation	After 659 days	Before Irradiation	After 489 days	After 659 days	Before Irradiation	After 489 days	After 659 days
>25.6	3	3	8	1	2	1	5	4	1	16	9	1
7.1-25.6	16	14	14	19	21	8	18	13	4	19	13	6
3.0-7.1	25	17	24	35	20	27	29	33	26	29	34	36
1.0-3.0	37	24	35	26	40	31	35	30	31	30	28	35
0.6-1.0	11	9	12	6	15	8	12	5	16	5	5	9
<0.6	8	34	6	13	2	26	1	15	22	1	11	13

At the end of the 489-day irradiation a calculated 0.09% of the thorium atoms were fissioned, and at 22 months, 0.12%. Both irradiations produced about 0.4% mass-233 isotopes. The effective neutron-capture cross section of thorium based on thermal flux alone under the conditions of the irradiation appeared to be about 8.4 barns.

The aluminum capsules in which the powders were canned were 1/2 in. OD, 1/4 in. ID, and 2-1/2 in. long. Each contained a cobalt and a titanium flux monitor. They were irradiated in such a way that the reactor cooling water flowed over the outside of the capsules.

12.2 HOUDRY-SPHERE SLURRY IRRADIATION

Particle-size data were obtained on the slurry of Houdry spheres, 18 μ in average size and containing 0.12% natural uranium, which was irradiated 48 days in a settled condition in hole C-43 of the LITR at a thermal flux of 2×10^{13} neutrons/cm^2·sec and temperatures from 180 to 280°C.[2] When the stainless steel irradiation autoclave was opened,[3] a dried plug of yellow solid was found at the top of the autoclave, apparently deposited as a result of the refluxing introduced by the downflow air cooling. Approximately 1.7 ml of slurry containing about 20% of the solids originally added was drained from the bomb. A comparison of particle-size data on the original Houdry spheres containing 0.12% of adsorbed uranium with both the dry- and wet-irradiated slurry solids (Table 12.3, Fig. 12.1) showed a substantial increase in the size fraction less than 9.6 μ for the irradiated materials. A similar thoria-sphere preparation of 11 μ average size showed essentially no degradation upon being pumped as a slurry for as long as 550 hr at 175°C in a 100A loop.[4]

About 0.06 wt % of mass-233 isotopes was produced during the irradiation, and 0.0004% of the thorium atoms were fissioned.

Table 12.3 Particle Size of Irradiated Houdry Spheres

Irradiation time: 48 days
Average thermal flux: 2.2×10^{13} neutrons/cm^2·sec
Dispersant: 0.001 *M* $Na_4P_2O_7$

Particle Size Increment (μ)	Wt % Within Indicated Size Increment		
	Spheres plus 0.12% U	Dried Slurry Fraction	Wet Slurry Fraction
>25.6	12	6	4
14.8-25.6	66	48	63
11.4-14.8	17	19	10
9.6-11.4	3	3	2
5.0-9.6	1	14	9
<5.0	1	10	12
<1.0	0	3	2

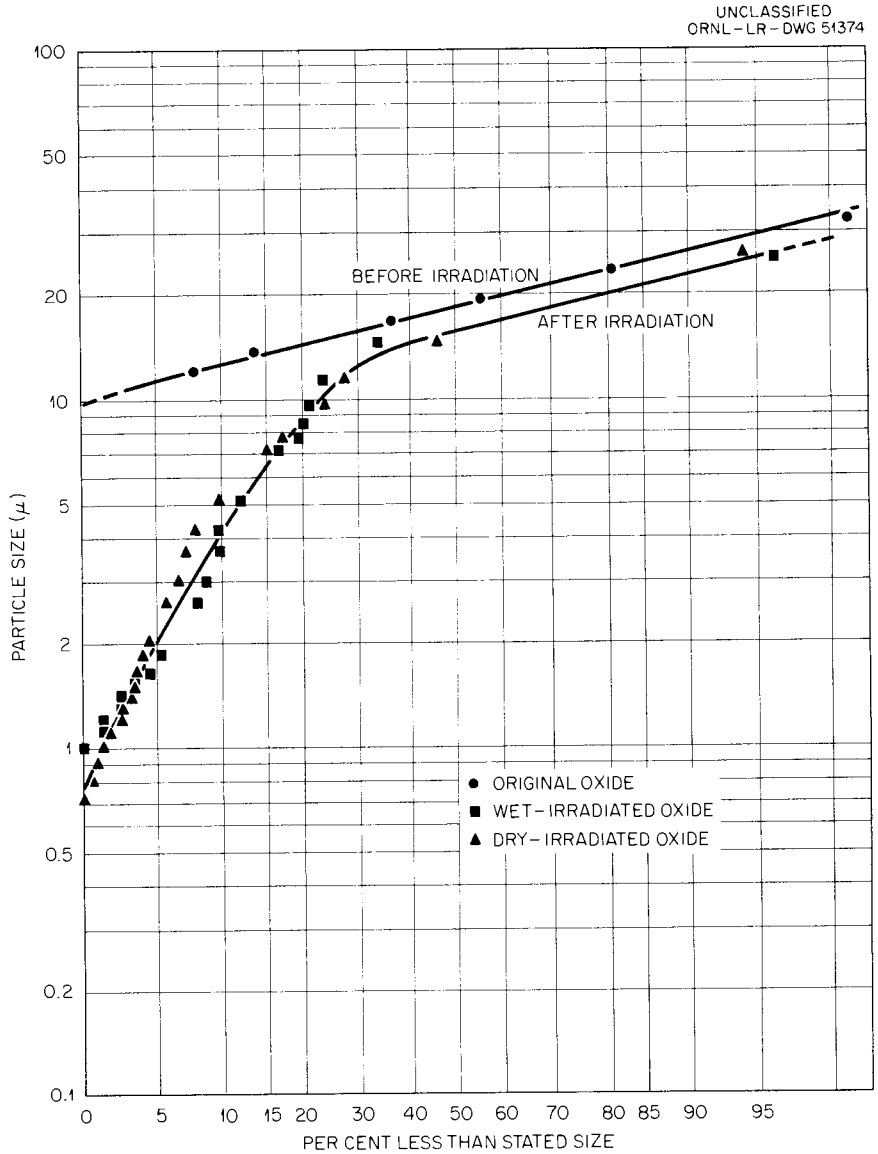

Fig. 12.1. Particle-Size Distribution in Irradiated Thoria Spheres. Irradiation time, 48 days; flux, 2×10^{13} neutrons/cm^2·sec; temperature, 180 to 280°C.

REFERENCES

1. W. H. Carr, HRP Quar. Prog. Rep. July 31, 1955, ORNL-1943, p 182-198.

2. J. P. McBride and O. O. Yarbro, HRP Quar. Prog. Rep. Apr. 31, 1960, ORNL-2947, pp. 82-86.

3. R. E. McDonald, Metallurgy Division.

4. E. L. Compere et al., HRP Quar. Prog. Rep. Apr. 30, 1959, ORNL-2743, p 126.

13. DEVELOPMENT OF GAS-RECOMBINATION CATALYST

J. P. McBride L. E. Morse

Studies of the reaction rates of deuterium or hydrogen and oxygen mixtures in aqueous thorium-uranium oxide slurries containing the "sol-prepared" palladium catalyst[1] were continued with slurries of interest to the in-pile slurry loop and corrosion programs of the HRP. Particular attention was given to the initial rates of reaction obtained when the gas mixtures were first added to the reaction autoclave and where the composition of the gas was most clearly defined. For a given series of experiments, an effort was made to keep one gas at a constant initial partial pressure and to vary the partial pressure of the other gas in an effort to define the pressure region where activity was maintained and to delineate the kinetics of the catalyzed recombination.

There was substantial evidence that the initial recombination rate observed was considerably influenced by the residual gas phase remaining at the end of the previous recombination experiment and the past history of the slurry-catalyst system. In addition, more often than not the recombination reaction was only partial and terminated in an apparent equilibrium or very slow recombination-rate condition in which both hydrogen and oxygen were present in the gas phase. Commonly, also, it was necessary to reach a certain threshold partial pressure for the gas not in excess in order to achieve any reaction whatsoever. Hence, while some empirical correlations were obtained between the gas-phase compositions and the observed reaction rates, the above considerations render such correlations of doubtful validity. They also point up the advantage of developing a continuous gas production-recombination apparatus which could be operated at steady state to obtain information on the kinetics of the catalyzed recombination reaction.

13.1 SLURRY SAMPLE FROM OUT-OF-PILE TEST RUN OF IN-PILE SLURRY LOOP

Experiments were carried out with a slurry sample (L2-26S-6-4) from the in-pile slurry loop test run. The slurry was prepared from a 1000°C-fired Th - 0.5% U oxide and contained 549 g of Th per kg of D_2O and 640 ppm of Pd (based on thorium) as catalyst. The slurry had been pumped several hundred hours under approximately 200-psi oxygen in excess of steam at 280°C, during which several deuterium-oxygen recombination experiments were performed in the loop and a dropoff in specific catalytic activity with a half life of several hundred hours was observed.[2]

Recombination experiments at 280°C were carried out with this sample over a period of 25 days. During the series the initial oxygen overpressure (added first to the reaction vessel) was maintained essentially constant at 220 to 245 psi. In the initial experiments about 100 psi of hydrogen was added, and the initial recombination rates were 23.7 to 27.3 psi/min; residual gas pressures, where recombination had essentially ceased, were 216 to 232 psi. The calculated H_2/O_2 ratios in the residual gases were 0.08 to 0.15. In subsequent experiments over the period of 25 days, it was necessary to increase the hydrogen

partial pressure successively to 200, 300, 350, 450, and 500 psi in order to obtain reaction. At the same time, the gas remaining when recombination had virtually ceased increased progressively to as high as 571 psi in excess of steam, and the calculated H_2/O_2 ratio in the residual gas increased to as high as 2.3 (Table 13.1). Hence it appears that the catalyst underwent considerable change during the period of operation, most of which time the system was under a partial pressure of oxygen in excess of stoichiometric. While it is difficult, in the absence of knowledge as to the exact role played by the hydrogen and oxygen in the recombination reaction, to say anything about changes in specific activity of the catalyst during this period, the data confirm, qualitatively, the apparent reduction in specific catalytic activity observed in the slurry loop experiments.

Table 13.1. Palladium Catalysis in Slurry Loop Sample

640 ppm Pd/Th; 549 g Th/kg D_2O; 1000°C-fired Th - 0.5% U oxide; 280°C
220-245 psi O_2 initial pressure

Time After Initial Experiment (days)	Initial Gas Phase: Total Pressure Minus Steam (psi)	Initial Gas Phase: D_2/O_2 Ratio	Initial Reaction Rate (moles H_2/liter·hr)	Residual Gas Phase*: Total Pressure Minus Steam (psi)	Residual Gas Phase*: Calculated D_2/O_2 Ratio
1	339	0.4	1.7	210	0.1
5	461	0.8	2.1	223	0.1
20	517	1.2	0.5	504	1.1
21	580	1.5	2.5	439	1.3
22	659	1.7	2.9	464	1.5
25	721	2.3	2.8	571	2.3

*Gas phase when reaction appeared to have stopped.

13.2 SLURRY SAMPLE FOR IN-PILE CORROSION STUDIES

Additional laboratory recombination studies were undertaken with a slurry of thorium - 13% uranium oxide containing 91.7 g of Th per kg H_2O and 113 ppm of Pd (based on thorium) of the "sol-prepared" palladium catalyst to obtain more information on conditions under which high catalytic activity could be maintained. An analogous slurry in D_2O at approximately eight times the slurry concentration and more than 20 times the catalyst concentration (i.e., Pd/Th) used in an in-pile experiment showed unusually low catalytic activity.

In 11 experiments at 280°C with total gas pressures in excess of steam which were increased from 350 to 800 psi and H_2/O_2 ratios in the gas phase from 0.38 to 0.78, only 4 showed reactions indicating a possible deactivation effect of excess oxygen. Where reactions were obtained, an over-all 1/2-order dependence of rate on Knallgas pressure was observed. Increasing the D_2/O_2 ratio to 0.9 and higher resulted in a consistent series of reactions, most of which showed a first-order rate dependence on Knallgas pressure. However, recombination of the hydrogen and oxygen was only partial in all cases.

Table 13.2 shows the results of a number of experiments in the above series in which the initial hydrogen pressure was maintained at about 300 psi by the

Table 13.2. Palladium Catalysis in Thorium - 13% Uranium Oxide Slurry

91.7 g of Th per kg of H_2O; 113 ppm Pd/Th; 280°C

Initial Gas Phase			Initial Reaction Rate (moles H_2/liter·hr)		Apparent Reaction Order Based on Knallgas	Final Gas Phase[b]		
O_2 (psi)	H_2 (psi)	H_2/O_2 Ratio	Observed	Calculated[a]		Total Pressure (psi)	Calculated[c] H_2/O_2 Ratio	Calculated[c] H_2 Partial Pressure (psi)
335	301	0.90	1.4	0.12	1	522	0.76	225
297	288	0.47	2.3	0.20	1	509	0.92	224
265	296	1.12	1.6	0.24	0.74	491	1.09	236
235	293	1.25	1.7	0.26	1	429	1.12	227
202	293	1.45	1.8	0.35	1	396	1.34	227
169	303	1.79	2.0	0.33	1	349	1.73	221
128	301	2.35	2.3	0.24	1	297	2.54	213
84	298	3.54	2.8	0.27	0.86	-	-	-

[a]From first-order rate constant based on Knallgas pressure and indicated initial hydrogen pressure.

[b]Gas phase when reaction appeared to have stopped.

[c]Calculated from H_2 addition and pressure decrease, assuming $H_2 + 1/2\ O_2 \rightarrow H_2O$.

addition of hydrogen alone after each recombination experiment, the only oxygen being that in the gas phase at the end of the previous run. As with the sample from the slurry loop experiments, there was a gradual increase in the calculated H_2/O_2 ratio in the residual gas phase as successive experiments were performed. The results are not inconsistent with a possible poisoning of the catalyst by a trace impurity in the added gases, possibly CO. An effort will be made to determine if this is the case.

An initial reaction rate based on the first-order rate constant and the initial hydrogen pressure was calculated. In addition to the differences between the observed and calculated rates, the observed initial rates increased (with one inconsistency) with decreasing oxygen concentration, while the calculated rates showed a pronounced maximum. Both relations are consistent with a reaction involving strong adsorption of oxygen on the catalyst.

REFERENCES

1. J. P. McBride and L. E. Morse, HRP Quar. Prog. Rep. Apr. 30, 1960, ORNL-2947, p 87.

2. E. L. Compere et al., HRP Quar. Prog. Rep. Apr. 30, 1960, ORNL-2947, p 107; see also Sec. 14.4 of this report.

14. SLURRY CORROSION AND BLANKET MATERIALS TESTS

E. L. Compere H. C. Savage

J. M. Baker
S. J. Ball
S. E. Bolt
V. A. DeCarlo
R. B. Gallaher
D. B. Hinton*
W. J. Leonard
R. A. Lorenz
R. E. McDonald
S. A. Reed
A. J. Shor
A. J. Taylor
L. F. Woo

14.1 THORIA-PELLET TEST PROGRAM

14.1.1 Introduction

As an aid to developing thoria pellets which would be suitable for a reactor blanket material,[1] a series of evaluation tests has been made to determine the integrity and relative attrition rates of a group of 24 experimental pellet preparations which were fabricated by the Ceramics Group of the ORNL Metallurgy Division.[2] The group of pellets resulted from a systematic study of composition and fabrication variables associated with the manufacture of pellets from a specific preparation (batch D-40) of thoria powder.

The group was comprised of both flat-ended and spherical-ended pellets (approximately 0.2 x 0.2 in.) which were made from ThO_2 precalcined at three temperatures, 800, 1200, and 1425°C. Final calcination of all pellet preparations was at 1650°C. Twelve of the preparations contained ~0.5 wt % CaO. Half of the samples had been tumbled after final firing to remove easily abraded projections; the rest of the group had not been tumbled.

By chemical analysis, it was found that the group of pellets to which no CaO was intentionally added contained calcium in an amount equivalent to ~0.05 wt % CaO.

14.1.2 Evaluation Tests

Each pellet preparation was evaluated in the same manner by determining weight changes after exposure at room temperature in ball-mill tests and in spouted-bed tests[3,4] before and after 72-hr tests in static autoclaves at 260°C.[3] The various fabrication variables and the results of the evaluation tests are shown in Table 14.1.

The room-temperature ball-mill tests were made at 155 rpm in a 3.75-in.-ID, 750-ml, rubber-lined steel jar mill, charged with 250 ml of H_2O and approximately 45 g of pellets (40 to 50 pellets). After each of two 1-hr exposures, the pellets were dried to constant weight in an oven at 120°C.

---

*Summer Research Participant, University of Tennessee

Table 14.1. Test Results in Evaluation of Thoria-Pellet Preparation Variables

PREPARATION		WEIGHT LOSS RATES										
		Ball Mill, %/hr			Initial Spouted Bed, %/hr			Static Autoclave %/hr x 10^5 (72 hr)	Ca Leached Out, % of Original	Final Spouted Bed, %/hr (Post-Autoclave)		
Code	Identification No.*	1st hr	2nd hr	Overall	1st hr	2nd hr	Overall			1st hr	2nd hr	Overall
0.5 wt % CaO Added												
					Flat-End Pellets							
P-53	1 C F T	0.96	0.96	0.96	0.30	0.36	0.33	20	0.67	1.69	1.12	1.40
-54	1 C F N	3.29	1.19	2.22	1.10	0.42	0.76	60	0.84	5.06	1.23	3.12
-55	2 C F T	1.03	1.21	1.11	0.26	0.35	0.31	4	0.35	0.64	0.79	0.71
-56	2 C F N	3.21	1.39	2.28	1.34	0.62	0.98	10	0.96	0.93	0.81	0.86
-57	3 C F T	2.04	1.14	1.59	0.41	0.50	0.45	20	0.50	1.00	0.69	0.84
-58	3 C F N	4.14	1.18	2.64	1.88	0.68	1.28	10	0.69	0.69	0.51	0.60
					Round-End Pellets							
P-59	1 C R T	1.53	1.43	1.47	0.88	0.76	0.82	400	2.98	72.85 H		
-60	1 C R N	4.12	1.67	2.86	1.80	0.95	1.37	600 H	4.51 H	56.06		
-61	2 C R T	0.76	0.88	0.82	0.21	0.25	0.23	8	0.28 L	0.62	0.69	0.65
-62	2 C R N	1.43	1.02	1.21	1.00	0.58	0.79	3 L	1.12	13.29	0.84	7.06 H
-63	3 C R T	0.20 L	0.25 L	0.22 L	0.12 L	0.14 L	0.13 L	40	0.34	0.30 L	0.36 L	0.33 L
-64	3 C R N	0.53	0.36	0.45	0.32	0.23	0.27	30	0.73	0.41	0.42	0.42
No CaO Added												
					Flat-End Pellets							
P-65	1 X F T	1.08	1.46	1.27	0.19	0.32	0.26	40		0.55	0.56	0.55
-66	1 X F N	3.62	1.77	2.66	1.45	0.76	1.10	70		0.81	0.79	0.80
-67	2 X F T	1.16	1.36	1.26	0.33	0.59	0.46	100		0.77	0.67	0.72
-68	2 X F N	3.67	1.56	2.59	1.90	0.52	1.21	100		0.88	0.92	0.90
-69	3 X F T	1.98	1.22	1.59	0.27	0.33	0.30	70		0.56	0.54	0.55
-70	3 X F N	5.03	1.50	3.23	1.85	0.78	1.31	90		0.74	0.72	0.73
					Round-End Pellets							
P-71	1 X R T	2.41	2.05	2.21	0.55	0.58	0.56	90		0.98	0.96	0.96
-72	1 X R N	7.14 H	2.34 H	4.65 H	4.33 H	1.32 H	2.80 H	100		1.20	1.24 H	1.21
-73	2 X R T	1.20	1.42	1.30	0.42	0.50	0.46	100		0.68	0.76	0.72
-74	2 X R N	2.11	1.32	1.70	1.09	0.45	0.77	100		0.71	0.78	0.74
-75	3 X R T	0.81	1.13	0.97	0.34	0.57	0.45	70		0.62	0.66	0.64
-76	3 X R N	1.82	1.16	1.48	1.34	0.85	1.09	70		0.65	0.65	0.65

*Thoria powder calcined at (1) 800°C, (2) 1200°C, (3) 1425°C; Pellets (N) not tumbled or (T) tumbled 4 hr in H_2O with 3/8" dia. Al_2O_3 balls. C - contains 0.5 wt % CaO; X - contains no CaO; R - round-end pellets; F - flat-end pellets.

(H) Highest and (L) lowest values in each series are so indicated.

14.1.3 Test Results

Average 2-hr weight loss rates of pellets in the ball-mill test ranged from 0.22 to 4.65%/hr. The highest rate was shown by a round-end, nontumbled, CaO-free preparation (code P-72) which was compacted from 800°C-calcined ThO_2. The lowest rate was displayed by a preparation (code P-63) which was made from 1425°C-calcined ThO_2 powder with 0.5 wt % CaO that had rounded ends and had been tumbled after final calcination at 1650°C.

Average 2-hr rates of pellets exposed in initial spouted-bed tests ranged from 0.13 to 2.80%/hr. The same preparation (code P-63) which displayed the lowest average rate in the ball-mill tests showed the lowest rate in the spouted-bed tests. Similarly, the highest rate was displayed by the same preparation (code P-72) in both tests. The average weight loss rate (0.90%/hr) of pellets containing no additive was a factor of about 1.5 greater than the average rate (0.64%/hr) of pellets containing CaO additive. The pellets from the spouted-bed tests were subsequently exposed in static autoclave tests.

With flat-ended pellets, attrition rates in both ball-mill and spouted-bed tests increased as the ThO_2 precalcination temperature was increased from 800 to 1425°C; conversely, the attrition rates of cylinders with rounded ends decreased as the ThO_2 precalcination temperature was increased.

In 72-hr static autoclave tests, weight loss rates varied between 3 and 600 x 10^{-5}%/hr. As shown in Table 14.1, some calcium was leached from all preparations containing CaO as additive. The two preparations (code P-59 and P-60) which displayed the highest weight losses were those which lost the highest percentages of calcium. During subsequent exposure in spouted-bed tests, several pellets of both preparations disintegrated during the first hour of exposure. In general, preparations from which the highest percentages of calcium were leached displayed the highest rates during the post-autoclave spouted-bed tests. Thus the quality of the pellets was changed significantly due to the reaction of high-temperature water and the additive.

For the group of pellets containing no CaO as additive, the preparations which were tumbled after final calcination at 1650°C displayed rates in spouted-bed tests approximately twofold higher after autoclaving. No trend in rates of nontumbled pellets was observed.

14.2 HYDRIDING OF ZIRCONIUM-BASE ALLOYS: VELOCITY AND TEMPERATURE EFFECTS

Previous investigations[5] of the variables associated with hydriding of zirconium-base alloys during exposure to circulating aqueous slurries in toroids were concerned with the relative effects of (1) thoria or thoria-urania preparation variables, (2) operating atmospheres, (3) amount of gas overpressure, and (4) zirconium-alloy composition. Recent studies have been directed toward evaluating the effects of slurry flow velocity and of operating temperatures on the severity of hydriding.

Effect of Flow Velocity On Hydriding.--To determine the relative effects of flow velocity, a group of four tests was made at 10 fps to compare with previous runs made at 26 fps. Other test conditions duplicated those of several earlier runs.[5] Slurries of two mixed Th-U oxide preparations (6% and 9% U/Th) were

circulated at a concentration of 500 g of Th-U per kg of D_2O in 300-hr tests at 280°C. Four pin specimens of Zircaloy-2, item 569, were exposed in each test. Deuterium gas was charged to the toroids to provide total pressures of 10 psig in two toroids and 50 and 100 psig respectively in the other two toroids.

In previous tests conducted at 26 fps, specimens of item-569 Zircaloy-2 were grossly hydrided in 300-hr periods with 100 psi deuterium overpressure and specimens picked up significant quantities of deuterium in tests in which 10 to 50 psi overpressure of D_2 was used.[5]

Gross hydriding of the type previously observed in the higher flow velocity runs was not observed in the tests at 10 fps. Metallographic examinations revealed a concentration of zirconium hydride needles on the upstream areas of the pins to a depth of approximately 15 mils. The same effect, which extended to a depth of approximately 8 mils, was noted on the downstream areas of the specimens.

The extent of attack as well as the degree of hydriding was less at the lower velocity; e.g., weight losses of scrubbed specimens exposed at 10 fps ranged from nil to 0.3 mg/cm^2 as compared to losses of 4.8 to 7 mg/cm^2 for specimens exposed at 26 fps. Thus the severity of hydriding appeared to be directly related to the flow velocity, presumably as a result of more severe attack at the higher velocity under slug-flow conditions in the toroids.

Effect of Temperature On Hydriding.--Examination of specimens from toroid tests at 200°C revealed no evidence of hydriding of zirconium alloys, whereas frequent and sometimes severe hydriding of the alloys occurred when the same slurries were used in tests at 280°C.[5] Recently, specimens from two batches of Zircaloy-2 (items 569 and 611) were examined for evidence of hydriding after they had been exposed at 330°C in 300-hr tests at 26 fps.

Two tests used a slurry of (batch DT-18) thoria - 0.3% urania at a concentration of 400 g of Th per kg of D_2O, with an atmosphere of 90 psig (room temperature) of D_2 in one toroid and of O_2 in another toroid. Comparison tests were made with the same overpressures of D_2 and O_2 but with only D_2O in the toroids.

Metallographic examination revealed some hydrogen pickup by all specimens. The two specimens exposed in oxygenated D_2O displayed an increase in apparent hydrogen content to a depth of 2 to 6 mils in isolated areas under defects in the oxide corrosion film. Specimens exposed in D_2O with deuterium atmosphere displayed a shallow penetration of hydride needles around the total circumference of the pins extending to a depth of about 5 mils on the upstream portions. No increase in hydride was noted in the interior of the pins.

More defects were noted in the oxide corrosion film of specimens exposed in slurry with an oxygen atmosphere. A thin layer containing hydride needles was detected around the circumference of the specimens. In slurry tests with a deuterium atmosphere a general increase in hydride needles was found throughout the pins, with heaviest formation on the upstream (~15 mils in depth) and downstream (~7 mils) areas.

Based on these findings, it appears that increased temperature promoted hydride needle formation in aqueous systems and that the effect was intensified under hydrogen atmosphere with slurry in slug flow in the toroids.

14.3 IN-PILE AUTOCLAVE SLURRY CORROSION STUDIES

14.3.1 Introduction

A Zircaloy-2 autoclave corrosion experiment, L5Z-153S, containing thoria - 13% urania slurry was irradiated for six days in HB-5 facility of the LITR. The experiment briefly developed an estimated fission power density of 26 w/ml at full insertion, the highest yet achieved in slurry systems. Due to the generation of excessive radiolytic gas at this fission power density, the autoclave was retracted to a lower neutron flux (7% of maximum) for continuous irradiation. The experiment was terminated because plugging of the 20-mil-ID capillary tubing prevented the obtainment of sensitive pressure readings. The slurry had given out-of-pile evidence of a tendency to form deposits, and there was some evidence of similar behavior in-pile.

14.3.2 Exposure of In-Pile Experiment L5Z-153S

Operation.--In-pile Zircaloy-2 autoclave experiment L5Z-153S was loaded with thoria-urania slurry at a concentration of 820 g of Th per kg of D_2O, with 13.2 wt % enriched uranium with respect to thorium and 0.019 m Pd added as a recombination catalyst. At an assumed flux in LITR beam hole HB-5 of 1×10^{13} neutrons/$cm^2 \cdot sec$, the fission power density in the autoclave in the fully inserted position was 26 w/ml at 280°C. The experiment was operated at 280°C out-of-pile for 250 hr, in-pile for 162 hr, of which 136 hr was irradiation time, and then out-of-pile for 11 hr.

Initially gamma-ray radiography at room temperature revealed the presence of a tenacious slurry cake in the bottom of the autoclave, apparently formed during the loading operation. Dispersion of the slurry was finally achieved by rapping the bottom of the autoclave with a tool. As observed previously with a thoria - 8% urania slurry in autoclave experiment L5Z-152S,[6] suspension of this slurry at 280°C was assured only by careful stagewise heating of the autoclave to 280°C with rocking at 39 cycles/min.

After insertion into LITR beam hole HB-5, the autoclave was irradiated overnight (17 hr) at a flux of 7.3% of fully inserted flux. The autoclave was then irradiated briefly in the fully inserted position and subsequently retracted because of the generation of excessive radiolytic gas. Thereafter, the highest flux to which the autoclave was irradiated continuously was 18% of fully inserted flux. After six days of in-pile operation, when the autoclave was cooled to 25°C during a reactor shutdown, a slow response of the Baldwin pressure cell implied a partial plug in the 20-mil-ID capillary connecting tubing. Generation of hydrostatic pressure, by turning down a valve in the capillary line filled with D_2O, and rapid thermal cycling of the autoclave three times between 280 and 25°C did not relieve the plug. Since sensitive pressure readings were prevented by the plug, the autoclave was withdrawn from the reactor. Readings of the pressure cell were followed at room temperature for six days to obtain a reliable value of the oxygen pressure inside the autoclave, and the experiment was terminated.

Catalyst Performance.--Catalyst performance indices in experiment L5Z-153S ranged between 2.5 and 6.5 w/ml at 100 psi D_2, as shown in Table 14.2, with the average millimolal (Pd) value, 0.24, a factor of 125 lower than that observed in experiment L5Z-152S.[7] In the last two insertion experiments the true equilibrium radiolytic-gas pressure was not determined with high accuracy because of an apparent shift from first to zero reaction order after a substantial buildup of radiolytic gas.

Table 14.2. Catalyst Performance in Experiment L5Z-153S

Hours at Temp.	Hours at 3000 kw	Type of Experiment*	Relative Flux (% Maximum) Before	Relative Flux (% Maximum) After	Max. Power of Exp. (w/ml)	Catalyst Performance Index, w/ml at 100 psi D_2
268.2	0	I	2	7.3	1.9	4.5
268.6	0	I	7.3	29.8	7.8	6.5
269.4	0.2	R	29.8	7.3	7.8	4.2
289.7	1.7	I	2	7.3	1.9	4.5
290.4	1.8	I	7.3	25.5	6.7	2.5**
383.5	9.8	I	7.3	25.3	6.6	2.6**

*"I" indicates insertion; "R" indicates retraction.

**Based on an extrapolation of the first portion of the curve, which appears to be first order; the final portion appears to be zero order.

Postrun Observations.--During dismantling of the autoclave, while breaking the Zr-2 to Zr-2 pressure seal between the autoclave head and the autoclave, a "click" was heard from the inside of the dismantling cell. At the same time a small flash, about 1/4 in. long and 1/8 in. in diameter, was seen emitted from the mouth of the autoclave, and the autoclave head was observed to rise about 1 in. and then fall back in place. None of the components of either the autoclave or the dismantling cell appeared to have been affected by the incident, and stereomicroscopic examination of the swage surface of the autoclave head did not reveal any area suggestive of burning or unusual heating.

No loss of D_2O from the autoclave during the high-temperature operation was indicated by slurry samples recovered. Also no significant deposits of slurry were observed around the autoclave thermowell. Silicone-rubber replication of the inner autoclave walls to detect any deposits will be attempted. Some evidence of deposition of slurry on the inner walls of the autoclave was given by a gradual rise in temperature of one of the autoclave wall thermocouples during periods of irradiation at greater than 18% of fully inserted flux.

14.3.3 Corrosion in Experiment L5Z-153S

Time and Radiation Effect On Generalized Corrosion.--Generalized corrosion in Zircaloy-2 autoclave experiment L5Z-153S was followed from the decrease in oxygen pressure as determined from gas measurements at 25°C during reactor shutdowns.[8,9] Results from this experiment are presented in Fig. 14.1. The data can be fitted by the expression:

$$\text{Corrosion rate, mils/year} = \frac{75}{\text{hours at temp.}} .$$

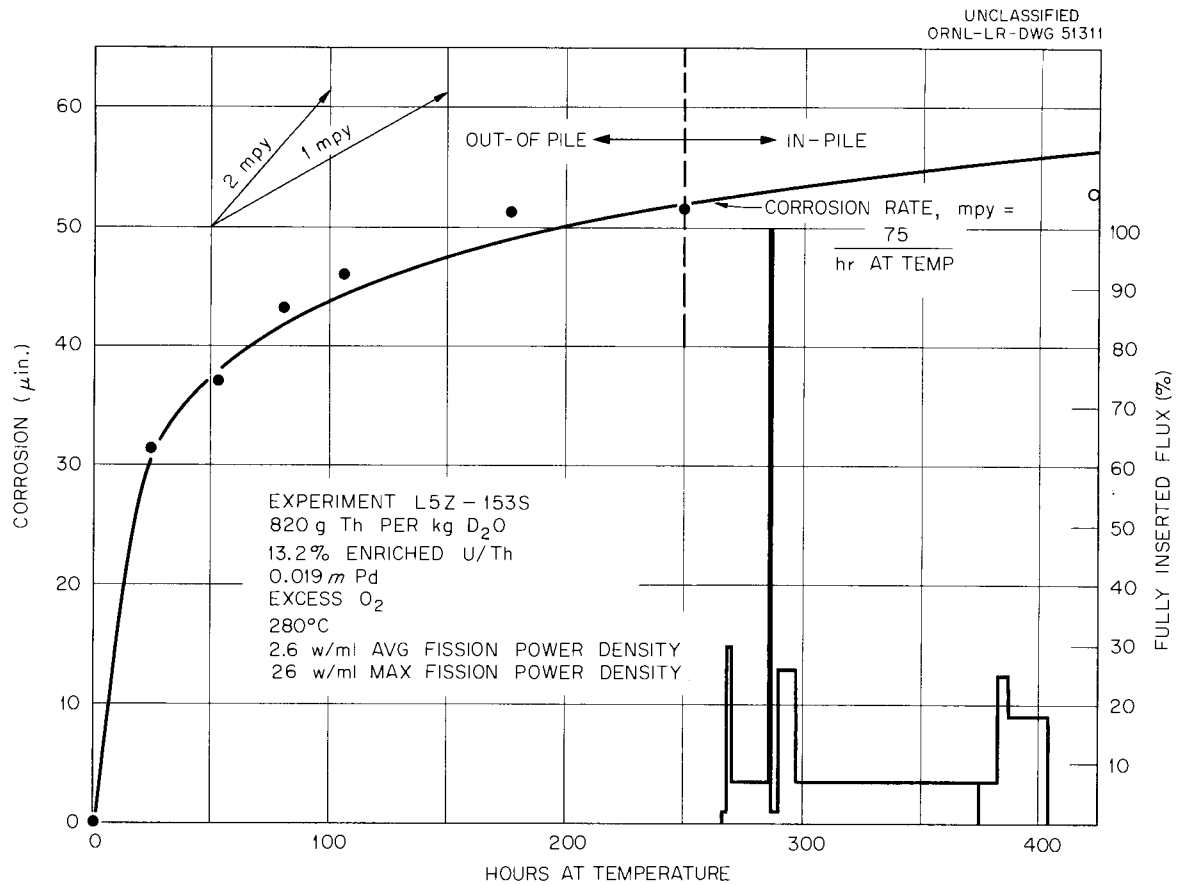

Fig. 14.1. Radiation Corrosion of Zircaloy-2 Autoclave by Thoria-Urania Slurry.

The radiation effect was not considered because at the low level of fission power density encountered in this experiment, 2.6 w/ml average, no radiation effect was observed.

Coupon Corrosion Specimens.--The corrosion results of coupon specimens in experiment L5Z-153S are presented in Table 14.3. A total corrosion of 53 μin. was indicated by oxygen consumption data, while coupon weight changes indicated 13 and 19 μin. As in previous experiments Y6Z-128S[10] and L5Z-152S,[11] all or most of the corrosion indicated by the consumption of oxygen had occurred out-of-pile under no radiation, and corrosion of Zircaloy-2 obtained by weight gain data showed poor agreement with that obtained by oxygen measurements.

Table 14.3. Radiation Corrosion of Coupon Specimens in Zircaloy-2 Autoclave Experiment L5Z-153S

Temperature, °C	280
Concentration of slurry, g Th per kg D_2O	820
Wt % enriched U, with respect to Th	13.2
Concentration of catalyst, m of Pd	0.019
Atmosphere	Excess O_2
Type of autoclave	Zr-2
Hours at temperature out-of-pile (including 11 hr after irradiation)	261
Total hours at temperature	422
Hours irradiated	136
Effective fraction of full irradiation time, fully inserted flux	0.101
Assumed flux, neutrons/cm^2.sec (in the fully inserted position)	1×10^{13}
Maximum power density, w/ml, at 280°C	26
Average power density while irradiated, w/ml, at 280°C	2.6
Autoclave generalized corrosion,[a] μin.	
Out-of-pile	52
Total	53
Coupon-specimen corrosion,[b] μin.	
Zircaloy-2[c]	13, 19
Type 347 SS	84
Titanium-75A	39

[a]Based on oxygen measurements.
[b]Corrosion of the first Zircaloy-2, the stainless steel, and titanium specimens based on weight loss; corrosion of the second Zircaloy-2 specimen based on weight gain.
[c]In a number of experiments Zircaloy-2 has been observed to gain in weight as a result of in-pile exposure. Consequently the results from the first Zircaloy-2 coupon represent the least amount of corrosion that could have occurred.

14.4 IN-PILE SLURRY LOOP

14.4.1 In-Pile Operation

Out-of-pile testing of the in-pile slurry loop, L-2-27S,[12] was completed during the past quarter. Satisfactory performance of the loop and auxiliary equipment was demonstrated in more than 900 hr of slurry circulation at 280°C. This included 800 hr of operation in the mockup facility and 100 hr of out-of-pile operation at the LITR facility to evaluate the equipment and procedures to be used during in-pile operation. The loop was then installed in beam hole HB-2 and in-pile operation was begun with the reactor at full power (3 Mw) on July 19. The loop is charged with thoria slurry at a concentration of 1350 g of Th per kg of D_2O and contains 0.5 wt % enriched uranium and palladium catalyst for liquid-phase recombination of radiolytic gas. Operating temperature of the loop is 280°C, and the slurry is oxygenated by means of an oxygen atmosphere in the pressurizer vapor space.

14.4.2 Catalysis Studies

Radiolytic-gas recombination in in-pile slurry loop L-2-27S, circulating the thoria-urania preparation[13] (DT-22) to be used in-pile, and containing 0.8 g of Pd, was studied[14,15] over a period of 600 hr by means of D_2 additions. Initially the specific activity of the catalyst was 1 mole of D_2 recombined per hour per gram of Pd at 100 psi D_2, and the activity declined by a factor of 2 after 400 hr of catalyst circulation. To permit an estimated original in-pile radiolytic-gas steady-state pressure of 15 to 20 psi, the loop Pd loading was brought to 1.6 g.

To assist in analyzing in-pile pressure and temperature transients, the electronic analog study of the loop[16] was extended to relate rate of pressure response with catalytic activity and pressurizer flow rates, and temperature transients with different inputs of fission and gamma heat and various controller settings. It was found that at the present (out-of-pile) value of pressurizer flow rate (3 to 4 cc/sec), this factor rather than recombination dominated the pressure response. The control system appeared more than adequate for all changes in fission-gamma heat levels appropriate to the experiment.

REFERENCES

1. I. Spiewak et al., HRP Quar. Prog. Rep. Apr. 30, 1960, ORNL-2947, p 32-35.
2. A. Taboada et al., HRP Quar. Prog. Rep. Apr. 30, 1960, ORNL-2947, p 122.
3. E. L. Compere et al., HRP Quar. Prog. Rep. Apr. 30, 1960, ORNL-2947, p 92.
4. Max Leva, Fluidization, p 169-178, McGraw-Hill, New York, 1959.
5. E. L. Compere et al., HRP Prog. Rep. Oct. 31, 1959, p 191-195.
6. E. L. Compere et al., HRP Quar. Prog. Rep. Apr. 30, 1960, ORNL-2947, p 99.
7. Ibid., p 99-101.
8. E. L. Compere et al., HRP Quar. Prog. Rep. Jan. 31, 1958, ORNL-2493, p 113.
9. K. S. Warren and R. J. Davis, In-Reactor Autoclave Studies - LITR. I. - Outline of Methods and Procedures, ORNL CF-57-5-110.
10. E. L. Compere et al., HRP Quar. Prog. Rep. Oct. 31, 1959, ORNL-2879, p 199.
11. E. L. Compere et al., HRP Quar. Prog. Rep. Apr. 30, 1960, ORNL-2947, p 101.
12. H. C. Savage et al., HRP Quar. Prog. Rep. Apr. 30, 1960, ORNL-2947, p 105.
13. E. L. Compere et al., HRP Quar. Prog. Rep. Apr. 30, 1960, ORNL-2947, p 107.
14. Ibid.
15. E. L. Compere et al., HRP Quar. Prog. Rep. Jan. 31, 1960, ORNL-2920, p 111.
16. E. L. Compere et al., HRP Quar. Prog. Rep. Oct. 31, 1959, ORNL-2879, p 208.

PART V. FUEL MANUFACTURE

15. THORIUM OXIDE PREPARATION

O. C. Dean P. A. Haas

A. T. Kleinsteuber C. C. Haws
R. H. Winget

15.1 THORIA-PELLET PREPARATION

A special ceramic-grade thoria (DT-100 and -103) was evaluated for preparation of rounded pellets. The oxalate was precipitated by methods leading to small particle size with a relatively wide particle-size distribution. The precipitate was filtered immediately with no digestion and then dried and calcined at 800°C for 2 hr. Approximately 50% of the particles were between 1 and 2 μ in diameter, 13% were less than 1 μ, and the remainder were distributed uniformly between 2 and 7 μ.

In initial experiments with pressing, the untreated powder tended to stick to the die walls and punch faces, and it flowed poorly due to "bridging" of the fines. Samples of ~200 g each lubricated with 4% aluminum stearate applied in isopropyl alcohol were prepressed at 2500 to 5200 psi, crushed and classified to -20+100 mesh, pressed to rounded green pellets of ~4.8 g/cc density, and then calcined at 1750°C for 4 hr (Table 15.1). With aluminum stearate lubricant, increasing the prepressing pressure increased the granule density and reduced the breakage of green pellets, but decreased resistance to attrition. Visual observation of pellets tested in the spouting bed showed that material loss was from a fault at the junction of the hemispherical and cylindrical sections of the pellets.

It was concluded that the powder is satisfactory, and that prepressing and lubrication are necessary, but that when the granules are made too dense faults are generated which develop into cracks on firing. The sticky character of the powder is emphasized by the results obtained with carbowax and no lubricant. When kerosene (~1/4%) was added to the carbowax-bound pellets, or when the prefiring temperature was increased from 800 to 1000°C, the breakage of green pellets during press-forming was reduced.

In all sphere press-forming experiments, regardless of powder, prepressing, lubrication, or firing conditions, cracking has tended to appear at the junction of the hemispherical and cylindrical sections in a significant percentage of pellets. One set of die punches has been modified to decrease the angle of curvature of the faces of the punch, and a few pellets made with the modified dies indicate that the severity of cracks has been decreased.

The effects of firing temperature on densities and attrition rates of pellets prepared from various powders prefired at various temperatures and treated with different binders were studied in a series of experiments

Table 15.1. Fabrication of Round Pellets from DT-100 Thoria

Powder, oxalate-precipitated, ceramic grade; pellets press-formed in Stokes automatic press with ball-faced punches; calcined at 1750°C, 4 hr

Sample	Lubricant-Binder	Prepressing Pressure (psi)	Pour Density of Granules (g/cc)	Breakage on Pressing (%)	Breakage After Firing (%)	Bulk Density (g/cc)	Erosion Rate[a] (%/hr)	
							High	Low
45-1	4% Al stearate[b]	2500	2.19	>50	Not fired	-	-	-
45-2	4% Al stearate	3300	2.22	~20	16	9.4	0.49	0.12
45-3	4% Al stearate	4130	2.43	<10	16	9.5	1.33	0.21
53-1	4% Al stearate	5150	2.56	<5	7	8.6	1.48	0.77
57-1	2% carbowax	4130	-	>50	Not fired	-	-	-

[a]A series of 1-hr spouting-bed erosion tests. (See HRP Quar. Prog. Rep. Apr. 30, 1960, ORNL-2947, p 91-96.)

[b]Aluminum stearate, 3.4% Al plus 50% excess stearic acid.

(Table 15.2). Even with shorter times at higher temperatures, densities and attrition resistance were increased by increasing the calcination temperature from 1300 to 1750°C.

Table 15.2. Effects of Calcination Conditions on Density and Attrition Resistance of Spherical ThO_2 Pellets

Powder: ceramic-grade, oxalate-precipitated ThO_2
Firing schedule: 4-hr heatup, 4 hr at temperature, 8-hr cooldown times

Powder	Binder	Calcination Temp. (°C)	Calcination Time (hr)	Bulk Density (g/cc)	Attrition Loss (wt %/hr)
Single, 800°C-fired	4% Al stearate	1300	20	8.7	3.3
		1600	6	9.5	1.6
		1750	4	9.5	0.8
Blend, 20% 800°C-fired and 80% 950°C-fired	1% carbowax	1300	20	7.4	3.3
		1600	6	8.1	2.6
		1750	4	8.7	1.6
Blend, 30% 800°C-fired and 70% 950°C-fired	1% carbowax	1300	20	7.2	2.8
		1600	6	8.2	2.3
		1750	4	8.9	2.3

15.2 URANIUM-THORIUM OXIDE PELLET PREPARATION

Round 0.5% uranium - thorium oxide pellets in which the uranium is uniformly distributed through the pellets, and which will have <1 wt %/hr loss in the spouting-bed attrition test[1] have been requested for pebble-bed studies. In order to satisfy the uniform-distribution requirement, a powder made by coprecipitations of U(IV) and thorium oxalate and then firing to 650°C was used. The particle sizes were quite uniform and were between 0.5 and 1 μ in diameter. Rolling formed rounded aggregates of ~60-mesh size. Powder samples prefired at 850, 1000, 1100, and 1200°C were granulated by simply rolling, or by pressing, sieving, and rolling after lubrication with either 2% carbowax or kerosene. They were pressed to ~6 g/cc green density in the Stokes automatic tablet press, using dies with ball-face punches, prefired for 20 hr at 200 to 1200°C, calcined at 1600°C for 4 hr, and cooled slowly. It appears that the desired specifications can be met by prefiring the powder to 1100°C, prepressing to 4000 psi, prefiring and soaking at 1200°C, and firing at 1600-1750°C for 4 hr (Table 15.3, samples 59-3C, 64, and 65). Modification of the punch faces of the die also appeared to decrease cracking of the green and fired pellets.

15.3 FLAME-CALCINATION DEVELOPMENT

Studies were conducted on increasing the size of flame-calcined thoria-alumina particles. Significant increases in particle sizes, from the 1.2 μ previously obtained[2] to 2.0 μ (see Table 15.4), were effected by increasing the thorium concentration in the feed from 300 to 600 g/liter and by lowering the

Table 15.3. Fabrication of Round Pellets of 0.5% Uranium - Thorium Oxide Powder

Coprecipitated U(IV)-Th oxalate calcined to 650°C; press-forming in Stokes automatic press with ball-faced punch dies; calcined 4 hr at 1600°C; binder-lubricant, 2% Carbowax-4000

Sample	4-hr Powder Prefiring Temp. (°C)	Granulation Procedure	Powder Pour Density (g/cc)	20-hr Pellet Prefiring Temp. (°C)	Breakage on Pressing, Prefiring, and Rolling (%)	Fired Density (g/cc)	Spouting-Bed Erosion Rate (%/hr)		Cracked on Firing (%)
							High	Low	
59-1A	850	None	-	600	>50	Not fired	-	-	-
59-2	850	Prepressed, 1670 psi	1.98	1200	<5	7.60	3.28	2.63	<5
59-3A	850	Prepressed, 2480 psi	-	600	<5	9.74	5.69	1.05	>10
59-3B	850	Prepressed, 2480 psi	-	1000	>50	-	-	-	-
59-3C	850	Prepressed, 2480 psi	-	1200	<5	8.02	1.69	0.69	>10
62	1000	No pressing, rolled	-	600	<5	7.89	2.81	1.67	>10
64	1000	Prepressed,[a] 4130 psi	2.87	200	<1	7.67	1.00	0.81	~10
65	1100	Prepressed,[a] 4130 psi	2.70	200	<1	8.41	0.80	0.44	<10
66	1100[b]	No pressing rolled	2.39	200	<5	6.62	6.00	2.75	>10
67	1200[b]	No pressing,[a] rolled	-	200	<1	7.52	6.08	2.17	>10

[a]Pressed in dies with modified punch faces.

[b]Kerosene used instead of carbowax.

Table 15.4. Effects of Operating Parameters on Particle Size of Flame-Calcined Thoria-Alumina

Feed: Al present in same form as Th to give 5 wt % Al_2O_3 in product; water used for both $Th(NO_3)_4$ and ThO_2 sol feeds

Atomizing gas: Nitrogen at 2.19 scfm

Flame: Oxygen-propane

Run No.	Firing Temp. (°C)	Feed Material		Feed Rate (ml/min)	Estimated Maximum Droplet Dia. (μ)	Mean Particle Dia. (μ)	
		Form	Concentration (g/liter)			Calculated[a]	Observed
100A	600	$Th(NO_3)_4$	600	33	50	15	2.1
100B	600	$Th(NO_3)_4$	600	9	40	12	2.5
101A	1000	$Th(NO_3)_4$	600	8	35	11	1.9
101B	1000	$Th(NO_3)_4$	600	33	50	15	2.9[b]
102A	1500	$Th(NO_3)_4$	600	28	50	15	1.9
102B	1500	$Th(NO_3)_4$	600	6	30	9	2.1[c]
103	1500	$Th(SO_4)_2$	37	30	50	5	1.1[c]
104	1500	ThO_2 sol	264	26	-	-	1.8[d]
105	1000	ThO_2 sol	280	24	-	-	2.5
106	1500	$Th(NO_3)_4$	920	26	-	-	1.8
107	1450	$Th(NO_3)_4$	1226	e	-	-	2.0

[a]Calculated from amount of Th and Al in droplet of estimated diameter.

[b]Reference run with about 300 g/liter of $Th(NO_3)_4$ gave 1.8-μ diameter.

[c]Reference run with about 300 g/liter of $Th(NO_3)_4$ gave 1.3-μ diameter.

[d]Very low surface area, 0.94 m^2/g.

[e]Could not be controlled due to physical properties of solution.

furnace reflector temperature from 1500 to 1000°C. The size of entering droplets appears to have no effect on ultimate particle size. Substitution of thorium sulfate for thorium nitrate had no effect on particle size of product. The use of 1 *M* thoria sols prepared by nitration and denitration of ThO_2 at 95°C gave spherical ThO_2 particles comparable to those obtained with thorium nitrate feed solutions.

REFERENCES

1. E. L. Compere et al., HRP Quar. Prog. Rep. Apr. 30, 1960, ORNL-2947, p 91-96.

2. O. C. Dean, P. A. Haas, et al., HRP Quar. Prog. Rep. Apr. 30, 1960, ORNL-2947, p 117.

PART VI. METALLURGY

16. METALLURGY

A. Taboada

T. M. Kegley, Jr. P. L. Rittenhouse
W. J. Leonard R. L. Stephenson

16.1 ZIRCONIUM-ALLOY DEVELOPMENT

A study was begun on the effects of beta homogeneization time, quenching temperature, quenching rate, and room-temperature aging after quenching, on the incubation time for the formation of omega phase at 400°C in Zr-15Nb alloys. Specimens were quenched in water-cooled mercury after homogeneization at 850 or 950°C for 30, 60, or 120 min. Delay times were <1 sec and 5, 15, and 30 sec from the time of removal of the specimen from the furnace to the instant of entrance into the quenching bath. The specimens were thus cooled to different and unknown temperatures in a purified argon atmosphere before entering the quenching bath. Since the study was intended to be only a rough evaluation of some of the variables of possible importance, it was necessary only that the temperatures just before quenching be appreciably different and that all specimens for a given quenching temperature and delay receive exactly the same treatment by heat-treating them together. Considerably more work on the study is intended, with the values of the variables better controlled and better known.

The principal results of the study to date are that higher homogeneization temperatures, longer homogeneization times, and higher temperatures when entering the quenching bath consistently resulted in shorter incubation times and in higher hardnesses at the maximum aging time of 60 min. The data also indicate that longer aging times at room temperature before aging at 400°C resulted in longer incubation times.

Data reported previously in this series of reports[1] show that small amounts of cold work decrease the incubation time, that the concentration of omega phase is homogeneous throughout a specimen (being essentially the same in a grain boundary as in the center of a grain), that omega-phase particles very rapidly reach their maximum size, and that oxygen decreases the incubation time.

The only explanation, consistent with all the observations, which can be postulated at the present time is that the vacancy concentration in the specimen strongly influences the nucleation and the concentration of omega phase; that is, an increased number of vacancies increases the rate of nucleation of omega phase and thereby the volume of omega phase present after any given time interval. Vacancy concentration should be affected by alloying element, homogeneization temperature, homogeneization time, quenching temperature, quenching rate, cold work, and aging at room temperature after beta quenching, in a manner consistent with the data determined to date for the change in the incubation period for the omega-phase formation.

The results of the study have also shown that the lack of reproducibility for aging data for the Zr-15Nb alloys for different ingots of alloy is probably due to minor differences in homogeneization and quenching treatments experienced by specimen material prepared at different times.[1]

Specimens of Zr-1Cu, Zr-1.6Cu, Zr-4Mo, and Zr-7.5Mo (weight per cent) were transformed isothermally or by beta-quench and reheat aging at 400, 500, 600 and 700°C for times up to 60 min. The hardness data collected show that an age-hardening reaction occurs in all four alloys for both types of transformation at temperatures of 400 and 500°C and that the hardness continually decreases for transformation by both techniques at 600 and 700°C. Metallographic examination has been difficult and of little aid in following the transformation behavior. The microstructures of the Mo alloys show very little change occurring after the initial change on aging at any temperature for the shortest period of time. The microstructures of the Cu alloys show that some type of nodular transformation product is produced at the grain boundaries. The nodular product grows slowly and appears to be the same whether the transformation technique has been beta-quench and reheat or true isothermal. Anodizing of the specimens after chemical polishing has been the only metallographic technique found to reveal the structures. The transformation studies for these alloys are being extended to both shorter and longer times at several temperatures intermediate to those already used.

16.2 ZIRCALOY-2 FABRICATION STUDY

The anisotropy of mechanical properties of Zircaloy-2 plate and sheet is known to be a function of the preferred orientation and of the mechanical fibering which occurs during fabrication. A study has been conducted on the evaluation of various fabrication procedures and the effects of specific fabrication variables on the final state of anisotropy. The aims, experimental procedures, variables studied, experimental data, and a number of the conclusions have been reported previously.[2,3]

The study has been terminated and the collection and analysis of the data determined in the study are reported in two topical reports now in press.[4] The principal conclusions reported previously remain unchanged. The fabrication procedure which produced the least preferred orientation was that which has been used for several years to fabricate Zircaloy-2 for HRP use.

REFERENCES

1. G. M. Adamson et al., HRP Quar. Prog. Reps. Oct. 31, 1956, ORNL-2222, p 114-16; Jan. 31, 1957, ORNL-2272, p 119-23; Apr. 31, 1957, ORNL-2331, p 124-28; July 31, 1957, ORNL-2379, p 122-26; Oct. 31, 1957, ORNL-2432. p 131-33; Jan. 31, 1958, ORNL-2493, p 141-43; Apr. 30 and July 31, 1958, ORNL-2561, p 245; Oct. 31, 1958, ORNL-2654, p 188; May 1 through Oct. 31, 1959, ORNL-2879, p 242; Jan. 31, 1960, ORNL-2920, p 128; Apr. 30, 1960, ORNL-2947, p 122.

2. G. M. Adamson et al., HRP Quar. Prog. Reps. Oct. 31, 1958, ORNL-2654, p 184-86; Apr. 30, 1959, ORNL-2743, p 182-91; Oct. 31, 1959, ORNL-2879, p 240-241; Jan. 31, 1960, ORNL-2920, p 127-128.

3. M. L. Picklesimer et al., Met. Div. Ann. Prog. Rep. Sept. 1, 1959, ORNL-2839, p 115-27.

4. P. L. Rittenhouse and M. L. Picklesimer, Metallurgy of Zircaloy-2: Part I - The Effects of Fabrication Variables on the Anisotropy of Mechanical Properties, ORNL-2944 (in press); P. L. Rittenhouse and M. L. Picklesimer, Metallurgy of Zircaloy-2: Part II - The Effects of Fabrication Variables on the Preferred Orientation and Anisotropy of Strain Behavior, ORNL-2948 (in press).

INTERNAL DISTRIBUTION

1. C. E. Center
2. Biology Library
3. Health Physics Library
4. Metallurgy Library
5-6. Reactor Experimental Engineering Library
7-9. Central Research Library
10-14. Laboratory Records Department
15. Laboratory Records, ORNL R. C.
16. G. M. Adamson
17. A. L. Bacarella
18. J. E. Baker
19. S. J. Ball
20. J. C. Banter
21. S. E. Beall
22. L. L. Bennett
23. A. M. Billings
24. D. S. Billington
25. E. P. Blizard
26. R. Blumberg
27. E. G. Bohlmann
28. S. E. Bolt
29. C. J. Borkowski
30. G. E. Boyd
31. J. C. Bresee
32. F. R. Bruce
33. J. R. Buchanan
34. W. D. Burch
35. C. A. Burchsted
36. S. R. Buxton
37. A. D. Callihan
38. W. L. Carter
39. G. H. Cartledge
40. R. H. Chapman
41. R. A. Charpie
42. R. D. Cheverton
43. C. J. Claffey
44. H. C. Claiborne
45. T. E. Cole
46. C. W. Collins
47. E. L. Compere
48. F. L. Culler
49. D. G. Davis
50. R. J. Davis
51. V. A. DeCarlo
52. W. K. Eister
53. L. B. Emlet (K-25)
54. J. L. English
55. D. E. Ferguson
56. D. F. Frech
57. J. H. Frye, Jr.
58. C. H. Gabbard
59. J. L. Gabbard
60. W. R. Gall
61. R. B. Gallaher
62. E. H. Gift
63. H. E. Goeller
64. A. T. Gresky
65. J. C. Griess
66. W. R. Grimes
67. E. Guth
68. R. H. Guymon
69. L. A. Haack
70. P. A. Haas
71. J. Halperin
72. P. H. Harley
73. R. J. Harvey
74. P. N. Haubenreich
75. D. N. Hess
76. J. W. Hill
77. E. C. Hise
78. A. Hollaender
79. P. P. Holz
80. H. P. House
81. A. S. Householder
82. S. Jaye
83. G. H. Jenks
84. D. T. Jones
85. E. V. Jones
86. J. E. Jones Jr.
87. W. H. Jordan
88. P. R. Kasten
89. C. P. Keim
90. M. T. Kelley
91. F. Kertesz
92. J. O. Kolb
93. U. Koskela
94. K. A. Kraus
95. N. A. Krohn
96. J. A. Lane
97. C. G. Lawson
98. S. C. Lind
99. R. S. Livingston
100. R. A. Lorenz
101. M. I. Lundin
102. R. N. Lyon
103. J. L. Marsh (C&CC, South Charleston)

104. W. L. Marshall
105. J. P. McBride
106. H. F. McDuffie
107. H. A. McLain
108. J. R. McWherter
109. E. C. Miller
110. R. L. Moore
111. C. S. Morgan
112. K. Z. Morgan
113. L. E. Morse
114. J. P. Murray (Y-12)
115. M. L. Nelson
116. P. D. Neumann
117. A. R. Olsen
118. L. F. Parsly
119. F. N. Peebles
120. M. L. Picklesimer
121. H. B. Piper
122. B. E. Prince
123. L. R. Quarles
124. S. A. Reed
125. W. D. Reel
126. P. M. Reyling
127. S. A. Reynolds
128. L. Rice
129. D. M. Richardson
130. R. C. Robertson
131. W. Robinson
132. H. C. Roller
133. M. W. Rosenthal
134. H. C. Savage
135. C. E. Schilling
136. H. E. Seagren
137. C. H. Secoy
138. C. L. Segaser
139. E. D. Shipley
140. A. J. Shor
141. M. D. Silverman
142. M. J. Skinner
143. A. N. Smith
144. A. H. Snell
145. I. Spiewak
146. H. H. Stone
147. R. W. Stoughton
148. C. D. Susano
149. J. A. Swartout
150. A. Taboada
151. E. H. Taylor
152. W. Terry
153. P. F. Thomason
154. M. Tobias
155. W. E. Unger
156. W. C. Ulrich
157. R. Van Winkle
158. D. W. Vroom
159. R. E. Wacker
160. H. O. Weeren
161. A. M. Weinberg
162. S. H. Wheeler
163. E. P. Wigner (Consultant)
164. H. D. Wills
165. G. C. Williams
166. J. C. Wilson
167. R. H. Winget
168. C. E. Winters
169. C. H. Wodtke
170. L. F. Woo
171. F. C. Zapp
172. H. E. Zittel
173. ORNL - Y-12 Technical Library, Document Reference Section
174. HRP Director's Office, Y-12

EXTERNAL DISTRIBUTION

175. F. P. Self, AEC, ORO
176. D. H. Groelsema, AEC, Washington
177. Division of Research and Development, AEC, ORO
178-754. Given distribution as shown in TID-4500 (15th ed.) under Reactors-Power Category (75 copies - OTS)

Reports previously issued in this series are as follows:

ORNL-527	Date Issued, December 28, 1949
ORNL-630	Period Ending February 28, 1950
ORNL-730	Feasibility Report - Date Issued, July 6, 1950
ORNL-826	Period Ending August 31, 1950
ORNL-925	Period Ending November 30, 1950
ORNL-990	Period Ending February 28, 1951
ORNL-1057	Period Ending May 15, 1951
ORNL-1121	Period Ending August 15, 1951
ORNL-1221	Period Ending November 15, 1951
ORNL-1280	Period Ending March 15, 1952
ORNL-1318	Period Ending July 1, 1952
ORNL-1424	Period Ending October 1, 1952
ORNL-1478	Period Ending January 1, 1953
ORNL-1554	Period Ending March 31, 1953
ORNL-1605	Period Ending July 31, 1953
ORNL-1658	Period Ending October 31, 1953
ORNL-1678	Period Ending January 31, 1954
ORNL-1753	Period Ending April 30, 1954
ORNL-1772	Period Ending July 31, 1954
ORNL-1813	Period Ending October 31, 1954
ORNL-1853	Period Ending January 31, 1955
ORNL-1895	Period Ending April 30, 1955
ORNL-1943	Period Ending July 31, 1955
ORNL-2004	Period Ending October 31, 1955
ORNL-2057	Period Ending January 31, 1956
ORNL-2096	Period Ending April 30, 1956
ORNL-2148	Period Ending July 31, 1956
ORNL-2222	Period Ending October 31, 1956
ORNL-2272	Period Ending January 31, 1957
ORNL-2331	Period Ending April 30, 1957
ORNL-2379	Period Ending July 31, 1957
ORNL-2432	Period Ending October 31, 1957
ORNL-2493	Period Ending January 31, 1958
ORNL-2561	Periods Ending April 30 and July 31, 1958
ORNL-2654	Period Ending October 31, 1958
ORNL-2696	Period Ending January 31, 1959
ORNL-2743	Period Ending April 30, 1959
ORNL-2879	Period May 1 Through October 31, 1959
ORNL-2920	Period Ending January 31, 1960
ORNL-2947	Period Ending April 30, 1960